
Wavelet Score-Based Generative Modeling

Florentin Guth

Computer Science Department,
ENS, CNRS, PSL University

Simon Coste

Computer Science Department,
ENS, CNRS, PSL University

Valentin De Bortoli

Computer Science Department,
ENS, CNRS, PSL University

Stéphane Mallat

Collège de France, Paris, France
Flatiron Institute, New York, USA

Abstract

Score-based generative models (SGMs) synthesize new data samples from Gaussian white noise by running a time-reversed Stochastic Differential Equation (SDE) whose drift coefficient depends on some probabilistic score. The discretization of such SDEs typically requires a large number of time steps and hence a high computational cost. This is because of ill-conditioning properties of the score that we analyze mathematically. We show that SGMs can be considerably accelerated, by factorizing the data distribution into a product of conditional probabilities of wavelet coefficients across scales. The resulting Wavelet Score-based Generative Model (WSGM) synthesizes wavelet coefficients with the same number of time steps at all scales, and its time complexity therefore grows linearly with the image size. This is proved mathematically over Gaussian distributions, and shown numerically over physical processes at phase transition and natural image datasets.

1 Introduction

Score-based Generative Models (SGMs) have obtained remarkable results to learn and sample probability distributions of image and audio signals (Song and Ermon, 2019; Nichol and Dhariwal, 2021; Dhariwal and Nichol, 2021). They proceed as follows: the data distribution is mapped to a Gaussian white distribution by evolving along a Stochastic Differential Equation (SDE), which progressively adds noise to the data. The generation is implemented using the time-reversed SDE, which transforms a Gaussian white noise into a data sample. At each time step, it pushes samples along the gradient of the log probability, also called *score function*. This score is estimated by leveraging tools from score-matching and deep neural networks (Hyvärinen and Dayan, 2005; Vincent, 2011). At sampling time, the computational complexity is therefore proportional to the number of time steps, i.e., the number of forward network evaluations. Early SGMs in Song and Ermon (2019); Song et al. (2021); Ho et al. (2020) used thousands of time steps, and hence had a limited applicability.

Diffusion models map a Gaussian white distribution into a highly complex data distribution. We thus expect that this process will require a large number of time steps. It then comes as a surprise that recent approaches have drastically reduced the the number of time steps. This is achieved by optimizing the discretization schedule or by modifying the original SGM formulation (Kadkhodaie and Simoncelli, 2020; Jolicœur-Martineau et al., 2021; Liu et al., 2022; Zhang and Chen, 2022; San-Roman et al., 2021; Nachmani et al., 2021; Song et al., 2020; Kong and Ping, 2021; Ho et al., 2020; Luhman and Luhman, 2021; Salimans and Ho, 2022; Xiao et al., 2021). High-quality score-based generative models have also been improved by cascading multiscale image generations (Saharia et al., 2021; Ho et al., 2022; Dhariwal and Nichol, 2021) or with subspace decompositions (Jing et al., 2022). We show that with an important modification, these approaches provably improve the performance of SGMs.

A key idea is that typical high-dimensional probability distributions coming from physics or natural images have complex multiscale properties. They can be simplified by factorizing them as a product of conditional probabilities of normalized wavelet coefficients across scales. These conditional probabilities are more similar to Gaussian white noise than the original image distribution, and can thus be sampled more efficiently. On the physics side, this observation is rooted in the renormalization group decomposition in statistical physics (Wilson, 1971), and has been used to estimate physical energies from data Marchand et al. (2022). In image processing, it relies on statistical observations of wavelet coefficient properties (Wainwright and Simoncelli, 1999). A Wavelet Score-based Generative Model (WSGM) generates normalized wavelet coefficients from coarse to fine scales, as illustrated in Figure 1. The conditional probability of each set of wavelet coefficients, given coarse scale coefficients, is sampled with its own (conditional) SGM. The main result is that a normalization of wavelet coefficients allows fixing the same discretization schedule at all scales. Remarkably, and as opposed to existing algorithms, it implies that the total number of sampling iterations per image pixel does not depend on the image size.

After reviewing score-based generation models, Section 2 studies the mathematical properties of its time discretization, with a focus on Gaussian models and multiscale processes. Images and many physical processes are typically non-Gaussian, but do have a singular covariance with long- and short-range correlations. In Section 3, we explain how to factorize these processes into probability distributions which capture interactions across scales by introducing orthogonal wavelet transforms. We shall prove that it allows considering SGMs with the same time schedule at all scales, independently of the image size. In Section 4, we present numerical results on Gaussian distributions, the φ^4 physical model at phase transition, and the CelebA-HQ image dataset (Karras et al., 2018). The main contributions of the paper are as follows:

- A Wavelet Score-based Generative Model (WSGM) which generates conditional probabilities of normalized wavelet coefficients, with the same discretization schedule at all scales. The number of time steps per image pixel does not need to depend upon the image size to reach a fixed error level.
- Theorems controlling errors of time discretizations of SGMs, proving accelerations obtained by scale separation with wavelets. These results are empirically verified by showing that WSGM provides an acceleration for the synthesis of physical processes at phase transition and natural image datasets.

2 Sampling and Discretization of Score-Based Generative Models

2.1 Score-Based Generative Models

Diffusions and time reversal A Score-based Generative Model (SGM) (Song and Ermon, 2019; Song et al., 2021; Ho et al., 2020) progressively maps the distribution of data x into the normal distribution, with a forward SDE which iteratively adds Gaussian white noise. It is associated with a *noising process* $(x_t)_t$, with x_0 distributed according to the data distribution p , and satisfying:

$$dx_t = -x_t dt + \sqrt{2} dw_t, \quad (1)$$

where $(w_t)_t$ is a Brownian motion. The solution is an Ornstein-Uhlenbeck process which admits the following representation for any $t \geq 0$:

$$x_t = e^{-t} x_0 + (1 - e^{-2t})^{1/2} z, \quad z \sim \mathcal{N}(0, \text{Id}). \quad (2)$$

The process $(x_t)_t$ is therefore an interpolation between a data sample x_0 and Gaussian white noise. The *generative process* inverts (1). Under mild assumptions on p (Cattiaux et al., 2021; Haussmann and Pardoux, 1986), for any $T \geq 0$, the reverse time process x_{T-t} satisfies:

$$dx_{T-t} = \{x_{T-t} + 2\nabla \log p_{T-t}(x_{T-t})\} dt + \sqrt{2} dw_t, \quad (3)$$

where p_t is the probability density of x_t , and $\nabla \log p_t$ is called the *Stein score*. Since x_T is close to a white Gaussian variable, one can approximately sample from x_T by sampling from the normal distribution. We can generate x_0 from x_T by solving this time-reversed SDE, if we can estimate an accurate approximation of the score $\nabla \log p_t$ at each time t , and if we can discretize the SDE without introducing large errors.

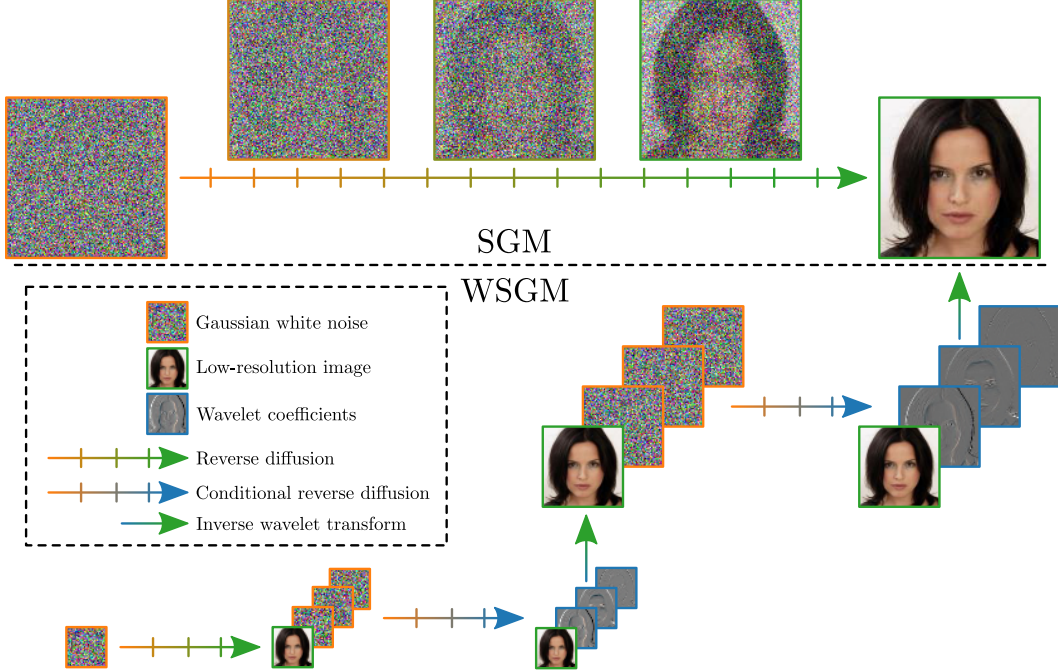


Figure 1: An SGM generates images by discretizing a reverse diffusion, which progressively transforms white Gaussian noise into a natural image. A WSGM generates increasingly higher-resolution images by discretizing reverse diffusions on wavelet coefficients at each scale. It begins by generating a first low-resolution image. Renormalized wavelet coefficients are then generated conditionally to this low-resolution image. A fast inverse wavelet transform reconstructs a higher-resolution image from these wavelet coefficients. This process is repeated at each scale. The number of steps is the same at each scale, and can be orders of magnitude smaller than for SGM.

Efficient approximations of the Stein scores are the workhorse of SGM. [Hyvärinen and Dayan \(2005\)](#) shows that the score $\nabla \log p_t$ can be approximated with parametric functions s_θ which minimize the following score matching loss:

$$s_t = \arg \min_{\theta} \mathbb{E}_{p_t} \left[\frac{1}{2} \|s_\theta(x_t)\|^2 + \text{div}(s_\theta)(x_t) \right]. \quad (4)$$

For image generation, s_θ is calculated by a neural network parameterized by θ . In statistical physics problems where the energy can be linearly expanded with coupling parameters, we obtain linear models $s_\theta(x) = \theta^\top \nabla U(x)$. This is the case for Gaussian processes where $U(x) = xx^\top$; it also applies to non-Gaussian processes, using non-quadratic terms in $U(x)$.

Time discretization of generation An approximation of the generative process (3) is computed by approximating $\nabla \log p_t$ by s_t and discretizing time. It amounts to approximating the time-reversed SDE by a Markov chain which is initialised by $\tilde{x}_T \sim \mathcal{N}(0, \text{Id})$, and computed over times t_k which decrease from $t_N = T$ to $t_0 = 0$, at intervals $\delta_k = t_k - t_{k-1}$:

$$\tilde{x}_{t_{k-1}} = \tilde{x}_{t_k} + \delta_k \{ \tilde{x}_{t_k} + 2s_{t_k}(\tilde{x}_{t_k}) \} + \sqrt{2\delta_k} z_k, \quad z_k \stackrel{\text{i.i.d.}}{\sim} \mathcal{N}(0, \text{Id}). \quad (5)$$

Ignoring the error due to the score model, the minimum number of time steps is limited by the Lipschitz regularity of the score $\nabla \log p_t$, see ([De Bortoli et al., 2021](#), Theorem 1). The overall complexity of this generation is $O(N)$ evaluations of the score $s_t(x)$.

2.2 Discretization of SGM and Score Regularity

We study how the regularity of the score $\nabla \log p$ affects the discretization of (5). Assuming that the score is known, i.e., that $s_t = \nabla \log p_t$, we prove that for Gaussian processes, the number of time steps to reach a fixed error ε depends on the condition number of its covariance. This result is generalized to non-Gaussian processes by relating this error to by the regularity of $\nabla \log p_t$.

Gaussian distributions Suppose that the data distribution is a Gaussian $p = \mathcal{N}(0, \Sigma)$ with covariance matrix Σ , in dimension d . Let p_t be the distribution of x_t . Using (2), we have:

$$\nabla \log p_t(x) = -(\text{Id} + (\Sigma - \text{Id})e^{-2t})^{-1}x.$$

Let \tilde{p}_t be the distribution of \tilde{x}_t obtained by the time discretization (5). The approximation error between the distribution \tilde{p}_0 obtained with the time-reversed SDE and the data distribution p stems from (i) the mismatch between the distributions of x_T and \tilde{x}_T , and (ii) the time discretization. The following theorem relates these two errors to the covariance Σ of x in the particular case of a uniform time sampling at intervals $\delta_k = \delta$. We normalize the signal energy by imposing that $\text{Tr}(\Sigma) = d$, and we write κ the condition number of Σ , which is the ratio between its largest and smallest eigenvalues.

Theorem 1. *We have $\text{KL}(p|\tilde{p}_0) \leq E_T + E_\delta + E_{T,\delta}$, with :*

$$E_T = f(e^{-4T} |\text{Tr}((\Sigma - \text{Id})\Sigma)|),$$

$$E_\delta = f(\delta |\text{Tr}(\Sigma^{-1} - \Sigma(\Sigma - \text{Id})^{-1} \log(\Sigma)/2 + (\text{Id} - \Sigma^{-1})/3)|),$$

where $f(t) = t - \log(1 + t)$ and $E_{T,\delta}$ is a higher-order term with $E_{T,\delta} = o(\delta + e^{-4T})$ when $\delta \rightarrow 0$ and $T \rightarrow +\infty$. Furthermore, for any $\varepsilon > 0$, there exists $T, \delta \geq 0$ such that:

$$(1/d)(E_T + E_\delta) \leq \varepsilon \text{ and } T/\delta \leq C\varepsilon^{-2}\kappa^3. \quad (6)$$

with $C \geq 0$ a universal constant.

This theorem specifies the dependence of the Kullback-Leibler error on the covariance matrix. It computes an upper bound on the number of time steps $N = T/\delta$ as a function of the condition number κ of Σ . As expected, it indicates that the number of time steps increases with the condition number of the covariance. This theorem is proved in a more general case in Section 10, which includes the case where p has a non-zero mean. An exact expansion of the Kullback-Leibler divergence is also given.

For stationary processes of images, the covariance eigenvalues are given by the power spectrum, which typically decays like $|\omega|^{-1}$ at a frequency ω . It results that κ is proportional to a power of the image size. Many physical phenomena produce such stationary images with a power spectrum having a power law decay. In these typical cases, the number of time steps must increase with the image size. This is indeed what is observed in numerical SGM experiments, as seen in Section 3.

General processes Theorem 1 can be extended to non-Gaussian processes. The number of time steps then depends on the regularity of the score $\nabla \log p_t$.

Theorem 2. *Assume that $\nabla \log p_t(x)$ is \mathcal{C}^2 in both t and x , and that:*

$$\sup_{x,t} \|\nabla^2 \log p_t(x)\| \leq K \text{ and } \|\partial_t \nabla \log p_t(x)\| \leq M e^{-\alpha t} \|x\|, \quad (7)$$

for some $K, M, \alpha > 0$. Then $\|p - \tilde{p}_0\|_{\text{TV}} \leq E_T + E_\delta + E_{T,\delta}$, where:

$$E_T = \sqrt{2}e^{-T} \text{KL}(p|\mathcal{N}(0, \text{Id}))^{1/2}, \quad (8)$$

$$E_\delta = 6\sqrt{\delta} [1 + \mathbb{E}_p(\|x\|^4)^{1/4}] [1 + K + M(1 + 1/(2\alpha)^{1/2})], \quad (9)$$

and $E_{\delta,T}$ is a higher order term with $E_{T,\delta} = o(\sqrt{\delta} + e^{-T})$ when $\delta \rightarrow 0$ and $T \rightarrow +\infty$.

The proof of Theorem 2 is postponed to Section 10 and we show that the result can be strengthened by providing a quantitative upper bound on $\|p - \tilde{p}_0\|_{\text{TV}}$. Theorem 2 improves on (De Bortoli et al., 2021, Theorem 1) by proving explicit bounds exhibiting the dependencies on the regularity constants K and M of the score and by eliminating an exponential growth term in T in the upper bound. Theorem 2 is much more general but not as tight as Theorem 1.

The first error term (8) is due to the fact that T is chosen to be finite. The second error term (9) controls the error depending upon the discretization time step δ . Since p_t is obtained from p through a high-dimensional convolution with a Gaussian convolution of variance proportional to t , the regularity of $\nabla \log p_t(x)$ typically increases with t so $\|\nabla^2 \log p_t(x)\|$ and $\|\partial_t \nabla \log p_t(x)\|$ rather decrease when t increase. This qualitatively explains why a *quadratic* discretization schedule with non-uniform time steps $\delta_k \propto k$ are usually chosen in numerical implementations of SGMs (Nichol and Dhariwal, 2021; Song and Ermon, 2020). For simplicity, we focus on the uniform discretization schedule, but our result could be adapted to non-uniform time steps with no major difficulties.

If p is Gaussian, then the Hessian $\nabla^2 \log p$ is the negative inverse of the covariance matrix. We verify in Section 10 that in this case, the assumptions of Theorem 2 are satisfied. Furthermore, the constants K and M , and hence the number of discretization steps, are controlled using the condition number of Σ . We thus conjecture that non-Gaussian processes with an ill-conditioned covariance matrix will require many discretization steps to have a small error. This will be verified numerically. As we now explain, such processes are ubiquitous in physics and natural image datasets.

Multiscale processes Most images have variations on a wide range of scales. They require to use many time steps to sample using an SGM, because their score is not well-conditioned. This is also true for a wide range of phenomena encountered in physics, biology, or economics (Kolmogorov, 1962; Mandelbrot, 1983). We define a *multiscale process* as a stationary process whose power spectrum has a power law decay. The stationarity implies that its covariance is diagonalized in a Fourier basis. Its eigenvalues, also called power spectrum, have a power law decay defined by:

$$P(\omega) \sim (\xi^\eta + |\omega|^\eta)^{-1}, \quad (10)$$

where $\eta > 0$ and $2\pi/\xi$ is the maximum correlation length. Physical processes near phase transitions have such a power-law decay, but it is also the case of many disordered systems such as fluid and gas turbulence. Natural images also typically define stationary processes. Their power spectrum satisfy this property with $\eta = 1$ and $2\pi/\xi \approx L$ which is the image width. To efficiently synthesize images and more general multiscale signals, we must eliminate the ill-conditioning properties of the score. This is done by applying a wavelet transform.

3 Wavelet Score-Based Generative Model

The numerical complexity of the SGM algorithm depends on the number of time steps, which itself depends upon the regularity of the score. We show that an important acceleration is obtained by factorizing the data distribution into normalized wavelet conditional probability distributions, which are closer to normal Gaussian distributions, and so whose score is better-conditioned.

3.1 Wavelet Whitening and Cascaded SGMs

Normalized orthogonal wavelet coefficients Let x be the input signal of width L and dimension $d = L^n$, with $n = 2$ for images. We write x_j its low-frequency approximation subsampled at intervals 2^j , of size $(2^{-j}L)^n$, with $x_0 = x$. At each scale $2^{j-1} \geq 1$, a fast wavelet orthogonal transform decomposes x_{j-1} into (\bar{x}_j, x_j) where \bar{x}_j are the wavelet coefficient which carries the higher frequency information over $2^n - 1$ signals of size $(2^{-j}L)^n$ Mallat (1999). They are calculated with convolutional and subsampling operators G and \bar{G} specified in Section 9:

$$x_j = \gamma_j^{-1} G x_{j-1} \quad \text{and} \quad \bar{x}_j = \gamma_j^{-1} \bar{G} x_{j-1}. \quad (11)$$

The normalization factor γ_j guarantees that $\mathbb{E}[\|\bar{x}_j\|^2] = (2^n - 1)(2^{-j}L)^n$. We consider wavelet orthonormal filters where (G, \bar{G}) is a unitary operator, i.e.:

$$\bar{G}G^\top = G\bar{G}^\top = 0 \quad \text{and} \quad G^\top G + \bar{G}^\top \bar{G} = \text{Id}.$$

It results that x_{j-1} is recovered from (\bar{x}_j, x_j) with:

$$x_{j-1} = \gamma_j G^\top x_j + \gamma_j \bar{G}^\top \bar{x}_j.$$

The wavelet transform is computed over $J \approx \log_2 L$ scales by iterating J times on (11). The last x_J has a size $(2^{-J}L)^n \sim 1$. The choice of wavelet filters G and \bar{G} specifies the properties of the wavelet transform and the number of vanishing moments of the wavelet, as explained in Section 9.

Renormalized probability distribution A conditional wavelet renormalization factorizes the distribution $p(x)$ of signals x into conditional probabilities over wavelet coefficients:

$$p(x) = \alpha \prod_{j=1}^J \bar{p}_j(\bar{x}_j | x_j) p_J(x_J). \quad (12)$$

where α (the Jacobian) depends upon all γ_j .

Although $p(x)$ is typically highly non-Gaussian, the factorization (12) involves distributions that are closer to Gaussians. The largest scale distribution p_J is usually close to a Gaussian when the image has independent structures, because x_J is an averaging of x over large domains of size 2^J . Remarkably, for large classes of signals and images, each conditional probabilities $\bar{p}_j(\bar{x}_j|x_j)$ also exhibit Gaussian properties. In images, the wavelet coefficients \bar{x}_j are usually sparse and thus have highly non-Gaussian distribution; however, it has been observed (Wainwright and Simoncelli, 1999) that their conditional distributions $\bar{p}_j(\bar{x}_j|x_j)$ become much more Gaussian, due to dependencies of wavelet coefficients across scales. Similarly, in statistical physics, factorization of probabilities of high frequencies conditioned by lower frequencies have been introduced in Wilson (1983). More recently, normalized wavelet factorizations (12) have been introduced in physics to implement renormalization group calculations, and model probability distributions with maximum likelihood estimators near phase transitions (Marchand et al., 2022).

Wavelet Score-based Generative Model Instead of computing a Score-based Generative Model (SGM) of the distribution $p(x)$, a Wavelet Score-based Generative Model (WSGM) applies an SGM at the coarsest scale $p_J(x_J)$ and then on each conditional distribution $\bar{p}_j(\bar{x}_j|x_j)$ for $j \leq J$. It is thus a cascaded SGM, similarly to Ho et al. (2022); Saharia et al. (2021), but calculated on $\bar{p}_j(\bar{x}_j|x_j)$ instead of $p_j(x_{j-1}|x_j)$. The normalization of wavelet coefficients \bar{x}_j effectively produces a whitening which can considerably accelerate the algorithm by reducing the number of time steps. This is not possible on x_{j-1} because its covariance is ill-conditioned. It will be proved for Gaussian processes.

A forward noising process is computed on each \bar{x}_j for $j \leq J$ and x_J :

$$d\bar{x}_{j,t} = -\bar{x}_{j,t} dt + \sqrt{2}d\bar{w}_{j,t} \quad \text{and} \quad dx_{J,t} = -x_{J,t} dt + \sqrt{2}dw_{J,t},$$

where the $\bar{w}_{j,t}, w_{J,t}$ are Brownian motions. Since \bar{x}_j is nearly white and has Gaussian properties, this diffusion converges much more quickly than if applied directly on x . Using (4), we compute a score function $s_{J,t}(x_{J,t})$ which approximates the score $\nabla \log p_{J,t}(x_{J,t})$. For each $j \leq J$ we also compute the conditional score $\bar{s}_{j,t}(\bar{x}_{j,t}|x_j)$ which approximates $\nabla \log \bar{p}_{j,t}(\bar{x}_{j,t}|x_j)$.

The inverse generative process is computed from coarse to fine scales as follows. At the largest scale 2^J , we sample the low-dimensional x_J by time discretizing the inverse SDE. Similarly to (5), the generative process is given by:

$$x_{J,t_{k+1}} = x_{J,t_k} + \delta_k \{x_{J,t_k} + 2s_{J,t_k}(x_{J,t_k})\} + \sqrt{2\delta_k} z_{J,k}, \quad z_{J,k} \stackrel{\text{i.i.d.}}{\sim} \mathcal{N}(0, \text{Id}).$$

For j going from J to 1, we then generate the wavelet coefficients \bar{x}_j conditionally to the previously calculated x_j , by keeping the same time discretization schedule at all scales:

$$\bar{x}_{j,t_{k+1}} = \bar{x}_{j,t_k} + \delta_k \{\bar{x}_{j,t_k} + 2\bar{s}_{j,t_k}(\bar{x}_{j,t_k}|x_j)\} + \sqrt{2\delta_k} z_{j,k}, \quad z_{j,k} \stackrel{\text{i.i.d.}}{\sim} \mathcal{N}(0, \text{Id}).$$

The inverse wavelet transform then approximately computes a sample of x_{j-1} from $(\bar{x}_{j,0}, x_j)$:

$$\tilde{x}_{j-1} = \gamma_j G^\top x_j + \gamma_j \bar{G}^\top \bar{x}_{j,0}. \quad (13)$$

The generative process is illustrated in Figure 1 and its pseudocode is given in Section 7, see Algorithm 1. The appendix also verifies that if x is of size d then its numerical complexity is $O(Nd)$ where N is the number of time steps, which is the same at each scale. For multiscale processes, we shall see that the number of time steps N does not depend upon d to reach a fixed error measured with a KL divergence.

Related work The use of wavelets in multiscale architectures is often motivated by the spectral bias phenomenon Rahaman et al. (2019): Huang et al. (2017) uses a wavelet CNN for super-resolution, Gal et al. (2021) incorporates spectral information by training GANs in the wavelet domain. Closer in spirit to our work, Yu et al. (2020) introduces Wavelet Flow, a normalizing flow with a cascade of layers generating wavelet coefficients conditionally on lower-scales, then aggregating them with an inverse wavelet transform. This method yields training time acceleration and high-resolution (1024x1024) generation.

WSGM is closely related to other cascading diffusion algorithms, such as the ones introduced in Ho et al. (2022); Saharia et al. (2021); Dhariwal and Nichol (2021). The main difference lies in that earlier works on cascaded SGMs do not model the *wavelet coefficients* $\{\bar{x}_j\}_{j=1}^J$ but the *low-frequency coefficients* $\{x_j\}_{j=1}^J$. As a result, cascaded models do not exploit the whitening properties of the

wavelet transform. We also point out the recent work of [Jing et al. \(2022\)](#) which, while not using the cascading framework, drop subspaces from the noising process at different times. This allows using only one SDE to sample approximately from the data distribution. However, the reconstruction is still computed with respect to $\{x_j\}_{j=1}^J$ instead of the wavelet coefficients.

Finally, we highlight that our work could be combined with other acceleration techniques such as the ones of [Jolicœur-Martineau et al. \(2021\)](#); [Liu et al. \(2022\)](#); [Zhang and Chen \(2022\)](#); [San-Roman et al. \(2021\)](#); [Nachmani et al. \(2021\)](#); [Song et al. \(2020\)](#); [Ho et al. \(2020\)](#); [Kong and Ping \(2021\)](#); [Luhman and Luhman \(2021\)](#); [Salimans and Ho \(2022\)](#); [Xiao et al. \(2021\)](#) in order to improve the empirical results of WSGM.

3.2 Discretization and Accuracy for Gaussian Processes

We now illustrate Theorem 1 and the effectiveness of WSGM on Gaussian multiscale processes. We use the whitening properties of the wavelet transform to show that the time complexity required in order to reach a given error is linear in the image dimension.

The following result proves that the normalization of wavelet coefficients performs a preconditioning of the covariance, whose eigenvalues then remain of the order of 1. This is a consequence of a theorem proved by [Meyer \(1992\)](#) on the representation of classes of singular operators in wavelet bases, see Section 9. As a result, the number of iterations T/δ required to reach an error ε is independent of the dimension.

Theorem 3. *Let x be a Gaussian stationary process of power spectrum $P(\omega) = c(\xi^\eta + |\omega|^\eta)^{-1}$ with $\eta > 0$ and $\xi > 0$. If the wavelet has a compact support, $q \geq \eta$ vanishing moments and is \mathcal{C}^q , then $\text{KL}(p\|\tilde{p}_0) = E_T + E_\delta + E_{\delta,T}$ with $E_{\delta,T}$ a higher order term such that $E_{T,\delta} = o(\delta + e^{-4T})$ when $\delta \rightarrow 0$ and $T \rightarrow +\infty$. Furthermore, for any $\varepsilon > 0$, there exists $C > 0$ such that for any δ, T :*

$$(1/d)(E_T + E_\delta) \leq \varepsilon \text{ and } T/\delta \leq C\varepsilon^{-2}. \quad (14)$$

To prove this result, we show that the conditioning number of the covariance matrix of the renormalized wavelet coefficients does not depend on the dimension using ([Meyer, 1992](#)). We conclude upon combining this result, the cascading property of the Kullback-Leibler divergence and an extension of Theorem 1 to the setting with non-zero mean. The detailed proof is postponed to Section 11.

Numerical results We illustrate Theorem 3 on a Gaussian field x , with power spectrum P as (10). In Figure 2, we display the sup-norm between P and the power spectrum \hat{P} of the samples obtained using either vanilla SGM or WSGM with uniform stepsize $\delta_k = \delta$. In the case of vanilla SGM, the number $N(\varepsilon)$ of time steps needed to reach a small error $\|P - \hat{P}\| = \varepsilon$ increases with the size of the image L Figure 2, right). Equation (6) suggests that $N(\varepsilon)$ scales like a power of the conditioning number κ of Σ , which, for multiscale gaussian processes, is $\kappa \sim L^\eta$. In the WSGM case, we sample conditional distributions \tilde{p}_j of wavelets \tilde{x}_j given low-frequencies x_j . At scale j , the conditioning numbers $\tilde{\kappa}_j$ of the conditional covariance become dimension-independent (Section 9), removing the dependency of $N(\varepsilon)$ on the image size L as suggested by (14).

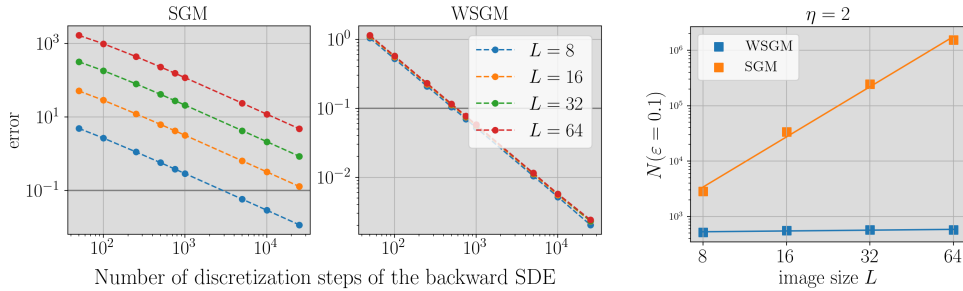


Figure 2: **Left and middle:** evolution of the error on the estimated covariance matrix using either SGM or WSGM w.r.t. the number of stepsizes used in the model ($T = 10$ is fixed). **Right:** number $N(\varepsilon)$ of discretization steps required to reach a given error $\varepsilon = 0.1$ using either SGM or WSGM.

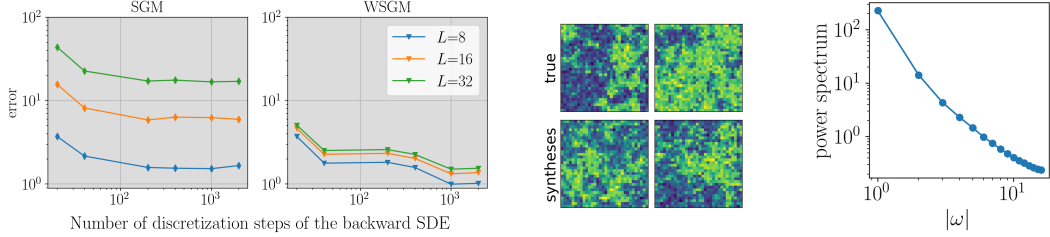


Figure 3: **Left:** error between ground-truth φ^4 datasets in various dimensions L , and the synthesized datasets with SGM and WSGM, for various number of discretization steps. **Middle:** realizations of φ^4 (top) and WSGM samples (bottom). **Right:** power spectrum of φ^4 for $L = 32$.

4 Acceleration with WSGM: Numerical Results

For multiscale Gaussian processes, we proved that with WSGMs, the number of time steps $N(\varepsilon)$ to reach a fixed error ε does not depend on the signal size, as opposed to SGMs. This section shows that this result applies to non-Gaussian multiscale processes. We consider a physical process near a phase transition and images from the CelebA-HQ database (Karras et al., 2018).

4.1 Physical Processes with Scalar Potentials

Gaussian stationary processes are maximum entropy processes conditioned by second order moments defined by a circulant matrix. More complex physical processes are modeled by imposing a constraint on their marginal distribution, with a so-called scalar potential. The marginal distribution of x is the probability distribution of $x(u)$, which does not depend upon u if x is stationary. Maximum entropy processes conditioned by second order moments and marginal distributions have a probability density which is a Gibbs distribution $p(x) = Z^{-1} e^{-E(x)}$ with:

$$E(x) = \frac{1}{2} x^\top C x + \sum_u V(x(u)) , \quad (15)$$

where C is a circulant matrix and $V: \mathbb{R} \rightarrow \mathbb{R}$ is a scalar potential. Section 13 explains how to parametrize V as a linear combination of a family of fixed elementary functions. The φ^4 model is a particular example where $C = \Delta$ is a Laplacian and V is a fourth order polynomial, adjusted in order to impose that $x(u) = \pm 1$ with high probability. For so-called critical values of these parameters, the resulting process becomes multiscale with long range interactions and a power law spectrum, see Figure 3-(c).

We train SGMs and WSGMs on critical φ^4 processes of different sizes; for the score model s_θ , we use a simple linear parametrization detailed in Section 13.2. To evaluate the quality of the generated samples, it is sufficient to verify that these samples have the same second order moment and marginals as φ^4 . We define the error metric as the sum of the L^2 error on the power spectrum and the total-variation distance between marginal distributions. Figure 3-(a) shows the decay of this error as a function of the number of time steps used in an SGM and WSGM with a uniform discretization. With vanilla SGM, the loss has a strong dependency in L , but becomes almost independent of L for WSGM. This empirically verifies the claim that an ill-conditioned covariance matrix leads to slow sampling of SGM, and that WSGM is unaffected by this issue by working with the conditional distributions of normalized wavelet coefficients.

4.2 Scale-Wise Time Reduction in Natural Images

Images are highly non-Gaussian multiscale processes whose power spectrum has a power law decay. We now show that WSGM also provides an acceleration over SGM in this case, by being independent of the image size.

We focus on the CelebA-HQ dataset (Liu et al., 2015) at a 128×128 resolution. Though non-stationary, its power spectrum still has a power law decay, as shown in Figure 4. We compare SGM Ho et al. (2020) samples at the 128×128 resolution with WSGM samples which start from the 32×32 resolution. Though smaller, the 32×32 resolution still suffers from a power law decay of its spectrum over several orders of magnitude. The reason why we limit this coarsest resolution is

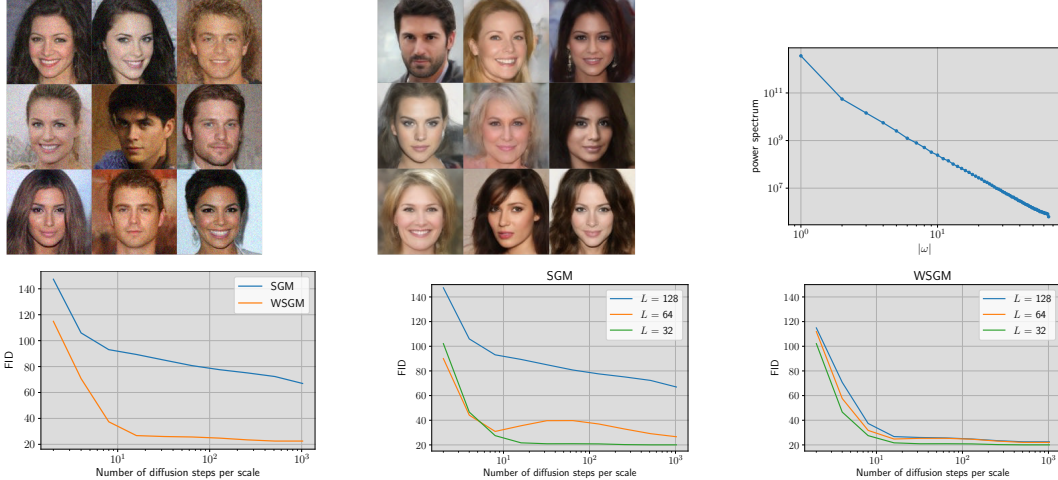


Figure 4: **Top.** (a): Generations from SGM with 16 discretization steps. (b): Generations from WSGM with 16 discretization steps at each scale. (c): Power spectrum of CelebA-HQ. **Bottom.** (a): Evolution of the FID w.r.t. the number of diffusion steps for SGM and WSGM with $L = 128$. (b): Evolution of the FID w.r.t. the number of diffusion steps for SGM at several image sizes L . (c) Evolution of the FID w.r.t. the number of diffusion steps for WSGM at several image sizes L .

because border effects become dominant at lower image sizes. To simplify the handling of border conditions, we use Haar wavelets.

Following [Nichol and Dhariwal \(2021\)](#), the global scores $s_\theta(x)$ are parametrized by a neural network with a UNet architecture. It has 3 residual blocks at each scale, and includes multi-head attention layers at lower scales. The conditional scores $s_\theta(\bar{x}_j|x_j)$ are parametrized in the same way, and the conditioning on the low frequencies x_j is done with a simple input concatenation along channels ([Nichol and Dhariwal, 2021](#); [Saharia et al., 2021](#)). The details of the architecture are in Section 14. We use a uniform discretization of the backward SDE to stay in the setting of Theorem 2.

The generation results are given in Figure 4. With the same computational budget of 16 discretizations steps at the largest scale (iterations at smaller scales having a negligible cost due to the exponential decrease in image size), WSGM achieves a much better perceptual generation quality. Notably, SGM generates noisy images due to discretization errors. This is confirmed quantitatively with the Fréchet Inception Distance (FID) ([Heusel et al., 2017](#)). The FID of the WSGM generations decreases with the number of steps, until it plateaus. This plateau is reached with at least 2 orders of magnitude less steps for WSGM than SGM. This number of steps is also independent of the image size for WSGM, thus confirming the intuition given in the Gaussian case by Theorem 1-3. Our results confirm that vanilla SGM on a wide range of multiscale processes, including natural images, suffers from ill-conditioning, in the sense that the number of discretization steps grows with the image size. WSGM, on the contrary, leads to uniform discretization schemes whose number of steps at each scale does not depend on the image size.

We also stress that there exists many techniques ([Kadkhodaie and Simoncelli, 2020](#); [Jolicœur-Martineau et al., 2021](#); [Liu et al., 2022](#); [Zhang and Chen, 2022](#); [San-Roman et al., 2021](#); [Nachmani et al., 2021](#); [Song et al., 2020](#); [Kong and Ping, 2021](#); [Ho et al., 2020](#); [Luhman and Luhman, 2021](#); [Salimans and Ho, 2022](#); [Xiao et al., 2021](#)) to accelerate the sampling of vanilla SGMs, with sometimes better FID-time complexity tradeoff curves. Notably, the FID plateaus at a relatively high value of 20 because the coarsest resolution 32×32 is still ill-conditioned and requires thousands of steps with a non-uniform discretization schedule to achieve FIDs less than 10 with vanilla SGM [Nichol and Dhariwal \(2021\)](#). Such improvements (including proper handling of border conditions) are beyond of the scope of this paper. The contribution of WSGM is rather to show the reason behind this sampling inefficiency and mathematically prove in the Gaussian setting that wavelet decompositions of the probability distribution allow solving this problem. We believe that extending this theoretical result to a wider class of non-Gaussian multiscale processes and combining WSGM with other sampling accelerations are interesting avenues for future work.

5 Discussion

This paper introduces a Wavelet Score-based Generative Model (WSGM) which applies an SGM to normalized wavelet coefficients conditioned by lower frequencies. We prove that the number of stepsizes in SGMs is controlled by the regularity of the score of the target distribution. For multiscale processes such as images, it requires a considerable number of time steps to achieve a good accuracy, which increases quickly with the image size. We show that a WSGM eliminates ill-conditioning issues by normalizing wavelet coefficients. As a result, the number of stepsizes in WSGM does not increase with the image dimension. We illustrated our results on Gaussian distributions, physical processes and image datasets.

One of the main limitations of WSGM is that it is limited to multiscale processes for which the conditional wavelet probabilities are close to white Gaussian distributions. A promising direction for future work is to combine WSGM with other acceleration techniques such as adaptive time discretizations to handle such cases. In another direction, one could strengthen the theoretical study of SGM and extend our results beyond the Gaussian setting, in order to fully describe SGM on physical processes which can be seen as perturbations of Gaussian distributions.

Acknowledgments

This work was supported by a grant from the PRAIRIE 3IA Institute of the French ANR-19-P3IA-0001 program. We would like to thank the Scientific Computing Core at the Flatiron Institute for the use of their computing resources.

References

- Bakry, D., Gentil, I., and Ledoux, M. (2014). *Analysis and Geometry of Markov Diffusion Operators*, volume 348. Springer.
- Cattiaux, P., Conforti, G., Gentil, I., and Léonard, C. (2021). Time reversal of diffusion processes under a finite entropy condition. *arXiv preprint arXiv:2104.07708*.
- De Bortoli, V., Thornton, J., Heng, J., and Doucet, A. (2021). Diffusion schrödinger bridge with applications to score-based generative modeling. *Advances in Neural Information Processing Systems*, 34.
- Dhariwal, P. and Nichol, A. (2021). Diffusion models beat GAN on image synthesis. *arXiv preprint arXiv:2105.05233*.
- Gal, R., Hochberg, D. C., Bermano, A., and Cohen-Or, D. (2021). Swagan: A style-based wavelet-driven generative model. *ACM Transactions on Graphics (TOG)*, 40(4):1–11.
- Gross, L. (1975). Logarithmic sobolev inequalities. *American Journal of Mathematics*, 97(4):1061–1083.
- Hausmann, U. G. and Pardoux, E. (1986). Time reversal of diffusions. *The Annals of Probability*, 14(4):1188–1205.
- Heusel, M., Ramsauer, H., Unterthiner, T., Nessler, B., Klambauer, G., and Hochreiter, S. (2017). Gans trained by a two time-scale update rule converge to a nash equilibrium. *CoRR*, abs/1706.08500.
- Ho, J., Jain, A., and Abbeel, P. (2020). Denoising diffusion probabilistic models. *Advances in Neural Information Processing Systems*.
- Ho, J., Saharia, C., Chan, W., Fleet, D. J., Norouzi, M., and Salimans, T. (2022). Cascaded diffusion models for high fidelity image generation. *Journal of Machine Learning Research*, 23(47):1–33.
- Huang, H., He, R., Sun, Z., and Tan, T. (2017). Wavelet-srnet: A wavelet-based cnn for multi-scale face super resolution. In *Proceedings of the IEEE International Conference on Computer Vision*, pages 1689–1697.
- Hyvärinen, A. and Dayan, P. (2005). Estimation of non-normalized statistical models by score matching. *Journal of Machine Learning Research*, 6(4).

- Ikeda, N. and Watanabe, S. (1989). *Stochastic Differential Equations and Diffusion Processes*, volume 24 of *North-Holland Mathematical Library*. North-Holland Publishing Co., Amsterdam; Kodansha, Ltd., Tokyo, second edition.
- Jing, B., Corso, G., Berlinghieri, R., and Jaakkola, T. (2022). Subspace diffusion generative models.
- Jolicœur-Martineau, A., Li, K., Piché-Taillefer, R., Kachman, T., and Mitliagkas, I. (2021). Gotta go fast when generating data with score-based models. *arXiv preprint arXiv:2105.14080*.
- Kadkhodaie, Z. and Simoncelli, E. P. (2020). Solving linear inverse problems using the prior implicit in a denoiser. *arXiv preprint arXiv:2007.13640*.
- Karras, T., Aila, T., Laine, S., and Lehtinen, J. (2018). Progressive growing of gans for improved quality, stability, and variation. arxiv 2017. *arXiv preprint arXiv:1710.10196*, pages 1–26.
- Kaupuvzs, J., Melnik, R., and Rimvsāns, J. (2016). Corrections to finite-size scaling in the φ^4 model on square lattices. *International Journal of Modern Physics C*, 27(09):1650108.
- Kolmogorov, A. N. (1962). A refinement of previous hypotheses concerning the local structure of turbulence in a viscous incompressible fluid at high reynolds number. *Journal of Fluid Mechanics*, 13(1):82–85.
- Kong, Z. and Ping, W. (2021). On fast sampling of diffusion probabilistic models. *arXiv preprint arXiv:2106.00132*.
- Léonard, C. (2014). Some properties of path measures. In *Séminaire de Probabilités XLVI*, pages 207–230. Springer.
- Liu, L., Ren, Y., Lin, Z., and Zhao, Z. (2022). Pseudo numerical methods for diffusion models on manifolds.
- Liu, Z., Luo, P., Wang, X., and Tang, X. (2015). Deep learning face attributes in the wild. In *International Conference on Computer Vision*.
- Luhman, E. and Luhman, T. (2021). Knowledge distillation in iterative generative models for improved sampling speed. *arXiv preprint arXiv:2101.02388*.
- Mallat, S. (1999). *A wavelet tour of signal processing*. Elsevier.
- Mallat, S. (July 1989). A theory for multiresolution signal decomposition: the wavelet representation. 11(7):674–693.
- Mandelbrot, B. (1983). *The fractal geometry of nature*/revised and enlarged edition. *New York*.
- Marchand, T., Ozawa, M., Biroli, G., and Mallat, S. (2022). Wavelet conditional renormalization group. *arXiv preprint arXiv:2207.04941*.
- Meyer, Y. (1992). *Wavelets and Operators*. Advanced mathematics. Cambridge university press.
- Meyn, S. P. and Tweedie, R. L. (1993). Stability of Markovian processes. III. Foster-Lyapunov criteria for continuous-time processes. *Advances in Applied Probability*, 25(3):518–548.
- Milchev, A., Heermann, D., and Binder, K. (1986). Finite-size scaling analysis of the φ^4 field theory on the square lattice. *Journal of statistical physics*, 44(5):749–784.
- Nachmani, E., Roman, R. S., and Wolf, L. (2021). Non gaussian denoising diffusion models. *arXiv preprint arXiv:2106.07582*.
- Nichol, A. and Dhariwal, P. (2021). Improved denoising diffusion probabilistic models. *arXiv preprint arXiv:2102.09672*.
- Rahaman, N., Baratin, A., Arpit, D., Draxler, F., Lin, M., Hamprecht, F., Bengio, Y., and Courville, A. (2019). On the spectral bias of neural networks. In *International Conference on Machine Learning*, pages 5301–5310. PMLR.

- Saharia, C., Ho, J., Chan, W., Salimans, T., Fleet, D. J., and Norouzi, M. (2021). Image super-resolution via iterative refinement. *arXiv preprint arXiv:2104.07636*.
- Salimans, T. and Ho, J. (2022). Progressive distillation for fast sampling of diffusion models. *arXiv preprint arXiv:2202.00512*.
- San-Roman, R., Nachmani, E., and Wolf, L. (2021). Noise estimation for generative diffusion models. *arXiv preprint arXiv:2104.02600*.
- Song, J., Meng, C., and Ermon, S. (2020). Denoising diffusion implicit models. *arXiv preprint arXiv:2010.02502*.
- Song, Y. and Ermon, S. (2019). Generative modeling by estimating gradients of the data distribution. In *Advances in Neural Information Processing Systems*.
- Song, Y. and Ermon, S. (2020). Improved techniques for training score-based generative models. In *Advances in Neural Information Processing Systems*.
- Song, Y., Sohl-Dickstein, J., Kingma, D. P., Kumar, A., Ermon, S., and Poole, B. (2021). Score-based generative modeling through stochastic differential equations. In *International Conference on Learning Representations*.
- Vincent, P. (2011). A connection between score matching and denoising autoencoders. *Neural Computation*, 23(7):1661–1674.
- Wainwright, M. J. and Simoncelli, E. (1999). Scale mixtures of gaussians and the statistics of natural images. *Advances in neural information processing systems*, 12.
- Wilson, K. G. (1971). Renormalization group and critical phenomena. ii. phase-space cell analysis of critical behavior. *Physical Review B*, 4(9):3184.
- Wilson, K. G. (1983). The renormalization group and critical phenomena. *Reviews of Modern Physics*, 55(3):583.
- Xiao, Z., Kreis, K., and Vahdat, A. (2021). Tackling the generative learning trilemma with denoising diffusion gans. *arXiv preprint arXiv:2112.07804*.
- Yu, J. J., Derpanis, K. G., and Brubaker, M. A. (2020). Wavelet flow: Fast training of high resolution normalizing flows. *Advances in Neural Information Processing Systems*, 33:6184–6196.
- Zhang, Q. and Chen, Y. (2022). Fast sampling of diffusion models with exponential integrator.

6 Organization of the Supplemental Material

We provide the pseudocode for the WSGM algorithm in Section 7. Details about wavelet transforms and their whitening properties are presented in Sections 8 and 9. The proofs of Section 2 and Section 3 are gathered Section 10 and Section 11 respectively. Details about the Gaussian model and the φ^4 model are given in Section 12 and Section 13 respectively. Finally, experimental details and additional experiments are described in Section 14.

7 WSGM Algorithm

In Algorithm 1, we provide the pseudo code for WSGM. Notice that the training of score models at each scale can be done in parallel, while the sampling is done sequentially one scale after the next. The sequential nature of sampling is the price to pay for the conditional decomposition, as we model only the conditional scores $\nabla_{\bar{x}_j} \log \bar{p}_j(\bar{x}_j|x_j)$. Generating all scales simultaneously would require learning the so-called free energy gradient $\nabla_{x_j} \log \bar{p}_j(\bar{x}_j|x_j)$. It is also required for likelihood computation. However, the conditional decomposition of WSGM allows not learning this free energy gradient and possibly reduces score estimation errors.

Algorithm 1 Wavelet Score-based Generative Model

```
Require:  $J, N_{\text{iter}}, N, T, \{\bar{\theta}_{j,0}, \theta_{j,0}\}_{j=0}^J, \{x_0^m\}_{m=1}^M$ 
1: /// WAVELET TRANSFORM ///
2: for  $j \in \{1, \dots, J\}$  do
3:   for  $m \in \{1, \dots, M\}$  do
4:      $x_j^m = \gamma_j^{-1} G x_{j-1}^m, \bar{x}_j^m = \gamma_j^{-1} \bar{G} x_{j-1}^m$  ▷ Wavelet transform of the dataset
5:   end for
6: end for
7: /// TRAINING ///
8: Train score network  $s_{\theta_j^*}$  at scale  $J$  with dataset  $\{x_j^m\}_{m=0}^M$  ▷ Unconditional SGM training
9: for  $j \in \{J, \dots, 1\}$  do ▷ Can be run in parallel
10:  for  $n \in \{0, \dots, N_{\text{iter}} - 1\}$  do
11:    Sample  $(\bar{x}_{j,0}, x_j)$  from  $\{\bar{x}_j^m, x_j^m\}_{m=1}^M$ 
12:    Sample  $t$  in  $[0, T]$  and  $\bar{Z} \sim N(0, \text{Id})$ 
13:     $\bar{x}_{j,t} = e^{-t} \bar{x}_{j,0} + (1 - e^{-2t})^{1/2} \bar{Z}$ 
14:     $\ell(\bar{\theta}_{j,n}) = \|(e^{-t} \bar{x}_{j,0} - \bar{x}_{j,t}) - (1 - e^{-2t})^{1/2} \bar{s}_{\bar{\theta}_{j,n}}(t, \bar{x}_{j,t} | x_j)\|^2$ 
15:     $\bar{\theta}_{j,n+1} = \text{optimizer\_update}(\bar{\theta}_{j,n}, \ell(\bar{\theta}_{j,n}))$  ▷ ADAM optimizer step
16:  end for
17:   $\bar{\theta}_j^* = \bar{\theta}_{j, N_{\text{iter}}}$ 
18: end for
19: /// SAMPLING ///
20:  $x_J = \text{unconditionalSGM}(T, N, s_{\theta_J^*})$  ▷ Unconditional SGM sampling
21: for  $j \in \{J, \dots, 1\}$  do
22:   $\bar{x}_j = \text{EulerMaruyama}(T, N, \bar{s}_{\bar{\theta}_j^*}(\cdot, \cdot | x_j))$  ▷ Euler-Maruyama recursion following (5)
23:   $x_{j-1} = \gamma_j G^T x_j + \gamma_j \bar{G}^T \bar{x}_j$  ▷ Wavelet reconstruction
24: end for
25: return  $\{\bar{\theta}_j^*, \theta_j^*\}_{j=1}^J, x_0$ 
```

8 Introduction to Orthogonal Wavelet Bases

This section introduces properties of orthogonal wavelet bases as specified by the operators G and \bar{G} . In this section, we drop the normalizing factors γ_j for clarity.

Let x_0 be a signal. The index u in $x_0(u)$ belongs to an n -dimensional grid of linear size L and hence with L^n sites, with $n = 2$ for images.

Let us denote x_j the coarse-grained version of x_0 at a scale 2^j defined over a coarser grid with intervals 2^j and hence $(2^{-j}L)^n$ sites. The coarser signal x_j is iteratively computed from x_{j-1} by applying a coarse-graining operator, which acts as a scaling filter G which eliminates high frequencies and subsamples the grid [Mallat \(1989\)](#):

$$(Gx_{j-1})(u) = \sum_{u'} x_{j-1}(u') G(2u - u'). \quad (16)$$

The index u on the left-hand side runs on the coarser grid, whereas u' runs on the finer one.

The degrees of freedom of x_{j-1} that are not in x_j are encoded in orthogonal wavelet coefficients \bar{x}_j . The representation (x_j, \bar{x}_j) is an orthogonal change of basis calculated from x_{j-1} . The coarse signal x_j is calculated in (16) with a low-pass scaling filter G and a subsampling. In dimension n , the wavelet coefficients \bar{x}_j have $2^n - 1$ channels computed with a convolution and subsampling operator \bar{G} . We thus have:

$$x_j = G x_{j-1} \text{ and } \bar{x}_j = \bar{G} x_{j-1}. \quad (17)$$

The wavelet filter \bar{G} computes $2^n - 1$ wavelet coefficients $\bar{x}_j(u, k)$ indexed by $1 \leq k \leq 2^n - 1$, with separable high-pass filters $\bar{G}_k(u)$:

$$\bar{x}_j(u, k) = \sum_{u'} x_{j-1}(u') \bar{G}_k(2u - u').$$

As an example, the Haar wavelet leads to a block averaging filter G :

$$x_j(u) = \frac{x_{j-1}(2u) + x_{j-1}(2u + 1)}{\sqrt{2}}.$$

In $n = 1$ dimension, there is a single wavelet channel in \bar{x}_j . The corresponding wavelet filter \bar{G} computes the wavelet coefficients with normalized increments:

$$\bar{x}_j(u) = \frac{x_{j-1}(2u) - x_{j-1}(2u+1)}{\sqrt{2}}.$$

If $n = 2$, then there are 3 channels as illustrated in Figure 1.

The fast wavelet transform cascades (17) for $1 \leq j \leq J$ to compute the decomposition of the high-resolution signal x_0 into its orthogonal wavelet representation over J scales:

$$\{x_J, \bar{x}_j\}_{1 \leq j \leq J}. \quad (18)$$

The wavelet orthonormal filters G and \bar{G} define a unitary transformation, which satisfies:

$$\bar{G}G^\top = G\bar{G}^\top = 0 \text{ and } G^\top G + \bar{G}^\top \bar{G} = \text{Id},$$

where Id is the identity. Mallat (1989) gives a condition on the Fourier transforms of G and \bar{G} to build such filters. The filtering equations (17) can then be inverted with the adjoint operators:

$$x_{j-1} = G^\top x_j + \bar{G}^\top \bar{x}_j. \quad (19)$$

The adjoint G^\top enlarge the grid size of x_j by inserting a zero between each coefficients, and then filters the output:

$$(G^\top x_j)(u) = \sum_{u'} x_j(u') G(2u' - u).$$

The adjoint of \bar{G} performs the same operations over the $2^n - 1$ channels and adds them:

$$(\bar{G}^\top \bar{x}_j)(u) = \sum_{k=1}^{2^n-1} \sum_{u'} \bar{x}_j(u', k) \bar{G}_k(2u' - u).$$

The fast inverse wavelet transform Mallat (1989) recovers x_0 from its wavelet representation (18) by progressively recovering x_{j-1} from x_j and \bar{x}_j with (19), for j going from J to 1.

9 Orthogonal Wavelet Transform

This appendix relates the fast discrete wavelet transform to decomposition of finite energy functions in orthonormal bases of $\mathbf{L}^2([0, 1]^n)$. We shall then prove that the covariance of normalized wavelet coefficients is a well-conditioned matrix, independently from scales. This is a central result to prove Theorem 3. The results of this appendix are based on the multiresolution theory Mallat (1999) and the representation of singular operators in wavelet orthonormal bases Meyer (1992).

Orthonormal wavelet transform From an input discrete signal $x_0(u) = x(u)$ defined over an n -dimensional grid of width L , we introduced in (11) a normalized wavelet transform which computes wavelet coefficients $\bar{x}_j(u, k)$ having $2^n - 1$ channels $1 \leq k < 2^n$. A non-normalized orthonormal wavelet transform is obtained by setting $\gamma_j = 1$:

$$x_j^w = G x_{j-1}^w \text{ and } \bar{x}_j^w = \bar{G} x_{j-1}^w, \quad (20)$$

with $x_0^w = x_0$ and where G is a low-pass filtering and subsampling by 2:

$$G x_{j-1}^w(u) = \sum_{u'} x_{j-1}^w(u') G(2u - u').$$

The wavelet convolutional and subsampling operator \bar{G} computes $2^n - 1$ wavelet signals $\bar{x}_j^w(u, k)$, with $2^n - 1$ high-pass filters $\bar{G}_k(u)$ indexed by $1 \leq k \leq 2^n - 1$:

$$\bar{x}_{j-1}^w(u, k) = \sum_{u'} x_{j-1}^w(u') \bar{G}_k(2u - u').$$

We write $\bar{x}^w = (\bar{x}_j^w, x_j^w)_{j \leq J}$ the vector of non-normalized wavelet coefficients.

The multiresolution wavelet theory Mallat (1999); Meyer (1992) proves that the coefficients of \bar{x}^w can also be written as the decomposition coefficients of a finite energy function, in a wavelet orthonormal basis of the space $\mathbf{L}^2(\mathbb{R}^n)$ of finite energy functions. These wavelets arise from the cascade of the

convolutional filters G and \bar{G} in (20) when we iterate on j Mallat (1999). This wavelet orthonormal basis is thus entirely specified by the choice of the filters G and \bar{G} . A wavelet orthonormal basis is defined by a *scaling function* $\psi^0(v)$ for $v \in \mathbb{R}^n$ which has a unit integral $\int \psi^0(v) dv = 1$, and $2^n - 1$ *wavelets* which have a zero integral $\int \psi^k(v) dv = 0$ for $1 \leq k < 2^n$. Each of these functions are dilated and translated by $u \in \mathbb{Z}^n$, for $1 \leq k < 2^n$ and $j \in \mathbb{Z}$:

$$\psi_{j,u}^k(v) = 2^{-nj/2} \psi^k(2^{-j}v - u).$$

The main result proved in Mallat (1999); Meyer (1992), is that for appropriate filters G and \bar{G} such that (G, \bar{G}) is unitary, the family of translated and dilated wavelets up to the scale 2^J :

$$\{\psi_{j,u}^0, \psi_{j,u}^k\}_{1 \leq k < 2^n, j \leq J, u \in \mathbb{Z}^n}$$

is an orthonormal basis of $\mathbf{L}^2(\mathbb{R}^n)$. A periodic wavelet basis of $\mathbf{L}^2([0, 1]^n)$ is defined by replacing each wavelet $\psi_{j,u}^k$ by the periodic function $\sum_{r \in \mathbb{Z}^n} \psi_{j,u}^k(v - r)$ which we shall still write $\psi_{j,u}^k$.

The properties of the wavelets $\psi_{j,u}^k$ depend upon the choice of the filters G and \bar{G} . If these filters have a compact support then one can verify Mallat (1999) that all wavelets $\psi_{j,u}^k$ have a compact support of size proportional to 2^j . With an appropriate choice of filters, one can also define wavelets having q vanishing moments, which means that they are orthogonal to any polynomial $Q(v)$ of degree strictly smaller than q :

$$\int_{[0,1]^n} Q(v) \psi_{j,u}^k(v) dv = 0.$$

One can also ensure that wavelet are q times continuously differentiable. Daubechies wavelets Mallat (1999) are examples of orthonormal wavelets which can have q vanishing moments and be \mathbf{C}^q for any q .

The relation between the fast wavelet transform and these wavelet orthonormal bases proves Mallat (1999) that any discrete signal $x_0(u)$ of width L can be written as a discrete approximation at a scale $2^\ell = L^{-1}$ ($\ell < 0$) of a (non-unique) function $f \in \mathbf{L}^2([0, 1]^n)$. The support of f is normalized whereas the approximation scale 2^ℓ decreases as the number of samples L increases. The coefficients $x_0(u)$ are inner products of f with the orthogonal family of scaling functions at the scale 2^ℓ for all $u \in \mathbb{Z}^n$ and $2^\ell u \in [0, 1]^n$:

$$x_0(u) = \int_{[0,1]^n} f(v) \psi_{\ell,u}^0(v) dv = \langle f, \psi_{\ell,u}^0 \rangle.$$

Let V_ℓ be the space generated by the orthonormal family of scaling functions $\{\psi_{\ell,u}^0\}_{2^\ell u \in [0,1]^n}$, and $P_{V_\ell} f$ be the orthogonal projection of f in V_ℓ . The signal x_0 gives the orthogonal decomposition coefficients of $P_{V_\ell} f$ in this family of scaling functions. One can prove Mallat (1999) that the non-normalized wavelet coefficients \bar{x}_j^w of x_0 computed with a fast wavelet transform are equal to the orthogonal wavelet coefficients of f at the scale $2^{j+\ell}$, for all $u \in \mathbb{Z}^n$ and $2^{j+\ell} u \in [0, 1]^n$:

$$\bar{x}_j^w(u, k) = \int_{[0,1]^n} f(v) \psi_{j+\ell,u}^k(v) dv = \langle f, \psi_{j+\ell,u}^k \rangle.$$

and at the largest scale 2^J

$$x_J^w(u, k) = \int_{[0,1]^n} f(v) \psi_{J+\ell,u}^k(v) dv = \langle f, \psi_{j+J,u}^k \rangle.$$

Normalized covariances We now consider a periodic stationary multiscale random process $x(u)$ of width L . Its covariance is diagonalised in a Fourier basis and its power spectrum (eigenvalues) has a power-law decay $P(\omega) = c(\xi^\eta + |\omega|^\eta)^{-1}$, for frequencies $\omega = 2\pi m/L$ with $m \in \{0, \dots, L-1\}^n$. The following lemma proves that the covariance matrix $\bar{\Sigma}$ of the normalized wavelet coefficients \bar{x} of x is well conditioned, with a condition number which does not depend upon L . It relies on an equivalence between Sobolev norms and weighted norms in a wavelet orthonormal basis.

Lemma 4. *For a wavelet transform corresponding to wavelets having $q > \eta$ vanishing moments, which have a compact support and are q times continuously differentiable, there exists $C_2 \geq C_1 > 0$ such that for any L the covariance $\bar{\Sigma}$ of $\bar{x} = (\bar{x}_j, x_j)_{j \leq J}$ satisfies:*

$$C_1 \text{ Id} \leq \bar{\Sigma} \leq C_2 \text{ Id}. \quad (21)$$

The remaining of the appendix is a proof of this lemma. Without loss of generality, we shall suppose that $\mathbb{E}[x] = 0$. Let $\sigma_{j,k}^2$ be the variance of $\bar{x}_j^w(u, k)$, and D be the diagonal matrix whose diagonal values are $\sigma_{j,k}^{-1}$. The vector of normalized wavelet coefficients $\bar{x} = (\bar{x}_j, x_J)_{j \leq J}$ are related to the non-normalized wavelet coefficients \bar{x}^w by a multiplication by D :

$$\bar{x} = D \bar{x}^w.$$

Let $\bar{\Sigma}_w$ be the covariance of \bar{x}^w . It results from this equation that the covariance $\bar{\Sigma}$ of \bar{x} and the covariance $\bar{\Sigma}_w$ of \bar{x}^w satisfy:

$$\bar{\Sigma} = D \bar{\Sigma}_w D.$$

The diagonal normalization D is adjusted so that the variance of each coefficient of \bar{x} is equal to 1, which implies that the diagonal of $\bar{\Sigma}$ is the identity. We must now prove that $\bar{\Sigma}$ satisfies (21), which is equivalent to prove that there exists C_1 and C_2 such that:

$$C_1 \text{Id} \leq D \bar{\Sigma}_w D \leq C_2 \text{Id}. \quad (22)$$

To prove (22), we relate it to Sobolev norm equivalences that have been proved in harmonic analysis. We begin by stating the result on Sobolev inequalities and then prove that it implies (22) for appropriate constants C_1 and C_2 .

Let Σ_∞ be the singular self-adjoint convolutional operator over $\mathbf{L}^2(\mathbb{R}^n)$ defined in the Fourier domain for all $\omega \in \mathbb{R}^n$:

$$\widehat{\Sigma_\infty f}(\omega) = \hat{f}(\omega) (\xi^\eta + |\omega|^\eta).$$

Observe that:

$$\langle \Sigma_\infty f, f \rangle = \frac{1}{(2\pi)^n} \int_{\mathbb{R}^n} |\hat{f}(\omega)|^2 (\xi^\eta + |\omega|^\eta) d\omega$$

is a Sobolev norm of exponent η . Such Sobolev norms are equivalent to weighted norms in wavelet bases, as proved in Theorem 4, Chapter 3 in Meyer (1992). To take into account the constant ξ , we introduce a maximum scale $2^{J'} = \xi^{-1}$. For all $f \in \mathbf{L}^2(\mathbb{R}^n)$, there exists $B \geq A > 0$ such that:

$$\begin{aligned} A \langle \Sigma_\infty f, f \rangle &\leq \sum_{u \in \mathbb{Z}^n} 2^{-J'\eta} |\langle f, \psi_{J',u}^0 \rangle|^2 \\ &+ \sum_{j=-\infty}^{J'} \sum_{u \in \mathbb{Z}^n} \sum_{k=1}^{2^n-1} 2^{-j\eta} |\langle f, \psi_{j,u}^k \rangle|^2 \leq B \langle \Sigma_\infty f, f \rangle. \end{aligned} \quad (23)$$

The remaining of the proof shows that these inequalities imply similar inequalities over the covariance of discrete wavelet coefficients. This is done by first restricting it to a finite support and then using the correspondence between the orthonormal wavelet coefficients of f and the discrete wavelet coefficients \bar{x}^w of x_0 .

One can verify that the equivalence (23) remains valid for functions $f \in \mathbf{L}^2([0, 1]^n)$ decomposed over periodic wavelet bases, because functions in $\mathbf{L}^2([0, 1]^n)$ can be written $f(v) = \sum_{r \in \mathbb{Z}^n} \tilde{f}(v - r)$ with $\tilde{f} \in \mathbf{L}^2(\mathbb{R}^n)$:

$$\begin{aligned} A \langle \Sigma_\infty f, f \rangle &\leq \sum_{2^j u \in [0, 1]^n} 2^{-j'\eta} |\langle f, \psi_{j',u}^0 \rangle|^2 \\ &+ \sum_{j=-\infty}^{J'} \sum_{2^j u \in [0, 1]^n} \sum_{k=1}^{2^n-1} 2^{-j\eta} |\langle f, \psi_{j,u}^k \rangle|^2 \leq B \langle \Sigma_\infty f, f \rangle. \end{aligned}$$

Applying this result to $f \in V_\ell$ is equivalent to restricting Σ_∞ to V_ℓ , which proves that $\Sigma_\ell = P_{V_\ell} \Sigma_\infty P_{V_\ell}$ satisfies:

$$\begin{aligned} A \langle \Sigma_\ell f, f \rangle &\leq \sum_{2^{j'} u \in [0, 1]^n} 2^{-j'\eta} |\langle f, \psi_{j',u}^0 \rangle|^2 \\ &+ \sum_{j=\ell+1}^{J'} \sum_{2^j u \in [0, 1]^n} \sum_{k=1}^{2^n-1} 2^{-j\eta} |\langle f, \psi_{j,u}^k \rangle|^2 \leq B \langle \Sigma_\ell f, f \rangle. \end{aligned} \quad (24)$$

The operator $\Sigma_\ell = P_{V_\ell} \Sigma_\infty P_{V_\ell}$ is covariant with respect to shifts by any $m2^\ell$ for $m \in \mathbb{Z}^n$ because P_{V_ℓ} and Σ_∞ are covariant to such shifts. Its representation in the basis of scaling functions $\{\psi_{\ell,u}^0\}_{2^\ell u \in [0, 1]^n}$ is thus a Toeplitz matrix which is diagonalized by a Fourier transform. There exists $0 < A_1 \leq B_1$ such that for all $\ell < 0$ and all $\omega \in [-2^{-\ell}\pi, 2^{-\ell}\pi]^n$,

$$A_1 (\xi^\eta + |\omega|^\eta) \leq P_\ell(\omega) \leq B_1 (\xi^\eta + |\omega|^\eta). \quad (25)$$

Indeed, the spectrum of Σ_∞ is $c(\xi^\eta + |\omega|^\eta)$ for $\omega \in \mathbb{R}^n$ and P_{V_ℓ} performs a filtering with the scaling function ψ_ℓ^0 whose support is essentially restricted to the frequency interval $[-\pi 2^{-\ell}, \pi 2^{-\ell}]$ so that the spectrum of $P_{V_\ell} \Sigma_\infty P_{V_\ell}$ is equivalent to the spectrum of Σ_∞ restricted to this interval.

The lemma hypothesis supposes that the covariance $\tilde{\Sigma}$ of x_0 has a spectrum equal to $c(\xi^\eta + |\omega|^\eta)^{-1}$ and hence that the spectrum of $\tilde{\Sigma}^{-1}$ is $c^{-1}(\xi^\eta + |\omega|^\eta)$. Since x_0 are decomposition coefficients of $f \in V_\ell$ in the basis of scaling functions, (25) can be rewritten for any $f \in V_\ell$:

$$A_1 c \langle \tilde{\Sigma}^{-1} x_0, x_0 \rangle \leq \langle \Sigma_\ell f, f \rangle \leq B_1 c \langle \tilde{\Sigma}^{-1} x_0, x_0 \rangle. \quad (26)$$

Since the orthogonal wavelet coefficients \bar{x}^w defines an orthonormal representation of x_0 , the covariance $\bar{\Sigma}_w$ of \bar{x}^w satisfies $\langle \bar{\Sigma}_w^{-1} \bar{x}^w, \bar{x}^w \rangle = \langle \tilde{\Sigma}^{-1} x_0, x_0 \rangle$. Moreover, we saw that that the wavelet coefficients \bar{x}^w of x_0 satisfy $\bar{x}_j^w(u, k) = \langle f, \psi_{j+\ell, u}^k \rangle$ and at the largest scale $\bar{x}_J^w(u, k) = \langle f, \psi_{J+\ell, u}^0 \rangle$. Hence for $J + \ell = J'$, we derive from (24) and (26) that:

$$\begin{aligned} A A_1 c \langle \bar{\Sigma}_w^{-1} \bar{x}^w, \bar{x}^w \rangle &\leq \sum_{2^j u \in [0, 1]^n} 2^{-(j+\ell)\eta} |x_J^w(u)|^2 \\ &+ \sum_{j=1}^J \sum_{2^j u \in [0, 1]^n} \sum_{k=1}^{2^{n-1}} 2^{-(j+\ell)\eta} |\bar{x}_j^w(u, k)|^2 \leq B B_1 c \langle \bar{\Sigma}_w^{-1} \bar{x}^w, \bar{x}^w \rangle. \end{aligned}$$

It results that for $A_2 = A A_1 c$ and $B_2 = B B_1 c$ we have:

$$A_2 \langle \bar{\Sigma}_w^{-1} \bar{x}^w, \bar{x}^w \rangle \leq 2^{-(J+\ell)\eta} \|\bar{x}_J^w\|^2 + \sum_{j=1}^J 2^{-(j+\ell)\eta} \|\bar{x}_j^w\|^2 \leq B_2 \langle \bar{\Sigma}_w^{-1} \bar{x}^w, \bar{x}^w \rangle.$$

Let \tilde{D} be the diagonal operator over the wavelet coefficients \bar{x}^w , whose diagonal values are $2^{-\eta(j+\ell)/2}$ at all scales 2^j . These inequalities can be rewritten as operator inequalities:

$$A_2 \bar{\Sigma}_w^{-1} \leq \tilde{D}^2 \leq B_2 \bar{\Sigma}_w^{-1},$$

and hence:

$$A_2 \text{Id} \leq \tilde{D} \bar{\Sigma}_w \tilde{D} \leq B_2 \text{Id}. \quad (27)$$

Since D^{-2} is the diagonal of $\bar{\Sigma}_w$, we derive from (27) that:

$$A_2 \tilde{D}^{-2} \leq D^{-2} \leq B_2 \tilde{D}^{-2}.$$

Inserting this equation in (27) proves that:

$$A_2 B_2^{-1} \text{Id} \leq D \bar{\Sigma}_w D \leq B_2 A_2^{-1} \text{Id},$$

and since $\bar{\Sigma} = D \bar{\Sigma}_w D$ it proves the lemma result (22), with $C_1 = A_2 B_2^{-1}$ and $C_2 = B_2 A_2^{-1}$.

10 Proof of Section 2

In this section, we first present the continuous-time framework in a Gaussian setting in Section 10.1. The general outline of the proof of Theorem 1 is presented in Section 10.2. Technical lemmas are gathered in Section 10.3. The proof of Theorem 2 is presented in Section 10.4.

10.1 Gaussian setting

In what follows we present the Gaussian setting used in the proof of Theorem 1. We assume that $p_0 = \mathcal{N}(0, \Sigma)$ with $\Sigma \in \mathbb{S}_d(\mathbb{R})_+$. Let $D \in \mathcal{M}_d(\mathbb{R})_+$ a diagonal positive matrix such that $\Sigma = P^\top D P$ with P an orthonormal matrix. We consider the following forward dynamics

$$dx_t = -x_t dt + \sqrt{2} dw_t,$$

with $\mathcal{L}(x_0) = p_0$. We also consider the backward dynamics given by

$$dy_t = \{y_t + 2\nabla \log p_{T-t}(y_t)\} dt + \sqrt{2} dw_t,$$

with $\mathcal{L}(y_0) = p_\infty = \mathcal{N}(0, \text{Id})$. Note that since for any $t \in [0, T]$ and $x \in \mathbb{R}^d$, $\nabla \log p_t(x) = -\Sigma_t^{-1} x$ with $\Sigma_t = \exp[-2t]\Sigma + (1 - \exp[-2t]) \text{Id}$, we have that $(y_t)_{t \in [0, T]}$ is a Gaussian process. In particular, we can compute the mean and the covariance matrix of y_t in a closed form for any $t \in [0, T]$. The results of Proposition 5 will not be used to prove Theorem 1. However, they provide some insights regarding the evolution of the mean and covariance of the backward process.

Proposition 5. For any $t \in [0, T]$, we have that $\mathcal{L}(y_t) = \mathcal{N}(0, \bar{\Sigma}_t)$ with

$$\bar{\Sigma}_t = P^\top ((1 - \exp[-2t])\bar{D}_t + \exp[-2t]\bar{D}_t^2)P,$$

and

$$\bar{D}_t = (\text{Id} + (D - \text{Id}) \exp[-2(T - t)]) \circ (\text{Id} + (D - \text{Id}) \exp[-2T]).$$

Note that $\bar{D}_0 = \text{Id}$ and $\bar{D}_T = D \circ (\text{Id} + (D - \text{Id}) \exp[-2T]) \approx D$. Hence, we have $\bar{\Sigma}_T \approx \Sigma$ and therefore $\mathcal{L}(y_T) \approx p_0$.

Proof. First, note that for any $t \in [0, T]$ we have that

$$y_t = y_0 + \int_0^t (\text{Id} - 2\Sigma_{T-t}^{-1})y_t + \sqrt{2}w_t = y_0 + \int_0^t (\text{Id} - 2P^\top D_{T-t}^{-1}P)y_t + \sqrt{2}w_t,$$

with $D_{T-t} = \exp[-2(T - t)]D + (1 - \exp[-2(T - t)])\text{Id}$. Denote $\{y_t^P\}_{t \in [0, T]} = \{Py_t\}_{t \in [0, T]}$. Using that $P^\top P = \text{Id}$, we have that for any $t \in [0, T]$

$$y_t^P = y_0^P + \int_0^t (\text{Id} - 2D_{T-t}^{-1})y_t^P + \sqrt{2}w_t^P,$$

where $\{w_t^P\}_{t \in [0, T]} = \{Pw_t\}_{t \in [0, T]}$. Note that since P is orthonormal, $\{w_t^P\}_{t \in [0, T]}$ is also a d -dimensional Brownian motion. We also have that $\mathcal{L}(y_0^P) = \mathcal{N}(0, \text{Id})$. Hence for any $\{y_t^{P,i}\}_{t \in [0, T]}\}_{i=1}^d$ is a collection of d independent Gaussian processes, where for any $i \in \{1, \dots, d\}$ and $t \in [0, T]$, $y_t^{P,i} = \langle y_t^P, e_i \rangle$ and $\{e_i\}_{i=1}^d$ is the canonical basis of \mathbb{R}^d . Let $i \in \{1, \dots, d\}$ and for any $t \in [0, T]$ denote $u_t^i = \mathbb{E}[y_t^{P,i}]$ and $v_t^i = \mathbb{E}[(y_t^{P,i})^2]$. We have that for any $t \in [0, T]$, $\partial_t u_t^i = (1 - 1/D_t^i)u_t^i$ with $u_0 = 0$ and $D_t^i = \exp[-2t]D_i + 1 - \exp[-2t]$. Hence, we get that for any $t \in [0, T]$, $u_t^i = 0$. Using Itô's lemma we have that

$$\partial v_t^i = \{2 - 4/D_{T-t}^i\}v_t^i + 2, \quad (28)$$

with $v_0^i = 1$. Denote $\alpha_T^i = (D^i - 1)\exp[-2T]$, we have that for any $t \in [0, T]$, $D_{T-t}^i = 1 + \alpha_T^i \exp[2t]$. Therefore, we get that for any $t \in [0, T]$

$$2 - 4/D_{T-t}^i = -2 + 2 \times (2\alpha_T^i \exp[2t]) / (1 + \alpha_T^i \exp[2t]) = -2 + 2\partial_t \log(1 + \alpha_T^i \exp[2t]).$$

Hence, we have that for any $t \in [0, T]$

$$\int_0^t 2 - 4/D_{T-s}^i ds = -2t + \log((1 + \alpha_T^i \exp[2t])^2 / (1 + \alpha_T^i)^2).$$

Hence, there exists $C_t^i \in C^1([0, T], \mathbb{R})$ such that for any $t \in [0, T]$, $v_t^i = C_t^i \exp[-2t](1 + \alpha_T^i \exp[2t])^2 / (1 + \alpha_T^i)^2$. Using (28), we have that for any $t \in [0, T]$

$$\partial_t C_t^i = 2 \exp[2t]((1 + \alpha_T^i \exp[2t]) / (1 + \alpha_T^i))^{-2} = -(1/\alpha_T^i)(1 + \alpha_T^i)^2 \partial_t (1 + \alpha_T^i \exp[2t])^{-1}.$$

Hence, we have that for any $t \in [0, T]$

$$C_t^i = (1/\alpha_T^i)(1 + \alpha_T^i)^2 [(1 + \alpha_T^i)^{-1} - (1 + \alpha_T^i \exp[2t])^{-1}] + A,$$

with $A \geq 0$. Hence, we get that for any $t \in [0, T]$

$$v_t^i = (1/\alpha_T^i) \exp[-2t](1 + \alpha_T^i \exp[2t]) [(1 + \alpha_T^i \exp[2t]) / (1 + \alpha_T^i) - 1] + A \exp[-2t](1 + \alpha_T^i \exp[2t])^2 / (1 + \alpha_T^i)^2.$$

In addition, we have that $v_0^i = 1$ and therefore $A = 1$. Therefore, for any $t \in [0, T]$ we have

$$\begin{aligned} v_t^i &= (1/\alpha_T^i) \exp[-2t](1 + \alpha_T^i \exp[2t]) [(1 + \alpha_T^i \exp[2t]) / (1 + \alpha_T^i) - 1] \\ &\quad + \exp[-2t](1 + \alpha_T^i \exp[2t])^2 / (1 + \alpha_T^i)^2 \\ &= (1 - \exp[-2t])(1 + \alpha_T^i \exp[2t]) / (1 + \alpha_T^i) + \exp[-2t](1 + \alpha_T^i \exp[2t])^2 / (1 + \alpha_T^i)^2, \end{aligned}$$

which concludes the proof. \square

10.2 Convergence results for the discretization

In what follows, we denote $(Y_k)_{k \in \{0, \dots, N-1\}} = (\bar{x}_{t_k})_{k \in \{0, \dots, N-1\}}$, the sequence given by (5). The following result gives an expansion of the covariance matrix and the mean of Y_N , i.e. the output of SGM, in the case where $p = N(\mu, \Sigma)$.

Theorem 6. *Let $N \in \mathbb{N}$, $\delta > 0$ and $T = N\delta$. Then, we have that $\bar{x}_{t_N} \sim N(\hat{\mu}_N, \hat{\Sigma}_N)$ with*

$$\hat{\Sigma}_N = \Sigma + \exp[-4T]\hat{\Sigma}_T + \delta\hat{E}_T + \delta^2 R_{T,\delta}, \quad \hat{\mu}_N = \mu + \exp[-2T]\hat{\mu}_T + \delta\hat{e}_T + \delta^2 r_{T,\delta},$$

where $\hat{\Sigma}_T, \hat{E}_T, R_{T,\delta} \in \mathbb{R}^{d \times d}$, $\hat{\mu}_T, \hat{e}_T, r_{T,\delta} \in \mathbb{R}^d$ and $\|R_{T,\delta}\| + \|r_{T,\delta}\| \leq R$ not dependent on $T \geq 0$ and $\delta > 0$. We have that

$$\begin{aligned} \hat{\Sigma}_T &= -(\Sigma - \text{Id})(\Sigma\Sigma_T^{-1})^2, \\ \hat{E}_T &= \text{Id} - (1/2)\Sigma^2(\Sigma - \text{Id})^{-1} \log(\Sigma) + \exp[-2T]\tilde{E}_T. \end{aligned} \quad (29)$$

In addition, we have

$$\begin{aligned} \hat{\mu}_T &= -\Sigma_T^{-1}\Sigma\mu, \\ \hat{e}_T &= \{-2\Sigma^{-1} - (1/4)\Sigma(\Sigma - \text{Id})^{-1} \log(\Sigma)\}\mu + \exp[-2T]\tilde{\mu}_T, \end{aligned}$$

with $\tilde{E}_T, \tilde{\mu}_T$ bounded and not dependent on T .

Before turning to the proof of Theorem 6, we state a few consequences of this result.

Corollary 7. *Let $\{\bar{x}_{t_k}\}_{k=0}^N$ the sequence defined by (5). We have that $\bar{x}_{t_N} \sim N(\mu_N, \Sigma_N)$ with*

$$\begin{aligned} \Sigma_N &= \Sigma + \delta\Sigma_\delta + \exp[-4T]\Sigma_T + \Sigma_{\delta,T}, \\ \mu_N &= \mu + \delta\mu_\delta + \exp[-2T]\mu_T + \mu_{\delta,T}, \end{aligned}$$

with

$$\begin{aligned} \Sigma_T &= -(\Sigma - \text{Id})\Sigma^2, \\ \Sigma_\delta &= \text{Id} - (1/2)\Sigma^2(\Sigma - \text{Id})^{-1} \log(\Sigma), \\ \mu_T &= \Sigma\mu, \\ \mu_\delta &= \{-2\Sigma^{-1} - (1/4)\Sigma(\Sigma - \text{Id})^{-1} \log(\Sigma)\}\mu. \end{aligned}$$

In addition, we have $\lim_{\delta \rightarrow 0, T \rightarrow +\infty} \|\Sigma_{\delta,T}\|/(\delta + \exp[-4T]) = 0$ and $\lim_{\delta \rightarrow 0, T \rightarrow +\infty} \|\mu_{\delta,T}\|/(\delta + \exp[-2T]) = 0$

At first sight, it might appear surprising that Σ^{-1} does not appear in Σ_T and μ_T . Note that in the extreme case where $\Sigma = 0$ and $\delta \rightarrow 0$, i.e. we only consider the error associated with the fact that $T \neq +\infty$, then we have no error. This is because in this case the associated continuous-time process is an Ornstein-Uhlenbeck bridge which has distribution $N(\mu, 0)$ at time T .

We will use the following result.

Lemma 8. *Let $\pi_i = N(\mu_i, \Sigma_i)$ for $i \in \{0, 1\}$, with $\mu_0, \mu_1 \in \mathbb{R}^d$ and $\Sigma_0, \Sigma_1 \in \mathbb{S}_d(\mathbb{R})_+$. Then, we have that*

$$\text{KL}(\pi_0 \|\pi_1) = (1/2)\{\log(\det(\Sigma_1)/\det(\Sigma_0)) - d + \text{Tr}(\Sigma_1^{-1}\Sigma_0) + (\mu_1 - \mu_0)^\top \Sigma_1^{-1}(\mu_1 - \mu_0)\}.$$

In particular, applying Lemma 8 we have that for any $\Sigma \in \mathbb{S}_d(\mathbb{R})_+$

$$\text{KL}(N(0, \Sigma) \|\| N(0, \text{Id})) = (1/2)\{-\log(\det(\Sigma)) + \text{Tr}(\Sigma) - d\}. \quad (30)$$

Proposition 9. *Let $\{\bar{x}_{t_k}\}_{k=0}^N$ the sequence defined by (5). We have that $\bar{x}_{t_N} \sim N(\mu_N, \Sigma_N)$, with μ_N, Σ_N given by Corollary 7. We have that*

$$\text{KL}(N(\mu, \Sigma) \|\| N(\mu_N, \Sigma_N)) \leq \delta |\text{Tr}(\Sigma^{-1}\Sigma_\delta)| + \exp[-4T] |\text{Tr}(\Sigma^{-1}\Sigma_T)| + \exp[-4T] \mu^\top \Sigma \mu + E_{T,\delta},$$

with $E_{T,\delta}$ a higher order term such that $\lim_{T \rightarrow +\infty, \delta \rightarrow 0} E_{T,\delta}/(\delta + \exp[-4T]) = 0$.

We now prove Theorem 6.

Proof. For any k , denote $Y_k = \bar{x}_{t_{N-k}}$. First, we recall that for any $k \in \{0, \dots, N-1\}$ and $x \in \mathbb{R}^d$, $\nabla \log p_{T-k\gamma}(x) = -\Sigma_{T-k\gamma}^{-1}x$ where for any $t \in [0, T]$

$$\Sigma_t = (1 - \exp[-2t]) \text{Id} + \exp[-2t]\Sigma.$$

Hence, we get that for any $k \in \{0, \dots, N-1\}$

$$Y_{k+1} = ((1 + \gamma) \text{Id} - 2\gamma \Sigma_{T-k\gamma}^{-1})Y_k + 2\gamma \Sigma_{T-k\gamma}^{-1}M_{T-k\gamma} + \sqrt{2\gamma}Z_{k+1}, \quad (31)$$

where for any $t \in [0, T]$, $M_t = \exp[-t]\mu$. Therefore, we get that for any $k \in \{0, \dots, N\}$, Y_k is a Gaussian random variable. Using (39), we have that for any $k \in \{0, \dots, N-1\}$

$$\mathbb{E}[\hat{Y}_{k+1}\hat{Y}_{k+1}^\top] = ((1 + \gamma) \text{Id} - 2\gamma \Sigma_{T-k\gamma}^{-1})\mathbb{E}[\hat{Y}_k\hat{Y}_k^\top]((1 + \gamma) \text{Id} - 2\gamma \Sigma_{T-k\gamma}^{-1}) + 2\gamma \text{Id}, \quad (32)$$

where for any $k \in \{0, \dots, N\}$, $\hat{Y}_k = Y_k - \mathbb{E}[Y_k]$. There exists $P \in \mathbb{R}^{d \times d}$ orthogonal such that $D = P\Sigma P^\top$ is diagonal. Note that for any $k \in \{0, \dots, N-1\}$, we have that $\Lambda_k = P((1 + \gamma) \text{Id} - 2\gamma \Sigma_{T-k\gamma}^{-1})P^\top$ is diagonal. For any $k \in \{0, \dots, N\}$, define $H_k = P\mathbb{E}[\hat{Y}_k\hat{Y}_k^\top]P^\top$. Note that $H_0 = \text{Id}$. Using (32), we have that for any $k \in \{0, \dots, N-1\}$

$$H_{k+1} = \Lambda_k^2 H_k + 2\gamma \text{Id}. \quad (33)$$

Hence, for any $k \in \{0, \dots, N\}$, H_k is diagonal. For any diagonal matrix $C \in \mathbb{R}^{d \times d}$ denote $\{c^1, \dots, c^d\}$ its diagonal elements. Let $i \in \{1, \dots, d\}$. Using (33), we have that for any $k \in \{0, \dots, N-1\}$

$$h_{k+1}^i = (\lambda_k^i)^2 h_k^i + 2\gamma.$$

Using this result we have that for any $k \in \{0, \dots, N\}$

$$h_k^i = (\prod_{\ell=0}^{k-1} \lambda_\ell^i)^2 + 2\gamma \sum_{\ell=0}^{k-1} (\prod_{j=0}^{\ell-1} \lambda_{k-1-j}^i)^2 = (\prod_{\ell=0}^{k-1} \lambda_\ell^i)^2 + 2\gamma \sum_{\ell=0}^{k-1} (\prod_{j=k-\ell}^{k-1} \lambda_j^i)^2.$$

Let $k_1, k_2 \in \{0, \dots, N\}$ with $k_1 < k_2$. In what follows, we derive an expansion of $I_{k_1, k_2} = \prod_{k=k_1}^{k_2} \lambda_k^i$ w.r.t. $\gamma > 0$. We have that

$$I_{k_1, k_2} = \prod_{k=k_1}^{k_2} \lambda_k^i = \exp[\sum_{k=k_1}^{k_2} \log(\lambda_k^i)] = \exp[\sum_{k=k_1}^{k_2} \log(1 + \gamma a_k^i)], \quad (34)$$

where for any $k \in \{0, \dots, N\}$, $a_k^i = 1 - 2/d_{(N-k)\gamma}^i$, with $d_{(N-k)\gamma}^i = 1 + \exp[-2(N-k)\gamma](d^i - 1)$. Hence, there exist $(b_{k,\gamma}^i)_{k \in \{0, \dots, N\}}$ bounded such that for any $k \in \{0, \dots, N\}$ we have

$$\log(1 + \gamma a_k^i) = \gamma a_k^i - (\gamma^2/2)(a_k^i)^2 + \gamma^3 b_{k,\gamma}^i.$$

In addition, using Proposition 10, there exists $C_{k_1, k_2}^\gamma \geq 0$ such that $\gamma C_{k_1, k_2}^\gamma \leq C$ with $C \geq 0$ not dependent on $k_2, k_2 \in \{0, \dots, N\}, \gamma > 0$ and

$$\sum_{k=k_1}^{k_2} \log(1 + \gamma a_k^i) = \int_{t_1}^{t_2^+} a^i(t) dt - (\gamma/2) [\int_{t_1}^{t_2^+} a^i(t)^2 dt + a^i(t_2^+) - a^i(t_1)] + C_{k_1, k_2}^\gamma \gamma^3,$$

with $t_1 = k_1\gamma, t_2^+ = (k_2 + 1)\gamma$ and for any $t \in [0, T]$, $a_t = 1 - 2/d_{T-t}^i$ with $d_{T-t}^i = 1 + \exp[-2(T-t)](d^i - 1)$. Hence, using this result and (34), we get that there exists $D_{k_1, k_2}^\gamma \geq 0$ such that $\gamma D_{k_1, k_2}^\gamma \leq D$ with $D \geq 0$ not dependent on $k_2, k_2 \in \{0, \dots, N\}, \gamma > 0$ and

$$I_{k_1, k_2} = \exp[\int_{t_1}^{t_2^+} a^i(t) dt] - \exp[\int_{t_1}^{t_2^+} a^i(t) dt] (\gamma/2) [\int_{t_1}^{t_2^+} a^i(t)^2 dt + a^i(t_2^+) - a^i(t_1)] + \gamma^3 D_{k_1, k_2}^\gamma. \quad (35)$$

Using this result, we get that there exists $E_1^\gamma \geq 0$ such that $\gamma E_1^\gamma \leq E$ with $E \geq 0$ not dependent on γ such that

$$(\prod_{\ell=0}^{N-1} \lambda_\ell^i)^2 = \exp[2 \int_0^T a^i(t) dt] - \gamma \exp[2 \int_0^T a^i(t) dt] [\int_0^T a^i(t)^2 dt + a^i(T) - a^i(0)] + \gamma^3 E_1^\gamma. \quad (36)$$

Similarly, using (35), there exist $E \geq 0$ and $(E_{2,\ell}^\gamma)_{\ell \in \{0, \dots, N\}}$ such that for any $\ell \in \{0, \dots, N\}$, $E_{2,\ell}^\gamma \geq 0$ and $\gamma E_{2,\ell}^\gamma \leq E$ with $E \geq 0$ not dependent on γ and ℓ such that

$$2\gamma \sum_{\ell=0}^{N-1} (\prod_{j=N-\ell}^{N-1} \lambda_j^i)^2 = (2\gamma) \sum_{\ell=0}^{N-1} \exp[2 \int_{T-\ell\gamma}^T a^i(t) dt]$$

$$\begin{aligned}
& -2\gamma^2 \sum_{\ell=0}^{N-1} \{ \exp[2 \int_{T-\ell\gamma}^T a^i(t) dt] [\int_{T-\ell\gamma}^T a^i(t)^2 dt + a^i(T) - a^i(T - \ell\gamma)] \} \\
& + \gamma^4 \sum_{\ell=0}^{N-1} E_{2,\ell}^\gamma.
\end{aligned}$$

Therefore, using Proposition 10, there exists E_3^γ such that $\gamma E_3^\gamma \leq E$ with $E \geq 0$ not dependent on γ and

$$\begin{aligned}
2\gamma \sum_{\ell=0}^{N-1} (\prod_{j=N-\ell}^{N-1} \lambda_j^i)^2 &= 2 \int_0^T \exp[2 \int_{T-t}^T a^i(s) ds] dt + \gamma(1 - \exp[2 \int_0^T a^i(t) dt]) \\
& - 2\gamma \int_0^T \{ \exp[2 \int_{T-t}^T a^i(s) ds] [\int_{T-t}^T a^i(s)^2 dt + a^i(T) - a^i(T-t)] \} dt \\
& + \gamma^3 E_3^\gamma.
\end{aligned} \tag{37}$$

Hence, combining (36) and (37) we get that

$$h_N^i = c_T^i - \gamma e_T^i + \gamma^3 E^\gamma,$$

with

$$c_T^i = \exp[2 \int_0^T a^i(t) dt] + 2 \int_0^T \exp[2 \int_{T-t}^T a^i(s) ds] dt. \tag{38}$$

and

$$\begin{aligned}
e_T^i &= - \exp[2 \int_0^T a^i(t) dt] [\int_0^T a^i(t)^2 dt + a^i(T) - a^i(0)] + 1 - \exp[2 \int_0^T a^i(t) dt] \\
& - 2 \int_0^T \exp[2 \int_{T-t}^T a^i(s) ds] [\int_{T-t}^T a^i(s)^2 ds + a^i(T) - a^i(T-t)] dt.
\end{aligned}$$

In what follows, we compute c_T^i and e_T^i .

(i) Using Lemma 11 we have

$$\exp[2 \int_0^T a^i(t) dt] = d^2 \exp[-2T] / (1 + \exp[-2T](d-1))^2.$$

In addition, using Lemma 12 we have

$$\int_0^T \exp[2 \int_{T-t}^T a^i(s) ds] = (d/2)(1 - \exp[-2T]) / (1 + \exp[-2T](d-1)).$$

Combining these results and (38), we get that

$$\begin{aligned}
c_T^i &= d + d^2 \exp[-2T] (1 - (1 + \exp[-2T](d-1))^{-1}) / (1 + \exp[-2T](d-1)) \\
& = d + d^2 (d-1) \exp[-4T] / (1 + \exp[-2T](d-1))^2.
\end{aligned}$$

(ii) We conclude for e_T^i using Proposition 20 with $\lambda = d^i - 1$.

This concludes the proof of (29). Next, we compute the evolution of the mean. Using (39), we have

$$\mathbb{E}[Y_{k+1}] = ((1 + \gamma) \text{Id} - 2\gamma \Sigma_{T-k\gamma}^{-1}) \mathbb{E}[Y_k] + 2\gamma \mathbb{E}[\Sigma_{T-k\gamma}^{-1} M_{T-k\gamma}], \tag{39}$$

Note that for any $k \in \{0, \dots, N-1\}$, we have that $\Lambda_k = \text{P}((1 + \gamma) \text{Id} - 2\gamma \Sigma_{T-k\gamma}^{-1}) \text{P}^\top$ is diagonal. For any $k \in \{0, \dots, N\}$, define $\text{H}_k = \text{P} \mathbb{E}[Y_k] \text{P}^\top$. Note that $\text{H}_0 = 0$. For any $k \in \{0, \dots, N-1\}$ we have that

$$\text{H}_{k+1} = \Lambda_k \text{H}_k + 2\gamma \text{D}_{T-k\gamma}^{-1} \text{V}_{T-k\gamma}, \tag{40}$$

where for any $t \in [0, T]$, $\text{D}_t = \text{P} \Sigma_t \text{P}^\top$ and $\text{V}_t = \text{P} M_t$. Let $i \in \{1, \dots, d\}$. Using (40), we have for any $k \in \{0, \dots, N-1\}$

$$h_{k+1}^i = \lambda_k^i h_k^i + 2\gamma v_{T-k\gamma}^i / d_{T-k\gamma}^i. \tag{41}$$

In what follows, we define for any $t \in [0, T]$, $r(t)^i = v_{T-t}^i / d_{T-t}^i$ and note that for any $t \in [0, T]$

$$r(t)^i = \exp[-(T-t)] / (1 + \exp[-2(T-t)](d^i - 1)) (\text{P}\mu)^i. \tag{42}$$

Using (41) and that $h_0^i = 0$, we have that for any $k \in \{0, \dots, N\}$

$$h_k^i = 2\gamma \sum_{\ell=0}^{k-1} r((k-\ell-1)\gamma) \prod_{j=0}^{\ell-1} \lambda_{k-1-j}^i = 2\gamma \sum_{\ell=0}^{k-1} r((k-\ell-1)\gamma) \prod_{j=k-\ell}^{k-1} \lambda_j^i.$$

Using (35), we get that there exists $D^\gamma \geq 0$ such that $\gamma D^\gamma \leq D$ not dependent on γ and

$$h_N^i = 2\gamma \sum_{k=0}^{N-1} r(T - (k+1)\gamma) \exp[\int_{T-k\gamma}^T a^i(t) dt]$$

$$\begin{aligned}
& -\gamma^2 \sum_{k=0}^{N-1} r(T - (k+1)\gamma) \exp[\int_{T-k\gamma}^T a^i(t)dt] [\int_{T-k\gamma}^T a^i(t)^2 dt + a^i(T) - a^i(T - k\gamma)] \\
& + \sum_{k=0}^{N-1} \gamma^4 D_{k,N}^\gamma \\
= & 2\gamma \sum_{k=0}^{N-1} r(T - (k+1)\gamma) \exp[\int_{T-k\gamma}^T a^i(t)dt] \\
& -\gamma^2 \sum_{k=0}^{N-1} r(T - (k+1)\gamma) \exp[\int_{T-k\gamma}^T a^i(t)dt] [\int_{T-k\gamma}^T a^i(t)^2 dt + a^i(T) - a^i(T - k\gamma)] \\
& + \gamma^3 D^\gamma .
\end{aligned}$$

Using Proposition 10, we get that there exists $E^\gamma \geq 0$ such that $\gamma E^\gamma \leq E$ not dependent on γ and

$$\begin{aligned}
h_N^i & = 2\gamma \sum_{k=0}^{N-1} r(T - (k+1)\gamma) \exp[\int_{T-k\gamma}^T a^i(t)dt] \\
& -\gamma \int_0^T r(T-t) \exp[\int_{T-t}^T a^i(s)ds] [\int_{T-t}^T a^i(t)^2 dt + a^i(T) - a^i(T-t)] dt \\
& + \gamma^3 E^\gamma .
\end{aligned}$$

In addition, for any $k \in \{0, \dots, N\}$, there exists $u_k \geq 0$ with $u_k \leq u$ and $u \geq 0$ not dependent on k and

$$r(T - (k+1)\gamma) = r(T - k\gamma) - r'(T - k\gamma)\gamma + u_k \gamma^2 .$$

Using this result, we get that exists $F^\gamma \geq 0$ such that $\gamma F^\gamma \leq F$ not dependent on γ and

$$\begin{aligned}
h_N^i & = 2\gamma \sum_{k=0}^{N-1} r(T - k\gamma) \exp[\int_{T-k\gamma}^T a^i(t)dt] \\
& -2\gamma^2 \sum_{k=0}^{N-1} r'(T - k\gamma) \exp[\int_{T-k\gamma}^T a^i(t)dt] \\
& -\gamma \int_0^T r(T-t) \exp[\int_{T-t}^T a^i(s)ds] [\int_{T-t}^T a^i(t)^2 dt + a^i(T) - a^i(T-t)] dt \\
& + \gamma^3 F^\gamma .
\end{aligned}$$

Using Proposition 10, we get that there exists $G^\gamma \geq 0$ such that $\gamma G^\gamma \leq G$ not dependent on γ and

$$\begin{aligned}
h_N^i & = 2\gamma \sum_{k=0}^{N-1} r(T - k\gamma) \exp[\int_{T-k\gamma}^T a^i(t)dt] \\
& -2\gamma \int_0^T r'(T-t) \exp[\int_{T-t}^T a^i(t)ds] dt \\
& -\gamma \int_0^T r(T-t) \exp[\int_{T-t}^T a^i(s)ds] [\int_{T-t}^T a^i(t)^2 dt + a^i(T) - a^i(T-t)] dt \\
& + \gamma^3 G^\gamma .
\end{aligned}$$

In addition, using Proposition 10, we get that there exists $H^\gamma \geq 0$ such that $\gamma H^\gamma \leq H$ not dependent on γ and

$$\begin{aligned}
h_N^i & = 2 \int_0^T r(T-t) \exp[\int_{T-t}^T a^i(s)ds] dt \\
& -\gamma \{r(0) \exp[\int_0^T a^i(t)dt] - r(T)\} - 2\gamma \int_0^T r'(T-t) \exp[\int_{T-t}^T a^i(s)ds] dt \\
& -\gamma \int_0^T r(T-t) \exp[\int_{T-t}^T a^i(s)ds] [\int_{T-t}^T a^i(t)^2 dt + a^i(T) - a^i(T-t)] dt \\
& + \gamma^3 H^\gamma .
\end{aligned} \tag{43}$$

In addition, we have by integration by part

$$\begin{aligned}
& \int_0^T r'(T-t) \exp[\int_{T-t}^T a^i(s)ds] dt \\
& = -\{r(0) \exp[\int_0^T a^i(t)dt] - r(T)\} - \int_0^T r(T-t) a^i(T-t) \exp[\int_{T-t}^T a^i(s)ds] dt .
\end{aligned}$$

Combining this result and (43) we get that

$$\begin{aligned}
h_N^i & = 2 \int_0^T r(T-t) \exp[\int_{T-t}^T a^i(s)ds] dt \\
& + \gamma \{r(0) \exp[\int_0^T a^i(t)dt] - r(T)\} \\
& -\gamma \int_0^T r(T-t) \exp[\int_{T-t}^T a^i(s)ds] [\int_{T-t}^T a^i(t)^2 dt + a^i(T) - 3a^i(T-t)] dt \\
& + \gamma^3 H^\gamma .
\end{aligned} \tag{44}$$

In what follows, we assume that $d^i \neq 0$. The case where $d^i = 0$ is left to the reader. Finally using (42) and Lemma 11 we have that for any $t \in [0, T]$

$$\begin{aligned} \exp[\int_{T-t}^T a^i(s)ds]r(T-t)^i &= \exp[-2t]/(1 + \exp[-2t](d^i - 1))^2(P\mu)^i d^i \\ &= \exp[2 \int_{T-t}^T a^i(s)ds](P\mu)^i / d^i . \end{aligned}$$

Therefore, combining this result and (44), we get that

$$\begin{aligned} h_N^i &= (P\mu)^i / d^i [2 \int_0^T \exp[2 \int_{T-t}^T a^i(s)ds]dt \\ &\quad + \gamma \{ \exp[2 \int_0^T a^i(t)dt] - 1 \} \\ &\quad - \gamma \int_0^T \exp[2 \int_{T-t}^T a^i(s)ds] [\int_{T-t}^T a^i(t)^2 dt + a^i(T) - 3a^i(T-t)] dt \\ &\quad + \gamma^3 H^\gamma , \end{aligned}$$

which concludes the proof upon using Lemma 12 and Proposition 21. \square

10.3 Technical lemmas

We are going to make use of the following lemma which is a direct consequence of the Euler-MacLaurin formula.

Proposition 10. *Let $f \in C^\infty([0, T])$, and $(u_k^\gamma)_{k \in \{0, \dots, N-1\}}$ with $N \in \mathbb{N}$ and $\gamma = T/N > 0$ such that for any $k \in \{0, \dots, N-1\}$, $u_k^\gamma = f(k\gamma)$. Then, there exists $C \geq 0$ such that*

$$\int_0^T f(t)dt - \gamma \sum_{k=0}^{N-1} u_k^\gamma - (\gamma/2)\{f(T) - f(0)\} = C\gamma^2 .$$

Proof. Apply the classical Euler-MacLaurin formula to $t \mapsto f(t\gamma)$. \square

We will also use the following lemmas.

Lemma 11. *Let $\lambda \in (-1, +\infty)$ and $a : [0, T] \rightarrow \mathbb{R}$ such that for any $t \in [0, T]$,*

$$a(t) = 1 - 2/(1 + \exp[-2(T-t)]\lambda) .$$

Then, we have that for any $t \in [0, T]$,

$$\int_{T-t}^T a(s)ds = t + \log((1 + \lambda)/(\exp[2t] + \lambda)) .$$

In particular, we have that for any $t \in [0, T]$

$$\exp[2 \int_{T-t}^T a(s)ds] = \exp[-2t](1 + \lambda)^2 / (1 + \lambda \exp[-2t])^2 .$$

Proof. Let $t \in [0, T]$. We have that $\int_{T-t}^T a(s)ds = \int_0^t a(T-s)ds$. Define b such that for any $t \in [0, T]$, $b(t) = a(T-t)$. In particular, we have that for any $t \in [0, T]$

$$b(t) = 1 - 2/(1 + \lambda \exp[-2t]) .$$

Hence, we have

$$\begin{aligned} \int_0^t b(s)ds &= t - 2 \int_0^t (1 + \lambda \exp[-2s])^{-1} ds \\ &= t - \int_0^t 2 \exp[2s]/(\exp[2s] + \lambda) ds \\ &= t + \log((1 + \lambda)/(\exp[2t] + \lambda)) , \end{aligned}$$

which concludes the proof. \square

Lemma 12. *Let $\lambda \in (-1, +\infty)$ and $a : [0, T] \rightarrow \mathbb{R}$ such that for any $t \in [0, T]$,*

$$a(t) = 1 - 2/(1 + \exp[-2(T-t)]\lambda) .$$

Then, we have that for any $t \in [0, T]$,

$$\begin{aligned} \int_0^t \exp[2 \int_{T-s}^T a(u)du] ds &= (1/2)(1 + \lambda)^2 [(1 + \lambda \exp[-2t])^{-1} - 1/(1 + \lambda)] / \lambda \\ &= (1/2)(1 + \lambda)(1 - \exp[-2t]) / (1 + \lambda \exp[-2t]) . \end{aligned}$$

Proof. Let $t \in [0, T]$. Using Lemma 11 we have that for any $s \in [0, T]$

$$\exp[2 \int_{T-s}^T a(u)du] = (1 + \lambda)^2 \exp[2s]/(\lambda + \exp[2s])^2 = (1 + \lambda)^2 \exp[-2s]/(1 + \lambda \exp[-2s])^2 .$$

Assume that $\lambda \neq 0$. Then, we have that

$$\begin{aligned} \int_0^t \exp[2 \int_{T-s}^T a(u)du] ds &= (1/2)(1 + \lambda)^2/\lambda \int_0^t 2\lambda \exp[-2t]/(1 + \lambda \exp[-2t])^2 ds \\ &= (1/2)(1 + \lambda)^2[(1 + \lambda \exp[-2t])^{-1} - 1/(1 + \lambda)]/\lambda \\ &= (1/2)(1 + \lambda)(1 - \exp[-2t])/(1 + \lambda \exp[-2t]) . \end{aligned}$$

We conclude the proof upon remarking that his result still holds in the case where $\lambda = 0$. \square

Lemma 13. Let $\lambda \in (-1, +\infty)$ and $a : [0, T] \rightarrow \mathbb{R}$ such that for any $t \in [0, T]$,

$$a(t) = 1 - 2/(1 + \exp[-2(T - t)]\lambda) .$$

Then, if $\lambda \neq 0$, we have that for any $t \in [0, T]$,

$$\begin{aligned} \int_0^t \exp[2 \int_{T-s}^T a(u)du]/(1 + \lambda \exp[-2s]) ds &= (1/4)(1 + \lambda)^2[(1 + \lambda \exp[-2t])^{-2} - 1/(1 + \lambda)^2]/\lambda \\ &= (1/4)(1 - \exp[-2t])(2 + \lambda(1 + \exp[-2t]))/(1 + \lambda \exp[-2t])^2 . \end{aligned}$$

If $\lambda = 0$ we have

$$\int_0^t \exp[2 \int_{T-s}^T a(u)du]/(1 + \lambda \exp[-2s]) ds = (1/2)(1 - \exp[-2t]) .$$

Proof. Let $t \in [0, T]$. Using Lemma 11 we have that for any $s \in [0, T]$

$$\exp[\int_{T-s}^T a(u)du]/(1 + \lambda \exp[-2s]) = (1 + \lambda)^2 \exp[-2s]/(1 + \lambda \exp[-2s])^3 .$$

Assume that $\lambda \neq 0$. Then, we have that

$$\begin{aligned} \int_0^t \exp[\int_{T-s}^T a(u)du]/(1 + \lambda \exp[-2s]) ds &= (1/2)(1 + \lambda)^2/\lambda \int_0^t 2\lambda \exp[-2t]/(1 + \lambda \exp[-2t])^3 ds \\ &= (1/4)(1 + \lambda)^2[(1 + \lambda \exp[-2t])^{-2} - 1/(1 + \lambda)^2]/\lambda \\ &= (1/4)(1 - \exp[-2t])(2 + \lambda(1 + \exp[-2t]))/(1 + \lambda \exp[-2t])^2 . \end{aligned}$$

We conclude the proof upon remarking that his result still holds in the case where $\lambda = 0$. \square

Lemma 14. Let $\lambda \in (-1, +\infty)$ and $a : [0, T] \rightarrow \mathbb{R}$ such that for any $t \in [0, T]$,

$$a(t) = 1 - 2/(1 + \exp[-2(T - t)]\lambda) .$$

Then, we have that for any $t \in [0, T]$

$$\begin{aligned} \int_0^t \exp[2 \int_{T-s}^T a(u)du] a(T - s) ds &= -(1/2)(1 - \exp[-2t])(1 - \lambda^2 \exp[-2t])/(1 + \lambda \exp[-2t])^2 . \end{aligned}$$

Proof. Let $t \in [0, T]$. We have that

$$\begin{aligned} \int_0^t \exp[2 \int_{T-s}^T a(u)du] a(T - s) ds &= \int_0^t \exp[2 \int_{T-s}^T a(u)du] ds - 2 \int_0^t \exp[2 \int_{T-s}^T a(u)du]/(1 + \lambda \exp[-2s]) ds . \end{aligned} \quad (45)$$

Using Lemma 12, we have that

$$\int_0^t \exp[2 \int_{T-s}^T a(u)du] dt = (1/2)(1 + \lambda)(1 - \exp[-2t])/(1 + \lambda \exp[-2t]) . \quad (46)$$

In addition, using Lemma 13, we have

$$\begin{aligned} \int_0^t \exp[2 \int_{T-s}^T a(u)du]/(1 + \lambda \exp[-2s]) ds &= (1/4)(1 - \exp[-2t])(2 + \lambda(1 + \exp[-2t]))/(1 + \lambda \exp[-2t])^2 . \end{aligned} \quad (47)$$

Combining (46) and (47) in (45) we have that

$$\begin{aligned} & \int_0^t \exp[2 \int_{T-s}^T a(u) du] a(T-s) ds \\ &= (1/2)(1 - \exp[-2t])[(1 + \lambda)(1 + \lambda \exp[-2t])]/(1 + \lambda \exp[-2t])^2 \\ & \quad - (1/2)(1 - \exp[-2t])(2 + \lambda(1 + \exp[-2t]))/(1 + \lambda \exp[-2t])^2 \\ &= -(1/2)(1 - \exp[-2t])(1 - \lambda^2 \exp[-2t])/(1 + \lambda \exp[-2t])^2, \end{aligned}$$

which concludes the proof. \square

Lemma 15. Let $\lambda \in (-1, +\infty)$ we have that for any $t \in [0, T]$

$$\int_0^t (1 + \lambda \exp[-2s])^{-1} ds = (1/2) \log((\lambda + \exp[2t])/(\lambda + 1)).$$

In addition, we have for any $t \in [0, T]$

$$\int_0^t (1 + \lambda \exp[-2s])^{-2} ds = (1/2) \log((\lambda + \exp[2t])/(\lambda + 1)) + (\lambda/2)[(\exp[2t] + \lambda)^{-1} - (\lambda + 1)^{-1}].$$

Finally, we have that for any $t \in [0, T]$

$$\begin{aligned} \int_0^t (1 + \lambda \exp[-2s])^{-3} ds &= (1/2) \log((\lambda + \exp[2t])/(\lambda + 1)) + \lambda[(\exp[2t] + \lambda)^{-1} - (\lambda + 1)^{-1}] \\ & \quad - (\lambda^2/4)[(\exp[2t] + \lambda)^{-2} - (\lambda + 1)^{-2}]. \end{aligned}$$

Proof. Let $k \in \{1, 2, 3\}$. Using the change of variable $u \mapsto \exp[2u]$ we have that

$$\int_0^t (1 + \lambda \exp[-2s])^{-k} ds = (1/2) \int_1^{\exp[2t]} u^{k-1}/(u + \lambda) du.$$

Therefore, we have that

$$\int_0^t (1 + \lambda \exp[-2s])^{-1} ds = (1/2) \int_1^{\exp[2t]} (u + \lambda)^{-1} du = (1/2) \log((\lambda + \exp[2t])/(\lambda + 1)).$$

In addition, using that for any $u \in [0, T]$, $u = (u + \lambda) - \lambda$ we have that

$$\begin{aligned} \int_0^t (1 + \lambda \exp[-2s])^{-2} ds &= (1/2) \int_1^{\exp[2t]} u(u + \lambda)^{-2} du \\ &= (1/2) \int_1^{\exp[2t]} (u + \lambda)^{-1} du - (\lambda/2) \int_1^{\exp[2t]} (u + \lambda)^{-2} du \\ &= (1/2) \log((\lambda + \exp[2t])/(\lambda + 1)) + (\lambda/2)[(\exp[2t] + \lambda)^{-1} - (\lambda + 1)^{-1}]. \end{aligned}$$

Finally, using that for any $u \in [0, T]$, $u \in [0, T]$, $u^2 = (u + \lambda)^2 - 2\lambda(u + \lambda) + \lambda^2$ we have that

$$\begin{aligned} \int_0^t (1 + \lambda \exp[-2s])^{-3} ds &= (1/2) \int_1^{\exp[2t]} u^2(u + \lambda)^{-2} du \\ &= (1/2) \int_1^{\exp[2t]} (u + \lambda)^{-1} du - \lambda \int_1^{\exp[2t]} (u + \lambda)^{-2} du + (\lambda^2/2) \int_1^{\exp[2t]} (u + \lambda)^{-3} du \\ &= (1/2) \log((\lambda + \exp[2t])/(\lambda + 1)) + \lambda[(\exp[2t] + \lambda)^{-1} - (\lambda + 1)^{-1}] \\ & \quad - (\lambda^2/4)[(\exp[2t] + \lambda)^{-2} - (\lambda + 1)^{-2}], \end{aligned}$$

which concludes the proof. \square

Lemma 16. Let $\lambda \in (-1, +\infty)$ and $a : [0, T] \rightarrow \mathbb{R}$ such that for any $t \in [0, T]$,

$$a(t) = 1 - 2/(1 + \exp[-2(T - t)]\lambda).$$

Then, we have that for any $t \in [0, T]$,

$$\int_{T-t}^T a(s)^2 ds = t - 2\lambda(1 - \exp[-2t])/[(1 + \lambda)(1 + \lambda \exp[-2t])].$$

Proof. Let $t \in [0, T]$. Similarly to the proof of Lemma 11, we have that $\int_{T-t}^T a(s) ds = \int_0^t a(T - s) ds$. Define b such that for any $t \in [0, T]$, $b(t) = a(T - t)$. In particular, we have that for any $t \in [0, T]$

$$b(t) = 1 - 2/(1 + \lambda \exp[-2t]).$$

We have that

$$\int_{T-t}^T a(s)^2 ds = \int_0^t b(s)^2 ds = \int_0^t (1 - 4/(1 + \lambda \exp[-2s]) + 4/(1 + \lambda \exp[-2s])^2) ds.$$

Combining this result and Lemma 15, we have

$$\begin{aligned} \int_{T-t}^T a(s)^2 ds &= t + 2\lambda[(\lambda + \exp[2t])^{-1} - (\lambda + 1)^{-1}] \\ &= t - 2\lambda(1 - \exp[-2t])/[(1 + \lambda)(1 + \lambda \exp[-2t])]. \end{aligned}$$

\square

Lemma 17. Let $\lambda \in (-1, +\infty)$ and $a : [0, T] \rightarrow \mathbb{R}$ such that for any $t \in [0, T]$,

$$a(t) = 1 - 2/(1 + \exp[-2(T - t)]\lambda) .$$

Then, if $\lambda \neq 0$, we have that

$$\begin{aligned} \int_0^T \exp[2 \int_{T-t}^T a(s)ds] (\int_{T-t}^T a(s)^2 ds) dt &= -(T/2)(1 + \lambda)^2 \exp[-2T]/(1 + \lambda \exp[-2T]) \\ &\quad + (1 + \lambda)^2/(4\lambda) \log((1 + \lambda)/(1 + \lambda \exp[-2T])) \\ &\quad - (\lambda/2)(1 - \exp[-2T])^2/(1 + \lambda \exp[-2T])^2 . \end{aligned} \quad (48)$$

If $\lambda = 0$, we have that

$$\int_0^T \exp[2 \int_{T-t}^T a(s)ds] (\int_{T-t}^T a(s)^2 ds) dt = -(T/2) \exp[-2T] + (1/4)(1 - \exp[-2T]) . \quad (49)$$

Note that taking $\lambda \rightarrow 0$ in (48) we recover (49), using that for any $u > 0$, $\lim_{\lambda \rightarrow 0} \log(1 + \lambda u)/\lambda = u$.

Proof. We first start with the case $\lambda \neq 0$. Similarly to the proof of Lemma 11, we have that $\int_{T-t}^T a(s)ds = \int_0^t a(T - s)ds$. Define b such that for any $t \in [0, T]$, $b(t) = a(T - t)$. We have that

$$\int_0^T \exp[2 \int_{T-t}^T a(s)ds] (\int_{T-t}^T a(s)^2 ds) dt = \int_0^T \exp[2 \int_{T-t}^T a(s)ds] (\int_0^t b(s)^2 ds) dt .$$

Let $A : [0, T] \rightarrow \mathbb{R}$ such that for any $t \in [0, T]$,

$$A(t) = \int_0^t \exp[2 \int_{T-s}^T a(u)du] ds .$$

Note that $A(0) = 0$. Hence, by integration by parts, we have

$$\int_0^T \exp[2 \int_{T-t}^T a(s)ds] (\int_0^t b(s)^2 ds) dt = A(T) \int_0^T b(t)^2 dt - \int_0^T A(t) b(t)^2 dt .$$

In what follows, we compute $\int_0^T A(t) b(t)^2 dt$. First, we recall that for any $t \in [0, T]$

$$b(t)^2 = (1 - 2/(1 + \lambda \exp[-2t]))^2 = 1 - 4/(1 + \lambda \exp[-2t]) + 4/(1 + \lambda \exp[-2t])^2 . \quad (50)$$

In addition, using Lemma 12, we have that for any $t \in [0, T]$

$$A(t) = (1/2)\{(1 + \lambda)^2/(\lambda(1 + \lambda \exp[-2t])) - (1 + \lambda)/\lambda\} . \quad (51)$$

Using (50) and (51) we have that for any $t \in [0, T]$

$$\begin{aligned} 2A(t)b(t)^2 &= -(1 + \lambda)/\lambda + [4(1 + \lambda)/\lambda + (1 + \lambda)^2/\lambda]u_1(t) \\ &\quad - [4(1 + \lambda)^2/\lambda + 4(1 + \lambda)/\lambda]u_2(t) + [4(1 + \lambda)^2/\lambda]u_3(t) \\ &= -(1 + \lambda)/\lambda + [(1 + \lambda)(5 + \lambda)/\lambda]u_1(t) \\ &\quad - [4(1 + \lambda)(2 + \lambda)/\lambda]u_2(t) + [4(1 + \lambda)^2/\lambda]u_3(t) , \end{aligned} \quad (52)$$

where for any $k \in \{1, 2, 3\}$ and $t \in [0, T]$ we have

$$u_k(t) = (1 + \lambda \exp[-2t])^{-k} .$$

For any $k \in \{0, 1, 2\}$ denote $v_k : [0, T] \rightarrow \mathbb{R}$ such that for any $t \in [0, T]$ and $k \in \{1, 2\}$

$$v_0(t) = \log((\lambda + \exp[2t])/(\lambda + 1)) , \quad v_k(t) = (\exp[2t] + \lambda)^{-k} - (1 + \lambda)^{-k} .$$

Combining (52) and Lemma 15, we get that for any $t \in [0, T]$

$$\begin{aligned} 2 \int_0^t A(s)b(s)^2 ds &= -[(1 + \lambda)/\lambda]t \\ &\quad + (1/2)\{[(1 + \lambda)(5 + \lambda)/\lambda] - [4(1 + \lambda)(2 + \lambda)/\lambda] + [4(1 + \lambda)^2/\lambda]\}v_0(t) \\ &\quad + \{-\lambda/2[4(1 + \lambda)(2 + \lambda)/\lambda] + \lambda[4(1 + \lambda)^2/\lambda]\}v_1(t) \\ &\quad - (\lambda^2/4)[4(1 + \lambda)^2/\lambda]v_2(t) \\ &= -[(1 + \lambda)/\lambda]t + (1 + \lambda)^2/(2\lambda)v_0(t) + 2(1 + \lambda)\lambda v_1(t) - \lambda(1 + \lambda)^2 v_2(t) . \end{aligned}$$

In addition, we have that

$$\begin{aligned} & - [(1 + \lambda)/\lambda]t + (1 + \lambda)^2/(2\lambda)v_0(t) = -[(1 + \lambda)/\lambda]t + [(1 + \lambda)^2/\lambda]t \\ & \quad + (1 + \lambda)^2/(2\lambda) \log((1 + \lambda \exp[-2t])/(1 + \lambda)) \\ & = (1 + \lambda)t + (1 + \lambda)^2/(2\lambda) \log((1 + \lambda \exp[-2t])/(1 + \lambda)) . \end{aligned}$$

Therefore, we get that

$$\begin{aligned} 2 \int_0^t A(s)b(s)^2 ds & = (1 + \lambda)t + (1 + \lambda)^2/(2\lambda) \log((1 + \lambda \exp[-2t])/(1 + \lambda)) \\ & \quad + 2(1 + \lambda)\lambda v_1(t) + \lambda(1 + \lambda)^2 v_2(t) . \end{aligned} \quad (53)$$

In addition, we have that

$$(1 + \lambda)\lambda v_1(t) = -\lambda(1 - \exp[-2T])/(1 + \lambda \exp[-2T]) . \quad (54)$$

We also have that

$$\begin{aligned} \lambda(1 + \lambda)^2 v_2(t) & = \lambda(2\lambda + 1 - 2\lambda \exp[2T] - \exp[4T]) / (\exp[2T] + \lambda)^2 \\ & = \lambda(1 - \exp[2T])(1 + 2\lambda + \exp[2T]) / (\exp[2T] + \lambda)^2 \\ & = -\lambda(1 - \exp[-2T])(1 + (1 + 2\lambda) \exp[-2T]) / (1 + \lambda \exp[-2T])^2 . \end{aligned} \quad (55)$$

Finally, using Lemma 12 and Lemma 16 we have

$$\begin{aligned} A(T) \int_0^T b(t)^2 dt & = (1/2)(1 + \lambda)(1 - \exp[-2T]) / (1 + \lambda \exp[-2T]) \\ & \quad \times (T - 2\lambda(1 - \exp[-2T]) / ((1 + \lambda)(1 + \lambda \exp[-2T]))) \\ & = (T/2)(1 + \lambda)(1 - \exp[-2T]) / (1 + \lambda \exp[-2T]) \\ & \quad - \lambda(1 - \exp[-2T])^2 / (1 + \lambda \exp[-2T])^2 . \end{aligned} \quad (56)$$

Combining (53), (54), (55) and (56) we get

$$\begin{aligned} \int_0^T \exp[2 \int_{T-t}^T a(s) ds] (\int_{T-t}^T a(s)^2 ds) dt & = (T/2)(1 + \lambda)(1 - \exp[-2T]) / (1 + \lambda \exp[-2T]) \\ & \quad - \lambda(1 - \exp[-2T])^2 / (1 + \lambda \exp[-2T])^2 \\ & \quad - (1 + \lambda)(T/2) + (1 + \lambda)^2 / (4\lambda) \log((1 + \lambda) / (1 + \lambda \exp[-2T])) \\ & \quad + \lambda(1 - \exp[-2T]) / (1 + \lambda \exp[-2T]) \\ & \quad - (\lambda/2)(1 - \exp[-2T])((1 + 2\lambda) \exp[-2T] + 1) / (1 + \lambda \exp[-2T])^2 . \end{aligned} \quad (57)$$

In addition, we have that

$$\begin{aligned} & - (\lambda/2)(1 - \exp[-2T])^2 / (1 + \lambda \exp[-2T])^2 \\ & = -\lambda(1 - \exp[-2T])^2 / (1 + \lambda \exp[-2T])^2 \\ & \quad + \lambda(1 - \exp[-2T]) / (1 + \lambda \exp[-2T]) \\ & = -(\lambda/2)(1 - \exp[-2T])((1 + 2\lambda) \exp[-2T] + 1) / (1 + \lambda \exp[-2T])^2 . \end{aligned}$$

Combining this result and (57), we get

$$\begin{aligned} \int_0^T \exp[2 \int_{T-t}^T a(s) ds] (\int_{T-t}^T a(s)^2 ds) dt & = (T/2)(1 + \lambda)(1 - \exp[-2T]) / (1 + \lambda \exp[-2T]) \\ & \quad - (1 + \lambda)(T/2) + (1 + \lambda)^2 / (4\lambda) \log((1 + \lambda) / (1 + \lambda \exp[-2T])) \\ & \quad - (1/2)(1 - \exp[-2T])^2 / (1 + \lambda \exp[-2T])^2 . \end{aligned} \quad (58)$$

Finally, we have

$$\begin{aligned} & (T/2)(1 + \lambda)(1 - \exp[-2T]) / (1 + \lambda \exp[-2T]) - (T/2)(1 + \lambda) \\ & = -(T/2)(1 + \lambda)^2 \exp[-2T] / (1 + \lambda \exp[-2T]) , \end{aligned}$$

which concludes the proof in the case $\lambda \neq 0$ upon combining this result and (58). In the case $\lambda = 0$, we have that for any $t \in [0, T]$, $a(t) = -1$ and therefore by integration by part we have

$$\int_0^T \exp[2 \int_{T-t}^T a(s) ds] (\int_{T-t}^T a(s)^2 ds) dt = -(T/2) \exp[-2T] + (1/4)(1 - \exp[-2T]) ,$$

which concludes the proof. \square

We are now ready to prove the following results.

Proposition 18. Let $\lambda \in (-1, +\infty)$ and $a : [0, T] \rightarrow \mathbb{R}$ such that for any $t \in [0, T]$,

$$a(t) = 1 - 2/(1 + \exp[-2(T - t)]\lambda) .$$

Then, we have that for any $t \in [0, T]$,

$$\begin{aligned} \exp[2 \int_0^T a(t)dt] \{ \int_0^T a(t)^2 dt + a(T) - a(0) + 1 \} \\ = (T + 1) \exp[-2T] (\lambda + 1)^2 / (1 + \lambda \exp[-2T])^2 . \end{aligned}$$

Proof. First, we have that

$$\begin{aligned} a(T) - a(0) &= 1 - 2/(1 + \lambda) - 1 + 2/(1 + \lambda \exp[-2T]) \\ &= 2\lambda(1 - \exp[-2T]) / [(1 + \lambda)(1 + \lambda \exp[-2T])] . \end{aligned} \quad (59)$$

In addition, using Lemma 16 we have

$$\int_0^T a(s)^2 ds = T - 2\lambda(1 - \exp[-2T]) / [(1 + \lambda)(1 + \lambda \exp[-2T])] . \quad (60)$$

Finally, using Lemma 11 we have that

$$\exp[2 \int_0^T a(s)ds] = \exp[-2T] (\lambda + 1)^2 / (1 + \lambda \exp[-2T])^2 . \quad (61)$$

We conclude the proof upon combining (59), (60) and (61). \square

Finally, we have the following proposition.

Proposition 19. Let $\lambda \in (-1, +\infty)$ and $a : [0, T] \rightarrow \mathbb{R}$ such that for any $t \in [0, T]$,

$$a(t) = 1 - 2/(1 + \exp[-2(T - t)]\lambda) .$$

Then, if $\lambda \neq 0$, we have that for any $t \in [0, T]$,

$$\begin{aligned} \int_0^T \exp[2 \int_{T-t}^T a(s)ds] [\int_{T-t}^T a(s)^2 ds + a(T) - a(T - t)] dt \\ = -(T/2)(1 + \lambda)^2 \exp[-2T] / (1 + \lambda \exp[-2T]) \\ + (1 + \lambda)^2 / (4\lambda) \log((1 + \lambda) / (1 + \lambda \exp[-2T])) \\ + (\lambda/2) \exp[-2T] / (1 + \lambda \exp[-2T])^2 . \end{aligned}$$

If $\lambda = 0$, we have that

$$\begin{aligned} \int_0^T \exp[2 \int_{T-t}^T a(s)ds] [\int_{T-t}^T a(s)^2 ds + a(T) - a(T - t)] dt \\ = -(T/2) \exp[-2T] + (1/4)(1 - \exp[-2T]) . \end{aligned}$$

Proof. We assume that $\lambda \neq 0$. The case where $\lambda = 0$ is left to the reader. First, using Lemma 17, we have that

$$\begin{aligned} \int_0^T \exp[2 \int_{T-t}^T a(s)ds] (\int_{T-t}^T a(s)^2 ds) dt &= -(T/2)(1 + \lambda)^2 \exp[-2T] / (1 + \lambda \exp[-2T]) \\ &+ (1 + \lambda)^2 / (4\lambda) \log((1 + \lambda) / (1 + \lambda \exp[-2T])) \\ &+ (3\lambda/2) \exp[-2T] (1 - \exp[-2T]) (1 + \lambda) / (1 + \lambda \exp[-2T])^2 . \end{aligned} \quad (62)$$

Second, using Lemma 14, we have that

$$\begin{aligned} \int_0^T \exp[2 \int_{T-t}^T a(u)du] a(T - t) dt \\ = -(1/2)(1 - \exp[-2T]) (1 - \lambda^2 \exp[-2T]) / (1 + \lambda \exp[-2T])^2 . \end{aligned} \quad (63)$$

Third, using Lemma 12 and that $a(T) = 1 - 2/(1 + \lambda)$, we have that

$$\begin{aligned} a(T) \int_0^T \exp[2 \int_{T-t}^T a(s)ds] dt &= a(T)(1/2)(1 + \lambda)(1 - \exp[-2T]) / (1 + \lambda \exp[-2T]) \\ &= (1/2)(1 + \lambda)(1 - \exp[-2T]) / (1 + \lambda \exp[-2T]) \\ &- (1 - \exp[-2T]) / (1 + \lambda \exp[-2T]) . \end{aligned} \quad (64)$$

Combining (62), (63) and (64) we get

$$\begin{aligned}
& \int_0^T \exp[2 \int_{T-t}^T a(s) ds] [\int_{T-t}^T a(s)^2 ds + a(T) - a(T-t)] dt \\
&= -(T/2)(1 + \lambda)^2 \exp[-2T]/(1 + \lambda \exp[-2T]) \\
&\quad + (1 + \lambda)^2/(4\lambda) \log((1 + \lambda)/(1 + \lambda \exp[-2T])) \\
&\quad + (3\lambda/2) \exp[-2T](1 - \exp[-2T])(1 + \lambda)/(1 + \lambda \exp[-2T])^2 \\
&\quad + (1/2)(1 - \exp[-2T])(1 - \lambda^2 \exp[-2T])/(1 + \lambda \exp[-2T])^2 \\
&\quad + (1/2)(1 + \lambda)(1 - \exp[-2T])/(1 + \lambda \exp[-2T]) \\
&\quad - (1 - \exp[-2T])/(1 + \lambda \exp[-2T])
\end{aligned}$$

In addition, we have

$$\begin{aligned}
& (\lambda/2)(1 - \exp[-2T])/(1 + \lambda \exp[-2T])^2 \\
&= (1/2)(1 - \exp[-2T])(1 - \lambda^2 \exp[-2T])/(1 + \lambda \exp[-2T])^2 \\
&\quad + (1/2)(1 + \lambda)(1 - \exp[-2T])/(1 + \lambda \exp[-2T]) \\
&\quad - (1 - \exp[-2T])/(1 + \lambda \exp[-2T]) ,
\end{aligned}$$

Finally, we have

$$\begin{aligned}
& (\lambda/2) \exp[-2T]/(1 + \lambda \exp[-2T])^2 \\
&= -(\lambda/2)(1 - \exp[-2T])^2/(1 + \lambda \exp[-2T])^2 \\
&\quad + (\lambda/2)(1 - \exp[-2T])/(1 + \lambda \exp[-2T])^2 .
\end{aligned}$$

which concludes the proof. \square

Finally, we have the following result.

Proposition 20. *Let $\lambda \in (-1, +\infty)$ and $a : [0, T] \rightarrow \mathbb{R}$ such that for any $t \in [0, T]$,*

$$a(t) = 1 - 2/(1 + \exp[-2(T-t)\lambda]) .$$

Then, if $\lambda \neq 0$, we have that for any $t \in [0, T]$,

$$\begin{aligned}
& -\exp[2 \int_0^T a(t) dt] \{ \int_0^T a(t)^2 dt + a(T) - a(0) \} + 1 - \exp[2 \int_0^T a(t) dt] \\
&\quad - 2 \int_0^T \exp[2 \int_{T-t}^T a(s) ds] [\int_{T-t}^T a(s)^2 ds + a(T) - a(T-t)] dt \\
&= 1 - \exp[-2T](1 - \lambda T \exp[-2T])(\lambda + 1)^2/(1 + \lambda \exp[-2T])^2 \\
&\quad - (1 + \lambda)^2/(2\lambda) \log((1 + \lambda)/(1 + \lambda \exp[-2T])) \\
&\quad - \lambda \exp[-2T]/(1 + \lambda \exp[-2T])^2 .
\end{aligned}$$

In particular, we have that

$$\begin{aligned}
& -\exp[2 \int_0^T a(t) dt] \{ \int_0^T a(t)^2 dt + a(T) - a(0) \} + 1 - \exp[2 \int_0^T a(t) dt] \\
&\quad - 2 \int_0^T \exp[2 \int_{T-t}^T a(s) ds] [\int_{T-t}^T a(s)^2 ds + a(T) - a(T-t)] dt \\
&= 1 - (1/2)(1 + \lambda)^2 \log(1 + \lambda)/\lambda + O(\exp[-2T]) .
\end{aligned}$$

If $\lambda = 0$, we have that for any $t \in [0, T]$

$$\begin{aligned}
& -\exp[2 \int_0^T a(t) dt] \{ \int_0^T a(t)^2 dt + a(T) - a(0) \} + 1 - \exp[2 \int_0^T a(t) dt] \\
&\quad - 2 \int_0^T \exp[2 \int_{T-t}^T a(s) ds] [\int_{T-t}^T a(s)^2 ds + a(T) - a(T-t)] dt \\
&= (1/2)(1 - \exp[-2T]) .
\end{aligned}$$

Proof. The proof is a direct consequence of Proposition 18, Proposition 19 and the fact that

$$\begin{aligned}
& -\exp[-2T](1 - \lambda T \exp[-2T])(\lambda + 1)^2/(1 + \lambda \exp[-2T])^2 \\
&= -(T + 1) \exp[-2T](1 + \lambda^2)/(1 + \lambda \exp[-2T])^2 \\
&\quad + T(1 + \lambda)^2 \exp[-2T]/(1 + \lambda \exp[-2T]) .
\end{aligned}$$

\square

Proposition 21. Let $\lambda \in (-1, +\infty)$ and $a : [0, T] \rightarrow \mathbb{R}$ such that for any $t \in [0, T]$,

$$a(t) = 1 - 2/(1 + \exp[-2(T - t)]\lambda) .$$

Then, we have that

$$\begin{aligned} & \exp[2 \int_0^T a(t)dt] - 1 - \int_0^T \exp[2 \int_{T-t}^T a(s)ds] \{ \int_{T-t}^T a(s)^2 ds + a(T) - 3a(T-t) \} dt \\ &= \exp[-2T](1 + \lambda)^2 / (1 + \lambda \exp[-2T])^2 - 1 \\ & \quad - (1/2)(1 + \lambda)(1 - \exp[-2T]) / (1 + \lambda \exp[-2T])(1 - 2/(1 + \lambda)) \\ & \quad - (3/2)(1 - \exp[-2T])(1 - \lambda^2 \exp[-2T]) / (1 + \lambda \exp[-2T])^2 \\ & \quad + (T/2)(1 + \lambda)^2 \exp[-2T] / (1 + \lambda \exp[-2T]) \\ & \quad - (1 + \lambda)^2 / (4\lambda) \log((1 + \lambda) / (1 + \lambda \exp[-2T])) \\ & \quad + (\lambda/2)(1 - \exp[-2T])^2 / (1 + \lambda \exp[-2T])^2 . \end{aligned}$$

In particular, we have

$$\begin{aligned} & \exp[2 \int_0^T a(t)dt] - 1 - \int_0^T \exp[2 \int_{T-t}^T a(s)ds] \{ \int_{T-t}^T a(s)^2 ds + a(T) - 3a(T-t) \} dt \\ &= -2 - (1 + \lambda)^2 / (4\lambda) \log(1 + \lambda) + O(\exp[-2T]) . \end{aligned}$$

Proof. Using Lemma 11, we have that

$$\exp[2 \int_0^T a(t)dt] = \exp[-2T](1 + \lambda)^2 / (1 + \lambda \exp[-2T])^2 . \quad (65)$$

Using Lemma 12, we have

$$\int_0^T \exp[2 \int_{T-t}^T a(s)ds] dt = (1/2)(1 + \lambda)(1 - \exp[-2t]) / (1 + \lambda \exp[-2t]) . \quad (66)$$

Using Lemma 14, we have

$$\begin{aligned} & \int_0^T \exp[2 \int_{T-t}^T a(s)ds] a(T-t) dt \\ &= -(1/2)(1 - \exp[-2T])(1 - \lambda^2 \exp[-2T]) / (1 + \lambda \exp[-2T])^2 . \end{aligned} \quad (67)$$

Finally, using Lemma 17, we have

$$\begin{aligned} & \int_0^T \exp[2 \int_{T-t}^T a(s)ds] (\int_{T-t}^T a(s)^2 ds) dt = -(T/2)(1 + \lambda)^2 \exp[-2T] / (1 + \lambda \exp[-2T]) \\ & \quad + (1 + \lambda)^2 / (4\lambda) \log((1 + \lambda) / (1 + \lambda \exp[-2T])) \\ & \quad - (\lambda/2)(1 - \exp[-2T])^2 / (1 + \lambda \exp[-2T])^2 . \end{aligned} \quad (68)$$

We conclude upon combining (65), (66), (67), (68) and that $a(T) = 1 - 2/(1 + \lambda)$. \square

10.4 General setting

In this section, we prove Theorem 2. In order to compare our results with (De Bortoli et al., 2021, Theorem 1), we redefine a few processes. Let $p \in \mathcal{P}(\mathbb{R}^d)$ be the target distribution. Consider the Ornstein-Uhlenbeck forward dynamics $(x_t)_{t \in [0, T]}$ such that $dx_t = -x_t dt + \sqrt{2} dw_t$ and x_0 has distribution p_0 . We consider the backward chain $(X_k)_{k \in \{0, \dots, N\}}$ such that for any $k \in \{0, \dots, N-1\}$,

$$X_k = X_{k+1} + \gamma_{k+1} \{ X_{k+1} + 2\nabla \log p_{t_{k+1}}(X_{k+1}) \} + \sqrt{2\gamma_{k+1}} Z_{k+1}, \quad (69)$$

with $\{Z_k\}_{k \in \mathbb{N}}$ a family of i.i.d. Gaussian random variables with zero mean and identity covariance matrix, $t_k = \sum_{\ell=1}^k \gamma_\ell$, $\sum_{\ell=1}^N \gamma_\ell = T$ and X_N has distribution $p_0 = \mathcal{N}(0, \text{Id})$ (independent from $\{Z_k\}_{k \in \mathbb{N}}$). Notice that here we do not consider a score approximation in the recursion in order to clarify our approximation results. We recall the following result from (De Bortoli et al., 2021, Theorem 1).

Theorem 22. Assume that p_0 admits a bounded density (w.r.t. the Lebesgue measure) $p_0 \in \mathcal{C}^3(\mathbb{R}^d, (0, +\infty))$ and that there exist $d_1, A_1, A_2, A_3 \geq 0$, $\beta_1, \beta_2, \beta_3 \in \mathbb{N}$ and $m_1 > 0$ such that for any $x \in \mathbb{R}^d$ and $i \in \{1, 2, 3\}$

$$\|\nabla^i \log p_0(x)\| \leq A_i(1 + \|x\|^{\beta_i}), \quad \langle \nabla \log p_0(x), x \rangle \leq -m_1 \|x\|^2 + d_1 \|x\| ,$$

with $\beta_1 = 1$. Then there exist $B, C, D \geq 0$ such that for any $N \in \mathbb{N}$ and $\{\gamma_k\}_{k=1}^N$ with $\gamma_k > 0$ for any $k \in \{1, \dots, N\}$ we have

$$\|\mathcal{L}(X_0) - p_0\|_{\text{TV}} \leq C \exp[DT] \sqrt{\gamma^*} + B \exp[-T]. \quad (70)$$

where $\gamma^* = \sup_{k \in \{1, \dots, N\}} \gamma_k$ and $\mathcal{L}(X_0)$ is the distribution of X_0 given in (69).

In the rest of this note we improve the theorem in the following way:

- (a) We remove the exponential dependency w.r.t. the time in the first term of the RHS of (70).
- (b) We provide explicit bounds $B, C, D \geq 0$ depending on the parameters of p_0 .

Lemma 23. *Assume*

$$\sup_{x,t} \|\nabla^2 \log p_t(x)\| \leq K \text{ and } \|\partial_t \nabla \log p_t(x)\| \leq M e^{-\alpha t} \|x\|.$$

Then there exists $D \geq 0$ such that for any $x \in \mathbb{R}^d$ and $t \in [0, T]$, $\|\nabla \log p_t(x)\| \leq D(1 + \|x\|)$ with $D = \|\nabla \log p_0(0)\| + K + CT$.

Proof. Let $x \in \mathbb{R}^d$ and $t \in [0, T]$. Since $(t, x) \mapsto \log p_t(x) \in C^2([0, T] \times \mathbb{R}^d, (0, +\infty))$, we have that

$$\begin{aligned} \nabla \log p_t(x) &= \nabla \log p_0(x) + \int_0^t \partial_s \nabla \log p_s(x) ds \\ &= \nabla \log p_0(0) + \int_0^1 \nabla^2 \log p_0(ux)(x) du + \int_0^t \partial_s \nabla \log p_s(x) ds. \end{aligned}$$

Therefore, we have that

$$\begin{aligned} \|\nabla \log p_t(x)\| &\leq \|\nabla \log p_0(0)\| + K\|x\| + \int_0^t \|\partial_s \nabla \log p_s(x)\| ds \\ &\leq \|\nabla \log p_0(0)\| + K\|x\| + M \sum_{k=0}^{N-1} (t_k - t_{k-1}) \exp[-\alpha t_k] \|x\| \\ &\leq \|\nabla \log p_0(0)\| + K\|x\| + MT\|x\|, \end{aligned}$$

which concludes the proof. \square

Note that in the previous proposition we can derive a tighter bound for D which does not depend on the limiting time $T > 0$. However, we do not use the bound $D > 0$ in our quantitative result and therefore our simple bound suffices.

We also have the following useful lemma.

Lemma 24. *Let $T \geq \log(2\mathbb{E}[\|X_0\|^2]) + \log(2)/2$ and assume that there exists $\eta > 0$ such that*

$$\int_{\mathbb{R}^d} p_\infty(x_T)^2 / p_T(x_T) dx_T \leq \exp[4] + E_T,$$

with $E_T \sim C \exp[-T]$ when $T \rightarrow +\infty$ and $C \geq 0$.

If p_∞ satisfies the following Φ -entropy inequality for any $f : \mathbb{R}^d \rightarrow (0, \infty)$ measurable

$$\int_{\mathbb{R}^d} \|\nabla f(x)\|^2 / f(x)^3 p_\infty(x) dx \leq C [\int_{\mathbb{R}^d} (1/f(x)) p_\infty(x) dx - 1 / (\int_{\mathbb{R}^d} f(x) p_\infty(x) dx)], \quad (71)$$

with $C \geq 0$. Then, we have as in (Bakry et al., 2014, Proposition 7.6.1)

$$\chi^2(p_\infty | p_t) = \int_{\mathbb{R}^d} p_\infty^2(x) / p_t(x) dx - 1 \leq e^{-Ct},$$

which immediately concludes the proof of Lemma 24. However, to the best of our knowledge, establishing (71) remains an open problem. Note that controlling $\chi^2(p_t | p_\infty)$ is much easier as the exponential decay of this divergence is linked with the Poincaré inequality which is satisfied in our Gaussian setting. In what follows, we consider another approach which relies on the structure of the Ornstein-Uhlenbeck transition kernel and provide non-tight upper bounds.

Proof. Let $T \geq 0$, $\varepsilon > 0$ and $x_T \in \mathbb{R}^d$

$$\|x_T - e^{-T} x_0\|^2 \leq (1 + \varepsilon) \|x_T\|^2 + (1 + 1/\varepsilon) e^{-2T} \|x_0\|^2.$$

Let $\varepsilon > 0$ and $x_T \in \mathbb{R}^d$, we have

$$p_T(x_T)^{-2} \leq \exp[(1 + \varepsilon) / \sigma_T^2 \|x_T\|^2]$$

$$\times \left(\int_{\mathbb{R}^d} p(x_0) \exp[-e^{-2T}(1+1/\varepsilon)/(2\sigma_T^2)\|x_0\|^2] dx_0 \right)^{-2} (2\pi\sigma_T^2)^d.$$

For any $x_T \in \mathbb{R}^d$, we have

$$\begin{aligned} p_\infty(x_T)^2/p_T(x_T) &\leq \exp\{-1 + (1+\varepsilon)/(2\sigma_T^2)\|x_T\|^2\} (2\pi/\sigma_T^2)^{-d/2} \\ &\quad \left(\int_{\mathbb{R}^d} p(x_0) \exp[-e^{-2T}(1+1/\varepsilon)/(2\sigma_T^2)\|x_0\|^2] dx_0 \right)^{-1}. \end{aligned}$$

In what follows, we set $\varepsilon = e^{-T}$. We have that

$$-1 + (1+\varepsilon)/(2\sigma_T^2) = (2\sigma_T^2)^{-1}(-2\sigma_T^2 + 1 + \varepsilon) = -(1 - 2e^{-T} + \varepsilon)/(2\sigma_T^2) = -(1 - e^{-T})/(2\sigma_T^2).$$

Therefore, we get that

$$\int_{\mathbb{R}^d} \exp\{-1 + (1+\varepsilon)/(2\sigma_T^2)\|x_T\|^2\} (2\pi/\sigma_T^2)^{-d/2} dx_T = (1 - e^{-T})^{-d/2}. \quad (72)$$

In addition, we have that for any $R \geq 0$ using that $\sigma_T^2 \geq 1/2$ since $T \geq \log(2)/2$

$$\begin{aligned} \int_{\mathbb{R}^d} p(x_0) \exp[-e^{-2T}(1+1/\varepsilon)/\sigma_T^2\|x_0\|^2] dx_0 &\geq \mathbb{P}(X_0 \in \bar{B}(0, R)) \exp[-e^{-2T}(1+1/\varepsilon)/\sigma_T^2 R^2] \\ &\geq \mathbb{P}(X_0 \in \bar{B}(0, R)) \exp[-4e^{-T} R^2] \end{aligned} \quad (73)$$

Now let $R^2 = e^T$. We obtain

$$\int_{\mathbb{R}^d} p(x_0) \exp[-e^{-2T}(1+1/\varepsilon)/\sigma_T^2\|x_0\|^2] dx_0 \geq \mathbb{P}(X_0 \in \bar{B}(0, e^{T/2})) \exp[-4].$$

In addition, using Markov inequality, we have

$$\mathbb{P}(X_0 \in \bar{B}(0, e^{T/2})) = 1 - \mathbb{P}(\|X_0\|^2 \geq e^T) \geq 1 - \mathbb{E}[\|X_0\|^2] e^{-T} \geq 0.$$

Therefore, combining this result and (73), we have

$$\int_{\mathbb{R}^d} p(x_0) \exp[-e^{-2T}(1+1/\varepsilon)/\sigma_T^2\|x_0\|^2] dx_0 \geq \exp[-4](1 - \mathbb{E}[\|X_0\|^2] e^{-T}) > 0. \quad (74)$$

We conclude upon combining (72) and (74). \square

We are now ready to state the following lemma.

Lemma 25. *There exists a unique strong solution to the SDE $dy_t = \{y_t + 2\nabla \log p_{T-t}(y_t)\} dt + \sqrt{2} dw_t$ with initial condition $\mathcal{L}(y_0) = p_\infty$. In addition, we have that $\mathbb{E}[\sup_{t \in [0, T]} \|y_t\|^\alpha] < +\infty$ for any $\alpha > 0$.*

Proof. Let $b : [0, T] \times \mathbb{R}^d$ given for any $t \in [0, T]$ and $x \in \mathbb{R}^d$ by $b(t, x) = x + 2\nabla \log p_t(x)$. We have that $b \in C^1([0, T] \times \mathbb{R}^d, \mathbb{R}^d)$ and in particular is locally Lipschitz. In addition, using Lemma 23 we have that for any $t \in [0, T]$ and $x \in \mathbb{R}^d$, $\|b(t, x)\| \leq (1 + D)\|x\|$. Hence using (Ikeda and Watanabe, 1989, Theorem 2.3, Theorem 3.1) and (Meyn and Tweedie, 1993, Theorem 2.1) (with $V(x) = (1/2)\|x\|^2$) there exists a unique strong solution to the SDE $dy_t = \{y_t + 2\nabla \log p_{T-t}(y_t)\} dt + \sqrt{2} dw_t$ with initial condition $\mathcal{L}(y_0) = p_\infty$. Let $\alpha > 1$, then we have for any $t \in [0, T]$

$$\sup_{s \in [0, t]} \|y_t\|^\alpha \leq 3^{\alpha-1} [\|y_0\|^\alpha + t^{\alpha-1} (1 + D)^\alpha \int_0^t \sup_{u \in [0, s]} \|y_u\|^\alpha du + 2^{\alpha/2} \sup_{s \in [0, t]} \|w_u\|^\alpha].$$

Using that $\mathbb{E}[\sup_{s \in [0, T]} \|w_u\|^\alpha]$ and Grönwall's lemma, we get that $\mathbb{E}[\sup_{t \in [0, T]} \|y_t\|^\alpha] < +\infty$ for any $\alpha > 1$. The result is extended to any $\alpha > 0$ since for any $\alpha \in (0, 1]$ we have that

$$\mathbb{E}[\sup_{t \in [0, T]} \|y_t\|^\alpha] \leq \mathbb{E}[\sup_{t \in [0, T]} \|y_t\|]^\alpha < +\infty.$$

\square

We are now ready to prove Theorem 2.

Proof. The beginning of the proof is similar to the one of (De Bortoli et al., 2021, Theorem 1). For any $k \in \{1, \dots, N\}$, denote R_k the Markov kernel such that for any $x \in \mathbb{R}^d$, $A \in \mathcal{B}(\mathbb{R}^d)$ and $k \in \{0, \dots, N-1\}$ we have

$$R_{k+1}(x, A) = (4\pi\gamma_{k+1})^{-d/2} \int_A \exp[-\|\tilde{x} - \mathcal{T}_{k+1}(x)\|^2 / (4\gamma_{k+1})] d\tilde{x},$$

where for any $x \in \mathbb{R}^d$, $\mathcal{T}_{k+1}(x) = x + \gamma_{k+1}\{x + 2\nabla \log p_{t_{k+1}}(x)\}$. Define for any $k_0, k_1 \in \{1, \dots, N\}$ with $k_1 \geq k_0$ $Q_{k_0, k_1} = \prod_{\ell=k_0}^{k_1} R_{k_1+k_0-\ell}$. Finally, for ease of notation, we also define for any $k \in \{1, \dots, N\}$, $Q_k = Q_{k+1, N}$. Note that for any $k \in \{1, \dots, N\}$, X_k has distribution $p_\infty Q_k$, where $p_\infty \in \mathcal{P}(\mathbb{R}^d)$ with density w.r.t. the Lebesgue measure p_∞ . Let $\mathbb{P} \in \mathcal{P}(\mathcal{C})$ be the probability measure associated with the diffusion

$$dx_t = -x_t dt + \sqrt{2} dw_t, \quad x_0 \sim p_0,$$

First, we have for any $A \in \mathcal{B}(\mathbb{R}^d)$

$$p_0 \mathbb{P}_{T|0}(\mathbb{P}^R)_{T|0}(A) = \mathbb{P}_T(\mathbb{P}^R)_{T|0}(A) = (\mathbb{P}^R)_0(\mathbb{P}^R)_{T|0}(A) = (\mathbb{P}^R)_T(A) = p_0(A).$$

Hence $p_0 = p_0 \mathbb{P}_{T|0}(\mathbb{P}^R)_{T|0}$. Using this result we have

$$\begin{aligned} \|p_0 - p_\infty Q_0\|_{\text{TV}} &= \|p_0 \mathbb{P}_{T|0}(\mathbb{P}^R)_{T|0} - p_\infty Q_0\|_{\text{TV}} \\ &\leq \|p_0 \mathbb{P}_{T|0}(\mathbb{P}^R)_{T|0} - p_\infty(\mathbb{P}^R)_{T|0}\|_{\text{TV}} + \|p_\infty(\mathbb{P}^R)_{T|0} - p_\infty Q_0\|_{\text{TV}} \\ &\leq \|p_0 \mathbb{P}_{T|0} - p_\infty\|_{\text{TV}} + \|p_\infty(\mathbb{P}^R)_{T|0} - p_\infty Q_0\|_{\text{TV}}. \end{aligned}$$

Note that $\mathcal{L}(X_0) = p_\infty Q_0$ and therefore

$$\|\mathcal{L}(X_0) - p_0\|_{\text{TV}} \leq \|p_0 \mathbb{P}_{T|0} - p_\infty\|_{\text{TV}} + \|p_\infty(\mathbb{P}^R)_{T|0} - p_\infty Q_0\|_{\text{TV}}.$$

We now bound each one of these terms.

(a) First, we bound $\|p_0 \mathbb{P}_{T|0} - p_\infty\|_{\text{TV}}$. Using the Pinsker inequality (Bakry et al., 2014, Equation 5.2.2) we have that

$$\|p_0 \mathbb{P}_{T|0} - p_\infty\|_{\text{TV}} \leq \sqrt{2} \text{KL}(p_0 \mathbb{P}_{T|0} \| p_\infty)^{1/2}. \quad (75)$$

In addition, p_∞ satisfies the log-Sobolev inequality with constant $C = 1$, Gross (1975). Namely, for any $f \in C^1(\mathbb{R}^d, (0, +\infty))$ such that $f \in L^1(p_\infty)$ and $\int_{\mathbb{R}^d} \|\nabla \log f(x)\|^2 f(x) dp_\infty(x) < +\infty$ we have

$$\begin{aligned} \int_{\mathbb{R}^d} f(x) \log f(x) dp_\infty(x) - \left(\int_{\mathbb{R}^d} f(x) dp_\infty(x)\right) \left(\log \int_{\mathbb{R}^d} f(x) dp_\infty(x)\right) \\ \leq (C/2) \int_{\mathbb{R}^d} \|\nabla \log f(x)\|^2 f(x) dp_\infty(x), \end{aligned}$$

with $C = 1$. Therefore, using (Bakry et al., 2014, Theorem 5.2.1) we have that for any $f \in L^1(p_\infty)$ with $\int_{\mathbb{R}^d} |f(x)| |\log f(x)| dp_\infty(x) < +\infty$

$$\text{Ent}_{p_\infty}(\mathbb{P}_{T|0}[f]) \leq \exp[-2T] \text{Ent}_{p_\infty}(f), \quad (76)$$

where for any $g \in L^1(p_\infty)$ with $\int_{\mathbb{R}^d} |g(x)| |\log g(x)| dp_\infty(x) < +\infty$ we define

$$\text{Ent}_{p_\infty}(g) = \int_{\mathbb{R}^d} g(x) \log g(x) dp_\infty(x) - \left(\int_{\mathbb{R}^d} g(x) dp_\infty(x)\right) \left(\log \int_{\mathbb{R}^d} g(x) dp_\infty(x)\right).$$

Note that $(dp_T/dp_\infty) = \mathbb{P}_{T|0}[dp_0/dp_\infty]$ and that for any $\mu \in \mathcal{P}(\mathbb{R}^d)$ with $\text{KL}(\mu \| p_\infty) < +\infty$ we have $\text{Ent}_{p_\infty}(d\mu/dp_\infty) = \text{KL}(\mu \| p_\infty)$. Using these results, (75) and (76) we get that

$$\|p_0 \mathbb{P}_{T|0} - p_\infty\|_{\text{TV}} \leq \sqrt{2} \exp[-T] \text{KL}(p_0 \| p_\infty)^{1/2}. \quad (77)$$

In addition, we have that

$$\text{KL}(p_0 \| p_\infty) = (d/2) \log(2\pi) + \int_{\mathbb{R}^d} \|x\|^2 dp_0(x) - H(p_0),$$

where $H(p_0) = -\int_{\mathbb{R}^d} \log(p_0(x)) p_0(x) dx$. Combining this result and (77) we get that

$$\|p_0 \mathbb{P}_{T|0} - p_\infty\|_{\text{TV}} \leq \sqrt{2} \exp[-T] \left((d/2) \log(2\pi) + \int_{\mathbb{R}^d} \|x\|^2 dp_0(x) - H(p_0) \right)^{1/2},$$

which concludes the first part of the proof.

(b) First, let $\mathbb{Q} \in \mathcal{P}(\mathcal{C})$ such that $\mathbb{Q} = p_\infty \mathbb{P}_{|0}^R$, where $\mathbb{P}_{|0}^R$ is the disintegration of \mathbb{P}^R w.r.t. $\phi : \mathcal{C} \rightarrow \mathbb{R}^d$ given for any $\omega \in \mathcal{C}$ by $\phi(\omega) = \omega_T$, see [Léonard \(2014\)](#) for instance. Note that for any $f \in C(\mathcal{C})$ with f bounded we have

$$\begin{aligned} \mathbb{Q}[f] &= \int_{\mathbb{R}^d} \int_{\mathcal{C}} f(\omega) \mathbb{P}_{|0}^R(\omega_0, d\omega) dp_\infty(\omega_0) = \int_{\mathbb{R}^d} \int_{\mathcal{C}} f(\omega) \mathbb{P}_{|0}^R(\omega_0, d\omega) (dp_\infty/dp_T)(\omega_0) dp_T(\omega_0) \\ &= \int_{\mathcal{C}} f(\omega) (dp_\infty/dp_T)(\omega_0) d\mathbb{P}^R(\omega). \end{aligned}$$

Therefore, we get that for any $\omega \in \mathcal{C}$, $(d\mathbb{Q}/d\mathbb{P}^R)(\omega) = (dp_\infty/dp_T)(\omega_0)$. Let $\mathbb{R} = p_\infty \mathbb{P}_{|0}$. Note that for any $t \in [0, T]$, $\mathbb{R}_t = p_\infty$ and that \mathbb{R} is associated with the process $dx_t = -x_t dt + \sqrt{2} dw_t$ with $\mathcal{L}(x_0) = p_\infty$. In particular, \mathbb{R} satisfies ([Cattiaux et al., 2021](#), Hypothesis 1.8). Using ([Léonard, 2014](#), Theorem 2.4) we have that

$$\text{KL}(\mathbb{P} \parallel \mathbb{R}) = \text{KL}(p_0 \parallel p_\infty) + \int_{\mathbb{R}^d} \text{KL}(\mathbb{P}_{|0}(x_0) \parallel \mathbb{P}_{|0}(x_0)) dp_0(x_0) = \text{KL}(p_0 \parallel p_\infty) < +\infty.$$

Therefore, we can apply ([Cattiaux et al., 2021](#), Theorem 4.9). Let $u \in C_c^\infty(\mathbb{R}^d, \mathbb{R})$, we have that $(\mathbf{M}_t^u(y))_{t \in [0, T]}$ is a local martingale, where we have for any $t \in [0, T]$

$$\mathbf{M}_t^u(y) = u(y_t) - u(y_0) - \int_0^t \{ \langle \nabla u(y_s), y_s + 2\nabla \log p_{T-s}(y_s) \rangle + \Delta u(y_s) \} ds,$$

where $\mathcal{L}(y) = \mathbb{P}^R$. Since u is compactly supported we have that $\sup_{\omega \in \mathcal{C}} \sup_{t \in [0, T]} |\mathbf{M}_t^u(\omega)| < +\infty$ and therefore $(\mathbf{M}_t^u(y))_{t \in [0, T]}$ is a martingale. We now show that $(\mathbf{M}_t^u(y))_{t \in [0, T]}$ is a martingale, with $\mathcal{L}(y) = \mathbb{Q}$. Since $\sup_{\omega \in \mathcal{C}} \sup_{t \in [0, T]} |\mathbf{M}_t^u(\omega)| < +\infty$, we have that for any $t \in [0, T]$, $\mathbb{E}[|\mathbf{M}_t^u|] < +\infty$. Let $t, s \in [0, T]$ with $t > s$ and $g : \mathcal{C} \rightarrow \mathbb{R}^d$ bounded. We have that $\mathbb{E}[|g(\{x_{T-s}\}_{s \in [0, t]})|^2 (dp_\infty/dp_T)(x_T)^2] < +\infty$. Hence, we have that

$$\mathbb{E}[(\mathbf{M}_t^u(x_{T-\cdot}) - \mathbf{M}_s^u(x_{T-\cdot}))g(\{x_{T-s}\}_{s \in [0, t]}) (dp_\infty/dp_T)(x_T)] = 0.$$

Using this result and that for any $\omega \in \mathcal{C}$, $(d\mathbb{Q}/d\mathbb{P}^R)(\omega) = (dp_\infty/dp_T)(\omega_0)$ we get

$$\mathbb{E}[(\mathbf{M}_t^u(y) - \mathbf{M}_s^u(y))g(\{y_s\}_{s \in [0, t]})] = 0.$$

Hence, for any $u \in C_c^2(\mathbb{R}^d, \mathbb{R})$, $(\mathbf{M}_t^u(y))_{t \in [0, T]}$ is a martingale. In addition, $(\mathbf{M}_t^u(\mathbf{Z}))_{t \in [0, T]}$ is a martingale using Lemma 25 and Itô's lemma, where \mathbf{Z} is the solution to the SDE in Lemma 25. In addition, we have that $\mathcal{L}(\mathbf{Z}_0) = \mathcal{L}(y_0) = p_\infty$. Using Lemma 23 and the remark following ([Cattiaux et al., 2021](#), Hypothesis 1.8), we get that $\mathcal{L}(\mathbf{Z}) = \mathcal{L}(y) = \mathbb{Q}$. We have just shown that the time-reversed process with initialisation p_∞ can be obtained as a strong solution of an SDE. Using Lemma 23 and Lemma 25, we have that for any $t \in [0, T]$

$$\mathbb{E}[\int_0^t \|x_s + 2\nabla \log p_s(x_s)\|^2 ds + \int_0^t \|w_s + 2\nabla \log p_s(w_s)\|^2 ds] < +\infty.$$

Combining this result and ([De Bortoli et al., 2021](#), Lemma S13) we have that

$$\|p_\infty \mathbb{P}_{T|0}^R - p_\infty \mathbb{Q}_0\|_{TV}^2 \leq (1/2) \int_0^T \mathbb{E}[\|b_1(t, (y_s)_{s \in [0, T]}) - b_2(t, (y_s)_{s \in [0, T]})\|^2] dt, \quad (78)$$

where for any $t \in [0, T]$ and $\omega \in \mathcal{C}$ we have that

$$b_1(t, \omega) = \omega_t + 2\nabla \log p_{T-t}(\omega_t), \quad b_2(t, \omega) = \omega_{t_\gamma} + 2\nabla \log p_{T-t_\gamma}(\omega_{t_\gamma}),$$

where $t_\gamma = \sum_{k=0}^{N-1} \mathcal{N}_{[T-t_{k+1}, T-t_k]}(t)(T-t_{k+1})$. Noting that $(y_t)_{t \in [0, T]}$ is distributed according to \mathbb{Q} and using that $(d\mathbb{Q}/d\mathbb{P}^R)(\omega) = (dp_\infty/dp_T)(\omega_0)$, (78) and the Cauchy-Schwarz inequality we have

$$\begin{aligned} &\|p_\infty \mathbb{P}_{T|0}^R - p_\infty \mathbb{Q}_0\|_{TV}^2 \quad (79) \\ &\leq (1/2) \mathbb{E}[(dp_\infty/dp_T)(x_T)^2]^{1/2} \int_0^T \mathbb{E}^{1/2}[\|b_1(t, (x_{T-s})_{s \in [0, T]}) - b_2(t, (x_{T-s})_{s \in [0, T]})\|^4] dt \\ &\leq (1/2) \mathbb{E}[(dp_\infty/dp_T)(x_T)^2]^{1/2} \\ &\quad \times \int_0^T \mathbb{E}^{1/2}[\|b_1(T-t, (x_{T-s})_{s \in [0, T]}) - b_2(T-t, (x_{T-s})_{s \in [0, T]})\|^4] dt. \end{aligned}$$

In addition, we have that for any $t \in [0, T]$ and $\omega \in \mathcal{C}$ we have

$$\begin{aligned} &\|b_1(t, \omega) - b_2(t, \omega)\| \\ &\leq \|\omega_t - \omega_{t_\gamma}\| + 2\|\nabla \log p_{T-t}(\omega_t) - \nabla \log p_{T-t_\gamma}(\omega_t)\| \end{aligned}$$

$$\begin{aligned}
& + 2\|\nabla \log p_{T-t_\gamma}(\omega_t) - \nabla \log p_{T-t_\gamma}(\omega_{t_\gamma})\| \\
& \leq (1 + 2 \sup_{s \in [0, T]} \sup_{x \in \mathbb{R}^d} \|\nabla^2 \log p_s(x)\|) \|\omega_t - \omega_{t_\gamma}\| \\
& \quad + 2 \sup_{s \in [T-t, T-t_\gamma]} \|\partial_t \nabla \log p_t(\omega_t)\| (t - t_\gamma) \\
& \leq (1 + 2K) \|\omega_t - \omega_{t_\gamma}\| + 2 \sup_{s \in [T-t, T-t_\gamma]} \|\partial_s \nabla \log p_s(\omega_t)\| (t - t_\gamma).
\end{aligned}$$

Note that

$$T - (T - t)_\gamma = T - \sum_{k=0}^{N-1} \mathbb{1}_{[T-t_{k+1}, T-t_k)}(T - t)(T - t_{k+1}) = \sum_{k=0}^{N-1} \mathbb{1}_{(t_k, t_{k+1}]}(t) t_{k+1}.$$

For any $t \in [0, T]$, denote $t^\gamma = T - (T - t)_\gamma = \sum_{k=0}^{N-1} \mathbb{1}_{(t_k, t_{k+1}]}(t) t_{k+1}$. Therefore, we get that for any $t \in (t_k, t_{k+1}]$

$$\begin{aligned}
& \|b_1(T - t, \omega) - b_2(T - t, \omega)\| \\
& \leq (1 + 2K) \|\omega_{T-t} - \omega_{(T-t)_\gamma}\| + 2 \sup_{s \in [t, t^\gamma]} \|\partial_s \nabla \log p_s(\omega_{T-t})\| (t^\gamma - t) \\
& \leq (1 + 2K) \|\omega_{T-t} - \omega_{(T-t)_\gamma}\| + 2 \sup_{s \in [t_k, t_{k+1}]} \|\partial_s \nabla \log p_s(\omega_{T-t})\| \gamma_{k+1} \\
& \leq (1 + 2K) \|\omega_{T-t} - \omega_{(T-t)_\gamma}\| + 2S_{t_k}(\omega_{T-t}) \gamma_{k+1}.
\end{aligned}$$

Combining this result and that for any $a, b \geq 0$, $(a+b)^4 \leq 8a^4 + 8b^4$ we get that for any $t \in (t_k, t_{k+1}]$

$$\begin{aligned}
& \mathbb{E}[\|b_1(T - t, (x_{T-s})_{s \in [0, T]}) - b_2(T - t, (x_{T-s})_{s \in [0, T]})\|^4] \\
& \leq 8(1 + 2K)^4 \mathbb{E}[\|x_t - x_{t_k}\|^4] + 16\mathbb{E}[S_{t_k}(x_t)^4] \gamma_{k+1}^4.
\end{aligned} \tag{80}$$

In addition, we have that for any $t \in [0, T]$, $x_t = \exp[-t]x_0 + w_{(1-\exp[-2t])^{1/2}}$. Hence, for any $s, t \in [0, T]$ with $t > s$ we have

$$\|x_t - x_s\| \leq \exp[-s](\exp[t - s] - 1)\|x_0\| + \|w_{(1-\exp[-2t])} - w_{(1-\exp[-2s])}\|.$$

Therefore, we have that for any $s, t \in [0, T]$ with $t > s$

$$\begin{aligned}
\mathbb{E}[\|x_t - x_s\|^4] & \leq 8 \exp[-4s](1 - \exp[-t + s])^4 \mathbb{E}[\|x_0\|^4] + 8\mathbb{E}[\|w_{(1-\exp[-2t])} - w_{(1-\exp[-2s])}\|^4] \\
& \leq 8 \exp[-4s](1 - \exp[-t + s])^4 \mathbb{E}[\|x_0\|^4] + 24(\exp[-t] - \exp[-s])^2 \\
& \leq 8 \exp[-4s](1 - \exp[-t + s])^4 \mathbb{E}[\|x_0\|^4] + 24 \exp[-2s](1 - \exp[-t + s])^2 \\
& \leq 8\mathbb{E}[\|x_0\|^4] \exp[-4s](t - s)^4 + 24 \exp[-2s](t - s)^2.
\end{aligned} \tag{81}$$

In addition, using that for any $k \in \{0, \dots, N-1\}$ and $x \in \mathbb{R}^d$, $S_{t_k}(x) \leq M \exp[-\alpha t_k] \|x\|$ we get that

$$\mathbb{E}[S_{t_k}(x_t)^4] \leq 24M^4 \exp[-4\alpha t_k] \{1 + \mathbb{E}[\|x_0\|^4]\}.$$

Combining this result, (80) and (81) we get that for any $t \in (t_k, t_{k+1}]$

$$\begin{aligned}
& \mathbb{E}[\|b_1(T - t, (x_{T-s})_{s \in [0, T]}) - b_2(T - t, (x_{T-s})_{s \in [0, T]})\|^4] \\
& \leq 64(1 + 2K)^4 \mathbb{E}[\|x_0\|^4] \exp[-4t_k] \gamma_{k+1}^4 \\
& \quad + 192(1 + 2K)^4 \exp[-2t_k] \gamma_{k+1}^2 + 384M^4 \exp[-4\alpha t_k] \{1 + \mathbb{E}[\|x_0\|^4]\} \gamma_{k+1}^4.
\end{aligned}$$

Using this result and that for any $a, b \geq 0$, $(a+b)^{1/2} \leq a^{1/2} + b^{1/2}$, we have for any $t \in (t_k, t_{k+1}]$

$$\begin{aligned}
& \mathbb{E}^{1/2}[\|b_1(T - t, (x_{T-s})_{s \in [0, T]}) - b_2(T - t, (x_{T-s})_{s \in [0, T]})\|^4] \\
& \leq 8(1 + 2K)^2 \mathbb{E}^{1/2}[\|x_0\|^4] \exp[-2t_k] \gamma_{k+1}^2 \\
& \quad + 14(1 + 2K)^2 \exp[-t_k] \gamma_{k+1} + 20M^2 \exp[-2\alpha t_k] \{1 + \mathbb{E}^{1/2}[\|x_0\|^4]\} \gamma_{k+1}^2.
\end{aligned} \tag{82}$$

We have that for any $\beta > 0$,

$$\sum_{k=0}^{N-1} \exp[-\beta t_k] \leq \sum_{k \in \mathbb{N}} \exp[-\beta \gamma_* k] \leq (1 - \exp[-\beta \gamma_*])^{-1} \leq 1 + \beta / \gamma_*.$$

Then using this result, (82) and (79) we get that

$$\|p_\infty \mathbb{P}_{T|0}^R - p_\infty \mathbb{Q}_0\|_{TV}^2 \leq \mathbb{E}[(dp_\infty / dp_T)(x_T)^2]^{1/2} [4(1 + 2K)^2 \mathbb{E}^{1/2}[\|x_0\|^4] (1 + \beta / (2\gamma_*)) (\gamma^*)^3]$$

$$+ 7(1 + 2K)^2(1 + 1/\gamma_*)(\gamma^*)^2 + 10M^2\{1 + \mathbb{E}^{1/2}[\|x_0\|^4]\}(1 + 1/(2\alpha\gamma_*))(\gamma^*)^3\}.$$

Therefore, we get that

$$\begin{aligned} \|p_\infty \mathbb{P}_{T|0}^R - p_\infty Q_0\|_{\text{TV}} &\leq \mathbb{E}[(dp_\infty/dp_T)(x_T)^2]^{1/4} [2(1 + 2K)\mathbb{E}^{1/4}[\|x_0\|^4](1 + 1/(2\gamma_*)^{1/2})(\gamma^*)^{3/2} \\ &\quad + 3(1 + 2K)(1 + 1/\gamma_*^{1/2})\gamma^* + 4M\{1 + \mathbb{E}^{1/4}[\|x_0\|^4]\}(1 + 1/(2\alpha\gamma_*)^{1/2})(\gamma^*)^{3/2}] \\ &\leq \mathbb{E}[(dp_\infty/dp_T)(x_T)^2]^{1/4} [6(1 + 2K)(1 + \mathbb{E}^{1/4}[\|x_0\|^4]) \\ &\quad + 4M\{1 + \mathbb{E}^{1/4}[\|x_0\|^4]\}(1 + 1/(2\alpha)^{1/2})]((\gamma^*)^2/\gamma_*)^{1/2} \\ &\leq 6(1 + \mathbb{E}^{1/4}[\|x_0\|^4])\mathbb{E}[(dp_\infty/dp_T)(x_T)^2]^{1/4} [1 + K + M(1 + 1/(2\alpha)^{1/2})]((\gamma^*)^2/\gamma_*)^{1/2}, \end{aligned}$$

which concludes the proof upon using Lemma 24. \square

We now check that the assumption of Theorem 2 are satisfied in a Gaussian setting.

Proposition 26. *Assume that $p_0 = N(0, \Sigma)$ and that $T \geq 1 + (1/2)[\log^+(\|\Sigma\|) + \log(d + 1)]$ then we have that for any $t \in [0, T]$ and $x \in \mathbb{R}^d$*

$$\|\nabla^2 \log p_t(x)\| \leq \max(1, \|\Sigma^{-1}\|), \quad \|\partial_t \nabla \log p_t(x)\| \leq 2 \exp[-2t] \max(1, \|\Sigma^{-1}\|)^2 \|\Sigma - \text{Id}\| \|x\|.$$

In addition, we have that $\int_{\mathbb{R}^d} p_\infty(x)^2/p_T(x) dx \leq \sqrt{2}$.

Proof. Recall that for any $t \in [0, T]$, $x_t = \exp[-t]x_0 + w_{1-\exp[-2t]}$. Therefore, we have that for any $t \in [0, T]$, $p_t = N(0, \Sigma_t)$ with $\Sigma_t = \exp[-2t]\Sigma + (1 - \exp[-2t])\text{Id}$. Hence, we get that for any $t \in [0, T]$ and $x \in \mathbb{R}^d$, $\nabla^2 \log p_t(x) = (\exp[-2t]\Sigma + (1 - \exp[-2t])\text{Id})^{-1}$. Using this result, we have that for any $t \in [0, T]$ and $x \in \mathbb{R}^d$, $\|\nabla^2 \log p_t(x)\| \leq \max(1, \|\Sigma^{-1}\|)$. Similarly, for any $t \in [0, T]$ and $x \in \mathbb{R}^d$ we have

$$\partial_t \nabla \log p_t(x) = \partial_t \Sigma_t^{-1} x = -\Sigma_t^{-1} (\partial_t \Sigma_t) \Sigma_t^{-1} x.$$

Hence, for any $t \in [0, T]$ and $x \in \mathbb{R}^d$ we have $\|\partial_t \nabla \log p_t(x)\| \leq 2 \exp[-2t] \max(1, \|\Sigma^{-1}\|)^2 \|\Sigma - \text{Id}\| \|x\|$. Finally, we have that for any $t \in [0, T]$ and $x \in \mathbb{R}^d$

$$\langle x, [2\text{Id} - (\exp[-2t]\Sigma + (1 - \exp[-2t])\text{Id})^{-1}]x \rangle \geq (2 - (\exp[-2t]\|\Sigma^{-1}\|^{-1} + (1 - \exp[-2t])^{-1}))\|x\|^2.$$

Let $\varepsilon \in (0, 1/2]$. For any $t \in [0, T]$, we have that $2 - (\exp[-2t]\|\Sigma^{-1}\|^{-1} + (1 - \exp[-2t])^{-1}) \geq 1 - \varepsilon$ if and only if $\exp[-2t](1 - \|\Sigma^{-1}\|^{-1}) \leq 1 - (1 + \varepsilon)^{-1}$. Using that $-\log(1 - (1 + \varepsilon)^{-1}) = \log(1 + \varepsilon^{-1})$ we have that for any $t \geq (1/2) \log(1 + \varepsilon^{-1})$ and $x \in \mathbb{R}^d$

$$p_\infty(x)^2/p_t(x) \leq \exp[-\|x\|^2/4](2\pi)^{-d/2} \det(\Sigma_t).$$

Combining this result and the fact that $\int_{\mathbb{R}^d} \exp[-\|x\|^2/2(1 - \varepsilon)] dx = (2(1 - \varepsilon)\pi)^{d/2}$, we get that for any $t \geq (1/2) \log(1 + \varepsilon^{-1})$

$$\int_{\mathbb{R}^d} p_\infty(x)^2/p_t(x) dx \leq \int_{\mathbb{R}^d} \exp[-\|x\|^2/2(1 - \varepsilon)] (2\pi)^{-d/2} \det(\Sigma_t)^{1/2} dx \leq (1 - \varepsilon)^{d/2} \det(\Sigma_t)^{1/2}.$$

Let $\varepsilon = 1/(2d) \leq 1/2$. Note that $T \geq (1/2)\{-\log(\|\Sigma^{-1}\|^{-1} - 1) + \log(1 + 2d)\}$. Hence, we have that

$$\int_{\mathbb{R}^d} p_\infty(x)^2/p_T(x) dx \leq \exp[-\log(1 - 1/(2d))(d/2)] \det(\Sigma_T)^{1/2}.$$

Since for any $t \in [0, 1/2]$, $-\log(1 - t) \leq \log(2)t$ we get that

$$\int_{\mathbb{R}^d} p_\infty(x)^2/p_T(x) dx \leq 2^{1/4} \det(\Sigma_T)^{1/2}. \quad (83)$$

Finally, using that $\Sigma_T = \exp[-2T]\Sigma + (1 - \exp[-2T])\text{Id}$ we have that

$$\det(\Sigma_T)^{1/2} \leq (\exp[-2T]\|\Sigma\| + 1 - \exp[-2T])^{d/2} \leq (1 + \exp[-2T]\|\Sigma\|)^{d/2}.$$

Hence, using that result and that for any $t \geq 0$, $\log(1 + t) \leq t$ we have

$$\det(\Sigma_T)^{1/2} \leq \exp[\exp[-2T]\|\Sigma\|(d/2)].$$

Since, $T \geq (1/2)\{\log(\|\Sigma\|) + \log(d) + \log(2) - \log(\log(2^{1/4}))\}$, we get that $\det(\Sigma_T)^{1/2} \leq 2$, which concludes the proof upon combining this result and (83). \square

Therefore, we get the following simplified result in the Gaussian setting.

Corollary 27. *Assume that $p = \mathcal{N}(0, \Sigma)$, with $\|\Sigma^{-1}\| \geq 1$, $\gamma^* = \gamma_* = \gamma > 0$ and $T \geq 1 + (1/2)[\log^+(\|\Sigma\|) + \log(d+1)]$, then we have*

$$\begin{aligned} \|\mathcal{L}(X_0) - p_0\|_{\text{TV}} &\leq \exp[-T/2](\log^+(\|\Sigma^{-1}\|) + \|\Sigma - \text{Id}\|)^{1/2} \\ &\quad + 48(1 + \|\Sigma\|^{1/2}d^{1/2})\|\Sigma^{-1}\|^2[1 + \|\Sigma - \text{Id}\|]\sqrt{\gamma}. \end{aligned}$$

Proof. Using (30) and Proposition 26 we have

$$\begin{aligned} \|\mathcal{L}(X_0) - p_0\|_{\text{TV}} &\leq \exp[-T/2](-\log(\det(\Sigma)) + \text{Tr}(\Sigma) - d)^{1/2} \\ &\quad + 12(1 + (\int_{\mathbb{R}^d} \|x\|^4 dp_0(x))^{1/4})[1 + K + 2C]\sqrt{(\gamma^*)^2/\gamma_*} \\ &\leq \exp[-T/2](-\log(\det(\Sigma)) + \text{Tr}(\Sigma) - d)^{1/2} \\ &\quad + 12(1 + (\int_{\mathbb{R}^d} \|x\|^4 dp_0(x))^{1/4})[1 + \|\Sigma^{-1}\| + 2\|\Sigma^{-1}\|^2\|\Sigma - \text{Id}\|]\sqrt{(\gamma^*)^2/\gamma_*} \\ &\leq \exp[-T/2](-\log(\det(\Sigma)) + \text{Tr}(\Sigma) - d)^{1/2} \\ &\quad + 12(1 + 3^{1/4}\|\Sigma\|^{1/2}d^{1/2})[1 + \|\Sigma^{-1}\| + 2\|\Sigma^{-1}\|^2\|\Sigma - \text{Id}\|]\sqrt{(\gamma^*)^2/\gamma_*} \\ &\leq \exp[-T/2](-\log(\det(\Sigma)) + \text{Tr}(\Sigma) - d)^{1/2} \\ &\quad + 48(1 + \|\Sigma\|^{1/2}d^{1/2})\|\Sigma^{-1}\|^2[1 + \|\Sigma - \text{Id}\|]\sqrt{(\gamma^*)^2/\gamma_*} \\ &\leq \exp[-T/2](\log^+(\|\Sigma^{-1}\|) + \|\Sigma - \text{Id}\|)^{1/2} \\ &\quad + 48(1 + \|\Sigma\|^{1/2}d^{1/2})\|\Sigma^{-1}\|^2[1 + \|\Sigma - \text{Id}\|]\sqrt{(\gamma^*)^2/\gamma_*}. \end{aligned}$$

□

11 Proof of Theorem 3

Proof. For any x and j , denote $\bar{p}_{j,0}(\cdot|x)$ the distribution of $\bar{x}_{j,0}$ given $x_j = x$ and $p_{j,0}$ the distribution of $\tilde{x}_{j,0}$. For any j we have

$$\text{KL}(p_j \| p_{j,0}) = \text{KL}(p_{j+1} \| p_{j+1,0}) + \mathbb{E}[\text{KL}(\bar{p}_{j+1}(\cdot|x_{j+1}) \| \bar{p}_{j+1,0}(\cdot|x_{j+1}))].$$

By recursion, we have that

$$\text{KL}(p \| p_0) = \text{KL}(p_J \| p_{J,0}) + \sum_{j=1}^J \mathbb{E}[\text{KL}(\bar{p}_j(\cdot|x_j) \| \bar{p}_{j,0}(\cdot|x_j))].$$

Combining Proposition 9 and Lemma 4, we get that

$$\text{KL}(p \| p_0) \leq (\delta + \exp[-4T])(2^{-J}L)^n + \sum_{j=1}^J (\delta + \exp[-4T])(2^{-j}L)^n(2^n - 1) + E_{T,\delta}.$$

Therefore, $\text{KL}(p \| p_0) \leq (\delta + \exp[-4T])L^n + E_{T,\delta}$, which concludes the proof. □

12 Experimental Details on Gaussian Experiments

We now give some details on the experiments in Section 3.2 (Figure 2). We use the exact formulas for the Stein score of p_t in this case: if $x_0 \sim \mathcal{N}(M, \Sigma)$, then $x_t \sim \mathcal{N}(M_t, \Sigma_t)$ with $M_t = e^{-t}M$ and

$$\Sigma_t = e^{-2t}\Sigma + (1 - e^{-2t})\text{Id}.$$

Under an ideal situation where there is no score error, the discretization of the (backward) generative process is given by equation (39):

$$x_{k+1} = ((1 + \delta)\text{Id} - 2\delta\Sigma_{T-k\delta}^{-1})x_k + 2\delta\Sigma_{T-k\delta}^{-1}M_{T-k\delta} + \sqrt{2\delta}z_{k+1},$$

where δ is the uniform step size and z_k are iid white Gaussian random variables. For the SGM case, $M = 0$. The starting step of this discretization is itself $x_0 \sim \mathcal{N}(0, \text{Id})$. From this formula, the covariance matrix $\hat{\Sigma}_k$ of x_k satisfies the recursion (32):

$$\hat{\Sigma}_{k+1} = ((1 + \delta)\text{Id} - 2\delta\Sigma_{T-k\delta}^{-1})\hat{\Sigma}_k((1 + \delta)\text{Id} - 2\delta\Sigma_{T-k\delta}^{-1}) + 2\delta\text{Id},$$

from which we can exactly compute $\hat{\Sigma}_k$ for very k , and especially for $k = N = T/\delta$, as a function of Σ , the final time T , and the step size δ . In all our experiments, we choose stationary processes: their covariance Σ is diagonal in a Fourier basis, with eigenvalues (*power spectrum*) noted \hat{P}_k . All the x_k remain stationary so $\hat{\Sigma}_k$ is still diagonal in a Fourier basis, with power spectrum noted \hat{P}_k . The error displayed in the left panel of Figure 2 is:

$$\|\hat{P}_N - P\| = \max_{\omega} |\hat{P}_N(\omega) - P(\omega)| / \max_{\omega} |P(\omega)|,$$

normalized by the operator norm of Σ .

The illustration in the middle panel of Figure 2, for WSGM, is done for simplicity only at one scale (ie, at $j = 1$ in Algorithm 1): instead of stacking the full cascade of conditional distributions for all $j = J, \dots, 1$, we use the true low-frequencies $x_{j,0} = x_1$. Here, we use Daubechies-4 wavelets. We sample $\bar{x}_{j,0}$ using the Euler-Maruyama recursion (39)-(32) for the conditional distribution. We recall that in the Gaussian case, \bar{x}_1 and x_1 are jointly Gaussian. The conditional distribution of \bar{x}_1 given x_1 is known to be $\mathcal{N}(Ax_1, \Gamma)$, where:

$$A = -\text{Cov}(\bar{x}_1, x_1)\text{Var}(x_1)^{-1}, \quad \Gamma = \text{Var}(\bar{x}_1) - \text{Cov}(\bar{x}_1, x_1)\text{Var}(x_1)^{-1}\text{Cov}(\bar{x}_1, x_1)^\top.$$

We solve the recursion (32) with a step size δ and $N = T/\delta$ steps; the sampled conditional wavelet coefficients $\bar{x}_{j,0}$ have conditional distribution noted $\mathcal{N}(\hat{A}_N x, \hat{\Gamma}_N)$. The full covariance of $(\bar{x}_{j,0}, x_{j,0})$, written in the basis given by the high/low frequencies, is now given by

$$\hat{\Sigma}_N = \begin{bmatrix} \hat{\Gamma}_N & \text{Cov}(x_1, \bar{x}_1)\hat{A}_N^\top \\ \hat{A}_N \text{Cov}(x_1, \bar{x}_1)^\top & \text{Cov}(x_1, x_1) \end{bmatrix}.$$

Figure 2, middle panel compares the eigenvalues (power spectrum) of these covariances, as a function of δ , with the ones of Σ .

The right panel of Figure 2 gives the smallest N needed to reach $\|\hat{P}_N - P\| = 0.1$ in both cases (SGM and WSGM), based on a power law extrapolation of the curves $N \mapsto \hat{P}_N$.

13 Experimental Details on the φ^4 Model

In this section, we develop and precise the results in Section 4.1.

13.1 The Critical φ^4 Process and its Stein Score Regularity

The macroscopic energy of non-Gaussian distributions can be specified as shown in (15), where K is a coupling matrix and V is non-quadratic potential. The φ^4 -model over the $L \times L$ periodic grid is the special case defined by $C = \Delta$ (the two-dimensional discrete Laplacian) and V is a quartic potential:

$$E(x) = \frac{\beta}{2} \sum_{|u-v|=1} (x(u) - x(v))^2 + \sum_u (x(u)^2 - 1)^2.$$

Here, β is a parameter proportional to an inverse temperature.

In physics, the φ^4 model is a typical example of second-order phase transitions: the quadratic part reduces spatial fluctuations, and V favors configurations whose entries remain close to ± 1 (in physics, this is often called a *double-well potential*). In the thermodynamic limit $L \rightarrow \infty$, both term compete according to the value of β .

- For $\beta \ll 1$, the quadratic term becomes negligible and the marginals of the field become independent; this is the disordered state.
- For $\beta \gg 1$, the quadratic term favors configuration which are spatially smooth and the potential term drives the values towards ± 1 , resulting in an ordered state, where all values of the field are simultaneously close to either $+1$ or to -1 .

A phase transition occurs between these two regimes at a critical temperature $\beta_c \sim 0.68$ Milchev et al. (1986); Kaupuvz et al. (2016). At this point, the φ^4 field display very long-range correlations and an ill-conditioned Hessian $\nabla^2 \log p$. The sampling of φ^4 at this critical point becomes very difficult. This ‘‘critical slowing down’’ phenomenon is why, from a machine learning point of view, the critical

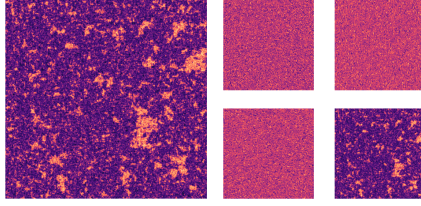


Figure 5: Example of a realization of a φ^4 critical field ($L = 256$) with its wavelet decomposition on the left (lower-frequencies are on bottom right panel).

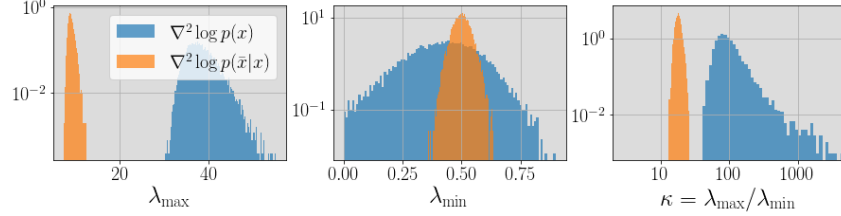


Figure 6: Histograms of 10^5 realizations of λ_{\min} , λ_{\max} and $\kappa = \lambda_{\max}/\lambda_{\min}$ of the Hessian matrices in (84) for the critical φ^4 model in dimension $L = 32$. The mean values of κ are respectively $\mu = 18.32$ and $\bar{\mu} = 210.53$; standard deviations are $\sigma = 1.78$ and $\bar{\sigma} = 9451.37$.

φ^4 field is an excellent example of hard-to-learn and hard-to-sample distribution, still accessible for mathematical analysis.

Our wavelet diffusion considers the sampling of the conditional probability $p(\bar{x}_1|x_1)$ instead of $p(x_0)$, by inverting the noise diffusion projected on the wavelet coefficients. Theorem 2 indicates that the loss obtained with any SGM-type method depends on the regularity parameters of $\nabla \log p_t$ in (7).

Strictly speaking, to get a bound on K we should control the norm of $\nabla^2 \log p_t$ over all x and t . However, a look at the proof of the theorem indicates that this control does not have to be uniform in x ; for instance, there is no need to control this Hessian in domains which have an extremely small probability under p_t . Moreover, since p_t is a convolution between p_0 and a Gaussian, we expect that a control over $\nabla^2 \log p_0(x)$ will actually be sufficient to control $\nabla^2 \log p_t(x)$ for all $t > 0$; these facts are non-rigorous for the moment. The distribution of some spectral statistics of $\nabla^2 \log p_0$ over samples drawn from the φ^4 -model are shown in Figure 6 (blue).

Considering conditional probabilities \bar{p} instead of p acts on the Hessian of the φ^4 -energy as a projection over the wavelet field: in the general context of (15),

$$-\nabla_x^2 \log p(x_0) = K + \nabla^2 V(x_0), \quad -\nabla_{\bar{x}_1}^2 \log p(\bar{x}_1|x_1) = \gamma^2 \bar{G}(K + \nabla^2 V(x_0))\bar{G}^\top. \quad (84)$$

The proof is in Section 13. The distribution of the conditioning number of $\nabla_x^2 \log p$ and $\nabla_{\bar{x}}^2 \log p$ over samples drawn from the φ^4 model is shown at Figure 6: the Hessian of the wavelet log-probability is orders-of-magnitude better conditioned than its single-scale counterpart, with a very concentrated distribution. The same phenomenon occurs at each scale j , and the same is true for λ_{\min} , λ_{\max} . It turns out that considering wavelet coefficient not only concentrates these eigenvalues, but also drives λ_{\min} away from 0. In the context of multiscale Gaussian processes, Lemma 4 gives a rigorous proof of this phenomenon. In the general case, $\nabla^2 \log p_t$ is not reduced to the inverse of a covariance matrix, but we expect the same phenomenon to be true.

13.2 Score Models and Details on our Numerical Experiments of φ^4

In this section, we give some details on our numerical experiments from Section 4.1.

Training Data and Wavelets

We used samples from the φ^4 model generated using a classical MCMC algorithm — the sampling script will be publicly available in our repository.

The wavelet decompositions of our fields were performed using Python’s `pywavelets` package and Pytorch `Wavelets` package. For synthetic experiments, we used the Daubechies wavelets with $p = 4$ vanishing moments (see (Mallat, 1999, Section 7.2.3)).

Score Model

At the first scale $j = 0$, the distribution of the φ^4 models falls into the general form given in (15), and it is assumed that at each scale j , the distribution of the field at scale j still assumes this shape — with modified constants and coupling parameters. The score model we use at each scale is given by:

$$s_{K,\theta}(x) = \frac{1}{2}x^\top Kx + \sum_u (\theta_1 v_1(x(u)) + \dots + \theta_m v_m(x(u))),$$

where the parameters are $K, \theta_1, \dots, \theta_m$ and v_i are a family of smooth functions. One can also represent this score as $s_{K,\theta} = K \cdot xx^\top + \theta^\top U(x)$ where $U_i(x) = \sum_u v_i(x(u))$.

Learning

We trained our various algorithms using SGM or WSGM up to a time $T = 5$ with $n_{\text{train}} = 2000$ steps of forward diffusion. At each step t , the parameters were learned by minimizing the score loss:

$$\ell(K, \theta) = \mathbb{E}[|\nabla s_{K,\theta}(x_t)|^2 + 2\Delta_x s_{K,\theta}(x_t)]$$

using the Adam optimiser with learning rate $\text{lr} = 0.01$ and default parameters α, β . At the start of the diffusion ($t = 0$) we use 10000 steps of gradient descent. For $t > 1$, we use only 100 steps of gradient descent, but initialized at (K_{t-1}, θ_{t-1}) .

Sampling

For the sampling, we used uniform steps of discretization.

For the error metric, we first measure the L^2 -norm between the power spectra P, \hat{P} of the true φ^4 samples, and our syntheses; more precisely, we set:

$$D_1 = \|P - \hat{P}\|^2.$$

This error on second-order statistics is perfectly suitable for Gaussian processes, but must be refined for non-Gaussian processes. We also consider the total variation distance between the histograms of the marginal distributions (in the case of two-dimensions, pixel-wise histograms). We note this error D_2 ; our final error measure is $D_1 + D_2$. This is the error used in Figure Figure 6.

13.3 Proofs of (84)

In the sequel, ∇f is the gradient of a function f , and ∇^2 is the Hessian matrix of f . The *Laplacian* of f is the trace of the Hessian.

Lemma 28. *Let $U : \mathbb{R}^n \rightarrow \mathbb{R}$ be smooth and M be a $n \times m$ matrix. We set $F(x) = U(Mx)$ where $x \in \mathbb{R}^m$. Then, $\nabla^2 F(x) = M^\top \nabla^2 U(x) M$.*

Proof. Let $U : \mathbb{R}^n \rightarrow \mathbb{R}$ be smooth and M be a $n \times m$ matrix. Then,

$$\partial_k F(x) = \sum_{i=1}^n M_{i,k} (\partial_i U)(Mx).$$

Similarly,

$$\partial_{k,\ell} F(x) = \sum_{i=1}^n \sum_{j=1}^n M_{i,k} M_{j,\ell} \partial_j (\partial_i U)(Mx). \quad (85)$$

This is equal to $(M^\top \nabla^2 U M)_{k,\ell}$. □

Lemma 29. *Under the setting of the preceding lemma, if $U(x) = \sum_{i=1}^n f(x_i)$, then (1) $\nabla^2 U(x) = \text{diag}(u''(x_1), \dots, u''(x_n))$ and (2) the Laplacian of $F(x) = U(Mx)$ is given by*

$$\Delta F(x) = \sum_{i=1}^n (M^\top M)_{i,i} u''(x_i).$$

Proof. The proof of (1) comes from the fact that $\partial_i U(x) = u'(x_i)$, hence $\partial_j \partial_i U(x) = u''(x_i)$ if $i = j$, zero otherwise. The proof of (2) consists in summing the $k = \ell$ terms in (85) and using (1). \square

For simplicity, let us note $p(x) = e^{-H(x)}/Z$ where Z_0 is a normalization constant and $H(x) = x^\top Kx/2 + V(x)$. Then,

$$\nabla_x p(x) = -\nabla_x H(x), \quad \nabla_x^2 p(x) = -\nabla_x^2 H(x),$$

and the formula in the left of (84) comes from the fact that the Hessian of $x^\top Kx$ is $2K$.

For the second term, let us first recall that if \bar{x}_1 and x_1 are the wavelet coefficients and low-frequencies of x , they are linked by (13). Consequently, the joint density of (\bar{x}_1, x_1) is:

$$q(\bar{x}_1, x_1) = e^{-H(\gamma G^\top x_1 + \gamma \bar{G}^\top \bar{x}_1)}/Z_1$$

where Z_1 is another normalization constant. The conditional distribution of \bar{x}_1 given x_1 is:

$$q(\bar{x}_1|x_1) = \frac{q(\bar{x}_1, x_1)}{Z_1(x_1)}$$

where $Z_1(x) = \int q(\bar{x}_1, u) du$. Consequently,

$$\begin{aligned} \nabla_{\bar{x}_1} \log q(\bar{x}_1|x_1) &= \nabla_{\bar{x}_1} (-H(\gamma G^\top x_1 + \gamma \bar{G}^\top \bar{x}_1) - \log Z_1) - \nabla_{\bar{x}_1} Z_1(x_1) \\ &= -\nabla_{\bar{x}_1} H(\gamma G^\top x_1 + \gamma \bar{G}^\top \bar{x}_1) \end{aligned}$$

and additionally:

$$\nabla_{\bar{x}_1}^2 q(\bar{x}_1|x_1) = -\nabla_{\bar{x}_1}^2 H(\gamma G^\top x_1 + \gamma \bar{G}^\top \bar{x}_1).$$

The RHS of (84) then follows from the lemmas in the preceding section.

14 Experimental Details on CelebA-HQ

Data We use Haar wavelets. The 128×128 original images are thus successively brought to the 64×64 and 32×32 resolutions, separately for each color channel. Each of the 3 channels of x_j and 9 channels of \bar{x}_j are normalized to have zero mean and unit variance.

Architecture Following Nichol and Dhariwal (2021), both the conditional and unconditional scores are parametrized by a neural network with a UNet architecture. It has 3 residual blocks at each scale, with a base number of channels of $C = 128$. The number of channels at the k -th scale is $a_k C$, where the multipliers $(a_k)_k$ depend on the resolution of the generated images. They are (1, 2, 2, 4, 4) for models at the 128×128 resolution, (2, 2, 4, 4) for models at the 64×64 resolution, (4, 4) for the conditional model at the 32×32 resolution, and (1, 2, 2, 2) for the unconditional model at the 32×32 resolution. All models include multi-head attention layers at in blocks operating on images at resolutions 16×16 and 8×8 . The conditioning on the low frequencies x_j is done with a simple input concatenation along channels, while conditioning on time is done through affine rescalings with learned time embeddings at each GroupNorm layer (Nichol and Dhariwal, 2021; Saharia et al., 2021).

Training The networks are trained with the (conditional) denoising score matching losses:

$$\begin{aligned} \ell(\theta_j) &= \mathbb{E}_{x_j, t, z} \left[\|s_{\theta_j}(t, e^{-t} x_j + \sqrt{1 - e^{-2t}} z) - z\|^2 \right] \\ \ell(\bar{\theta}_j) &= \mathbb{E}_{\bar{x}_j, x_j, t, z} \left[\|\bar{s}_{\bar{\theta}_j}(t, e^{-t} \bar{x}_j + \sqrt{1 - e^{-2t}} z | x_j) - z\|^2 \right] \end{aligned}$$

where $z \sim \mathcal{N}(0, \text{Id})$ and the time t is distributed as Tu^2 with $u \sim \mathcal{U}([0, 1])$. We fix the maximum time $T = 5$ for all scales. Networks are trained for 5×10^5 gradient steps with a batch size of 128 at the 32×32 resolution and 64 otherwise. We use the Adam optimizer with a learning rate of 10^{-4} and no weight decay.

Sampling For sampling, we use model parameters from an exponential moving average with a rate of 0.9999. For each number of discretization steps N , we use the Euler-Maruyama discretization with a uniform step size $\delta_k = T/N$ starting from $T = 5$. This discretization scheme is used at all scales. For FID computations, we generate 30,000 samples in each setting.